Activation of DNA Carbon−Hydrogen Bonds by Metal Complexes

Marguerite Pitié[†] and Geneviève Pratviel*[,‡]

CNRS, LCC (Laboratoire de Chimie de Coordination), 205 route de Narbonne, F-31077 Toulouse, France, and Université de Toulouse, Toulouse, France

Received July 11, 2009

Contents

Marguerite Pitié was born in Castres (France) in 1964. She studied biochemistry at University Paul Sabatier, Toulouse, and obtained her Ph.D. degree in 1993 working on the mechanisms of DNA cleavage by manganese porphyrins under the supervision of B. Meunier. She pursued as a postdoctoral fellowship (1994−1995) in the group of T. Le Doan, Museum d'Histoire Naturelle, Paris. She entered the CNRS in 1995 in the Laboratoire de Chimie de Coordination, Toulouse, where she is currently "Chargée de Recherche". Her main research interests concern the design of bioactive chelators and the DNA oxidation by copper complexes applied to the development of biologically active compounds and tools for molecular biology.

Geneviève Pratviel was born in 1959 in Toulouse, France, and received her Ph.D. in 1986 from Université Paul Sabatier, Toulouse (with B. Meunier). After a postdoc at Yale University, she joined the Laboratoire de Chimie de Coordination of CNRS in 1988. She is now Director of research at CNRS. Her major research interests include mechanism of oxidative DNA damage mediated by metal complexes, design of DNA-targeted reagents, and mechanism of action of antitumoral drugs.

1. Introduction

Inert C−H bond functionalization is usually performed by dioxygen-utilizing enzymes through the insertion of an oxygen atom into the C−H bond. Alternative reactions include halogenation, desaturation, cyclization, and epoxidation. Although DNA is highly resistant to hydrolysis, it is sensitive to oxidation. In a way reminiscent to the aerobic enzymes, the capacity of metal complexes to activate dioxygen, or its reduced form hydrogen peroxide, will lead to the functionalization of an inert C−H bond of DNA through the replacement of a C−H bond by a C−O bond. DNA oxidation by metal complexes occurs by C−H bond activation at the deoxyriboses. Oxidation of nucleobases, which are heterocyclic aromatic sites, follows other mech-

* To whom correspondence should be addressed. E-mail: pratviel@lcc-toulouse.fr.
† CNRS.
‡ Université de Toulouse.

10.1021/cr900247m
Published on Web 01/25/2010

anisms such as radical or electron transfer reactions. C−H bond activation involves as a first step a homolytic cleavage of the C−H bond, which produces a transient carbon-centered radical. The energy of C−H bonds of deoxyribose units of DNA range around ∼90 kcal/mol. For comparison, the methyl C−H of thymine nucleobase is ∼90 kcal/mol, while aromatic C−H or C−H bonds of methane are ∼100 kcal/mol. The susceptibility of an aliphatic C−H bond toward homolytic cleavage increases with the relative stabilization of the carbon-centered radical. Methine group (R_3C-H) leading to tertiary carbon radical is more reactive than methylene group ($-CH_2-$). C1′ and C4′ radicals are resonance stabilized by neighboring oxygen. Thus, the susceptibility of the C−H bonds of deoxyriboses toward activation is higher for C1′−H, C3′−H, and C4′−H, as compared to C2′−H and C5′−H. However, because they are not equally accessible, their reactivity will depend on the ways the metal complexes will approach and interact with the double helix of DNA.

Significant advances in our understanding of the exquisite chemistry of dioxygen-utilizing metalloenzymes as well as studies with biomimetic models[1−13] provide important insights on the mechanism of C−H bond activation by metal complexes. Several metal-centered active species able to perform C−H bond activation are now proposed in the literature. The nature of the metal, their number at the catalytic site, and the ligands differ. Among the species able to perform this reaction, one can find a high-valent metal−oxo entity, which is centered on the metal, or a simple hydroxyl radical (HO•), which is freely diffusing.

As soon as an active species is generated at the metal center, the presence of the substrate in close vicinity is extremely important to avoid the oxidation/degradation of the organic ligand(s) surrounding the activated metal center. As a consequence, C−H activation on DNA by metal complexes will concern metal complexes not only able to undergo oxygen activation but also complexes able to come within reach of C−H bonds of deoxyriboses. A tight and precise interaction between the active metal complex and DNA is the key of efficiency. In the case of proteins, the metal-centered active species is located in an enzyme pocket where the substrate finds a special place to bind, and a high-yield, stereo-, and regioselective reaction takes place. Furthermore, the activation of the metal core with O_2 takes place in general after the incoming of the substrate. In the case of biomimetic metal catalysts, small molecule substrates have an easy access to the metal catalyst, precluding its bleaching. Considering oxidative DNA damage, the activation of the metal complex before its binding to DNA will increase the probability of its self-degradation. DNA is not comparable to the usual small organic molecules. The C−H bonds of deoxyribose are not easily accessible to the bulk solvent except for neutral, small in size, and diffusible HO•. Thus, the best scenario consists of the activation of the metal core in situ, while in contact with DNA. Another important point is the stability of the metal complex. The affinity of the metal ion for the ligand must be high enough so that the metal is not lost under dilute solution conditions and activated at the precise site where the ligand places it in contact with DNA. Because of these absolute requirements for efficient C−H bond activation of DNA, examples of metal complexes able to perform precise chemistry on DNA are scarce.

We survey oxidative DNA damage mediated by metal complexes through deoxyribose oxidation. Possible active species and DNA products are reviewed. We focus then on the metal complexes for which molecular mechanisms have been studied in some details and that perform selective C−H activation of DNA, iron bleomycin (BLM), copper bis(1,10-phenanthroline) [$Cu(phen)_2$], and manganese tetramethylpyridiniumyl-porphyrin [Mn(TMPyP)].[14−17] They exemplify metal-centered active species in strict interaction with DNA that illuminate selective DNA C−H bond activation. Efforts toward the design of sequence selective DNA cleaving agents based on metal complexes will also be summarized.

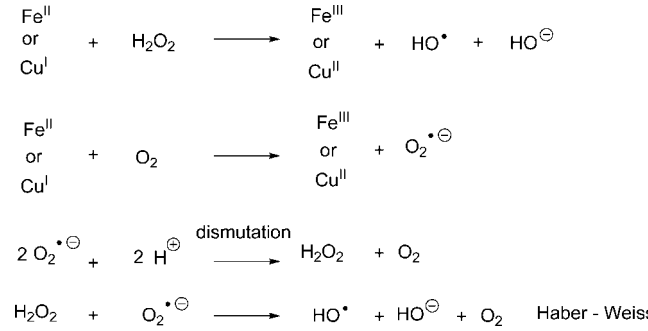

Figure 1. Redox events involved in the formation of diffusible reactive oxygen species by ferrous and cuprous complexes in the presence of reductant, O_2, and/or H_2O_2.

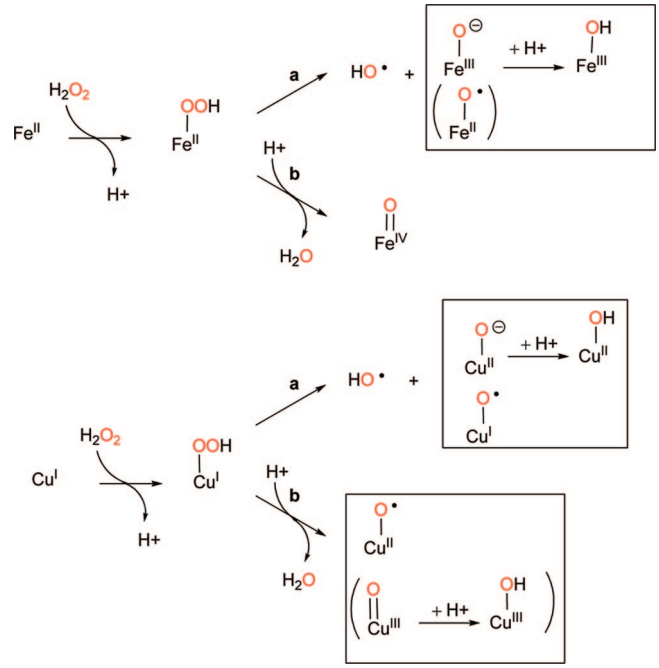

Figure 2. Coordination of H_2O_2 to ferrous and cuprous complexes. Formation of possible active species for C−H bond activation. Homolytic (a) and heterolytic cleavage (b) of the O−O bond of the coordinated peroxide.

2. Active Species Able To Perform C−H Bond Activation

Active species, formed by activation of O_2 or H_2O_2 with metal complexes, can be divided in three categories (presented in Figures 1, 2, and 3, respectively). Within these three general mechanisms, the process of C−H bond activation will be more or less controlled going from simple radical chemistry to advanced oxygen atom transfer with stereoselectivity and regioselectivity. The most used metals in the field of oxygen activation and DNA damage are iron, copper, and manganese. The mechanisms are presented with

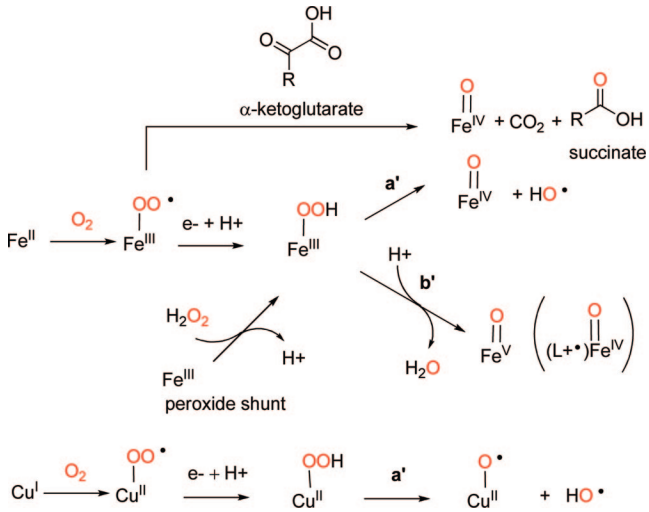

Figure 3. Coordination of O_2 to ferrous and cuprous complexes. Formation of possible active species for C−H bond activation. Homolytic (a′) and heterolytic cleavage (b′) of the O−O bond of the coordinated peroxide. L stands for ligand.

iron and copper; yet manganese follows the same reaction pathways as iron. We only focus on the case of mononuclear complexes because, at this time, oxygen activation with multinuclear metal complexes does not find any mechanistically defined example in the field of double-stranded DNA oxidation.

The first mechanism is related to radical chemistry. C−H bond oxidation can occur through a Fenton−Haber Weiss reaction (Figure 1). The reaction between metal ions and dioxygen or its reduced derivative, hydrogen peroxide, merely consists of a one-electron transfer reaction from a reduced metal ion to H_2O_2 and/or O_2, which generates hydroxyl radicals in solution. The hydroxyl radical is freely diffusing and reacts with any accessible site due to its small and neutral character. This reaction is common and easy. It is often encountered in the field of DNA damage mediated by metal complexes. The reaction of $HO^•$ with a C−H bond gives rise to a carbon radical associated with the formation of H_2O. This mechanism has no chance of being stereoselective and no chance of being regioselective because $HO^•$ may react at several C−H bonds.

On the other hand, a more sophisticated chemistry of C−H bond activation is possible with a metal-centered active species. In this case, one may expect a stereoselective and regioselective reaction. The formation of the metal-centered oxidative species requires the coordination of H_2O_2 (second mechanism) or O_2 (third mechanism) to a ferrous/cuprous ion. Coordination of H_2O_2 to a Fe^{II} (Cu^{I}) complex leads to an initial Fe^{II}−OOH (Cu^{I}−OOH) (Figure 2). Coordination of O_2 to a Fe^{II} (Cu^{I}) leads to a Fe^{III}−$OO^•$ (Cu^{II}−$OO^•$) species (Figure 3). The coordination of O_2 to the metal ion confers immediately a superior oxidizing power as compared to the coordination of hydrogen peroxide, even after a one-electron reduction followed by a protonation step that affords the Fe^{III}−OOH (Cu^{II}−OOH) entity from Fe^{III}−$OO^•$ (Cu^{II}−$OO^•$) (Figure 3). H_2O_2 can also coordinate onto Fe^{III} to give directly Fe^{III}−OOH (peroxide shunt, Figure 3). From these intermediate oxygenated metal complexes, the cleavage of the O−O bond will be possible.

Is Fe^{III}−OOH an active species able to perform C−H bond activation? Experimental data, indicating that oxygenation reactions by cytochrome P450 and synthetic transition metal reagents behave as though more than one oxidant species were involved in the process, led to a debate in the literature concerning the Fe^{III}−OOH species as being responsible for the activation of C−H bonds.[18–20] However, it appears that Fe^{III}−OOH may be rather considered as a precursor of active species in the form of high-valent metal−oxo species. The different product distributions may be due to a single oxidant under different environmental circumstances or from a two-state reactivity or multistate reactivity in high-valent metal−oxo reagents.[4,21–24] Furthermore, Fe^{III}−OOH proved to be a sluggish oxidant[25,26] and can be rather considered as a nucleophile for heme enzymes.[2]

What are the other possible active species? Starting from Fe^{II}−OOH (Cu^{I}−OOH), homolytic cleavage of the O−O bond of the coordinated peroxide produces $HO^•$ (pathway a, Figure 2). The hydroxyl radical is a one-electron oxidant and may react on its own. It may be generated in a confined volume (caged radical) and abstract a nearby hydrogen atom. After the homolytic cleavage of the peroxide, the Fe^{II}−OOH ends as Fe^{II}−$O^•$ or a Fe^{III}−OH, while Cu^{I}−OOH ends as Cu^{I}−$O^•$ or a Cu^{II}−OH (pathway a, Figure 2). These species may or may not be capable of oxidation by H-atom abstraction or electron transfer, probably as a function of the complex.[13]

Alternatively, the heterolytic cleavage of the peroxide of Fe^{II}−OOH or Cu^{I}−OOH leads to high-valent metal−oxo species in the form of Fe^{IV}=O for iron complexes and Cu^{II}−$O^•$, Cu^{III}=O, or Cu^{III}−OH after protonation for copper (pathway b, Figure 2). The same metal-centered oxygenated species can be obtained through the homolytic cleavage of the Fe^{III}−OOH (Cu^{II}−OOH) entity (pathway a′, Figure 3). Their formation in that case is associated with the release of an equivalent of $HO^•$.

Finally, the heterolytic cleavage of the O−O bond of Fe^{III}−OOH leads to the most powerful activated species (pathway b′, Figure 3). On the basis of the strong oxidant generated from the heterolytic cleavage of Fe^{III}−OOH, similar heterolytic cleavage from Cu^{II}−OOH was also envisioned, yet only at the level of computational studies (pathway b′, Figure 3).[27,28] This mechanism of oxygen activation corresponds to the chemistry of cytochrome P450, the most extensively studied hydroxylating enzymes.[2–4] The distal oxygen of the coordinated peroxide is released as a water molecule, and the metal center becomes a formally written Fe^{V}=O species (referred to as Compound I in the catalytic cycle of peroxidase and cytochrome P450). This species contains two oxidizing equivalents required to oxidize the substrate. Its oxidation state is two-redox equivalents above the corresponding Fe^{III} complex and is clearly more oxidizing than the previous iron−oxo, Fe^{IV}=O, which is two-redox equivalents above Fe^{II}. The two oxidizing equivalents of the formal Fe^{V}=O are distributed between the iron and the porphyrin ligand, in heme enzymes, so that the heterolytic cleavage of Fe^{III}−OOH leads to an oxo−iron(IV)−porphyrin cation radical ($P^{+•}$−Fe^{IV}=O). This type of active species is extremely efficient in C−H bond activation. It is not only able to abstract a hydrogen atom from a C−H bond, but it is able to immediately incorporate the oxygen atom from the metal onto the carbon centered radical by the so-called oxygen rebound mechanism. This mode of activation is the only one that guarantees the storage/use of two oxidizing equivalents by the metal-centered active species, because after a one-electron oxidation equivalent process, the system is clearly still an oxidant for a second oxidation step.

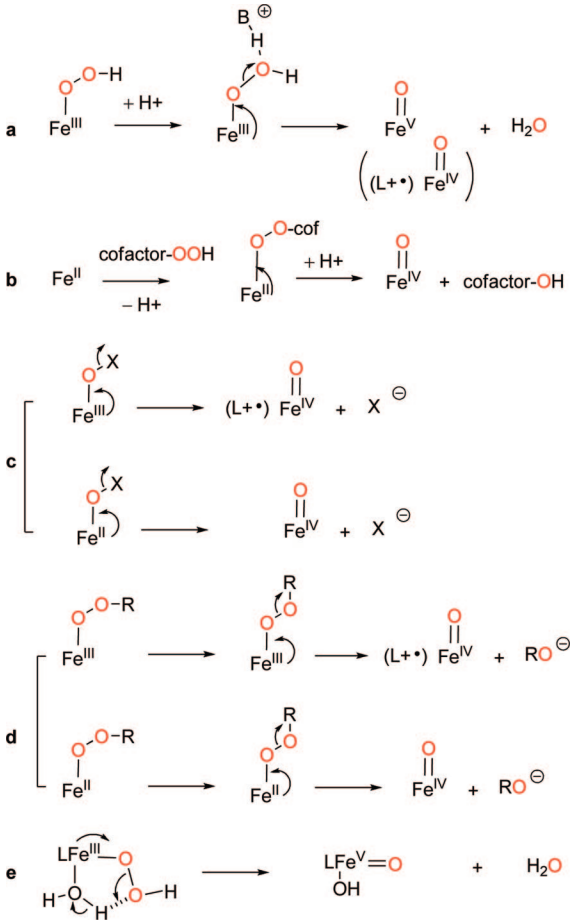

Figure 4. Examples of different pathways leading to heterolytic cleavage of the O−O bond of the coordinated peroxide. L stands for ligand.

Homolytic cleavage of the O−O bond of the coordinated peroxide will always produce HO•, whatever the starting species, Fe^{II}−OOH (Cu^{I}−OOH) (pathway a, Figure 2) or Fe^{III}−OOH (Cu^{II}−OOH) (pathway a′, Figure 3). The production of HO• must be avoided for a better control of the stereo- and regioselectivity of the reaction. Consequently, the heterolytic cleavage of the O−O bond of the coordinated peroxide must be favored. The presence of a good leaving group associated with the distal oxygen atom helps. This is illustrated in cytochrome P450 or iron porphyrins by the protonation of the distal oxygen atom (acid catalysis) and its release in the form of a molecule of water[1–3,29] (Figure 4a) or in pterin-dependent nonheme iron enzymes with the release of 4a-hydroxybiopterin (Figure 4b).[30] This is also illustrated by the use of dissymmetric hydroperoxides or single oxygen atom donors (X−O) with metallo-porphyrins and nonheme iron complexes (Figure 4c,d). The intramolecular protonation mechanism in nonheme iron models is also a key example (Figure 4e).[31–34]

Figure 4 shows that the oxygen atom of the formal Fe^{V}=O species originates from O_2, H_2O_2, HOOR, or OX initially coordinated to the metal ion. The oxygen rebound mechanism implies an oxygen atom transfer from the metal−oxo to the activated C−H bond. The oxygen atom of the formal Fe^{V}=O species exchanges with solvent through an oxo−hydroxo tautomerism involving a coordinated water molecule (hydroxo ligand) (Figure 5).[31,35,36] In $H_2{}^{18}O$, the subsequent alcohol is labeled with a mixture of ^{16}O and ^{18}O, depending on the extent of exchange. The maximum percentage of ^{18}O incorporated from water is 50%.

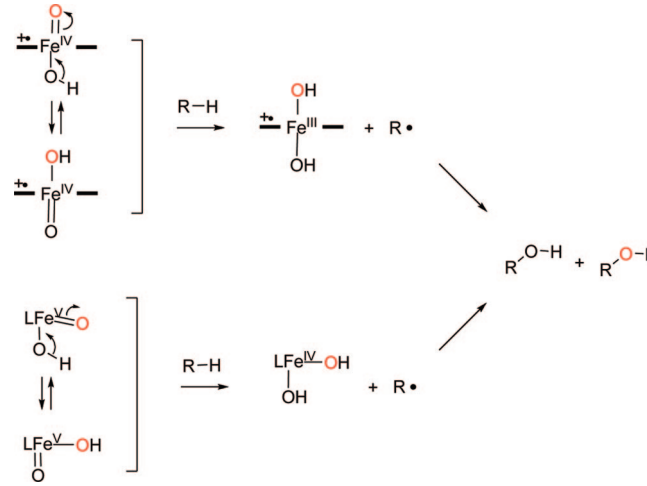

Figure 5. Oxygen rebound mechanism and oxo−hydroxo tautomerism of high-valent metal−oxo species in the case of iron porphyrins (top) or nonheme iron complexes (bottom). Mixed origin of the oxygen atom incorporated in the resulting alcohol. L stands for ligand.

Full characterizations in support for the various activated species that have been mentioned in Figures 2 and 3 are not always available. Fe^{III}−OOH exists as a transient precursor of activated species in the catalytic cycle of heme enzymes (Compound 0) and has been characterized not only for enzymes but also for porphyrins and nonheme iron complexes. However, as mentioned before, there is no experimental evidence that Fe^{III}−OOH would be sufficiently electrophilic at the distal oxygen to react with a C−H bond.

Fe^{IV}=O active species are similar to cytochrome P450 and peroxidase Compound II. They have also been characterized in the case of nonheme iron complexes.[7,37,38] A nonheme Fe^{IV}=O species was characterized for the nonheme iron α-ketoglutarate dependent hydroxylases and for pterin-dependent hydroxylases.[5,7,30,39] These species are capable of alkane hydroxylations not only for nonheme iron enzymes but also for model compounds.[13,40,41]

Oxo−iron(IV)−porphyrin cation radical ($P^{+•}$−Fe^{IV}=O) has been proposed for heme peroxidases (Compound I).[1] The evidence for this species for cytochrome P450 is not as compelling as for the peroxidases.[3] High-valent iron oxo species in the form of the formal Fe^{V}=O oxidation state, such as the oxo−iron(IV)−porphyrin cation radical, have been characterized for synthetic porphyrins.[12] Some examples of Fe^{V}=O species are now available with nonheme ligands.[42,43] These species are unambiguously able to perform C−H bond activation.

In the case of copper, the structures and mechanisms are less documented. The mechanism of monocopper enzymes (more precisely, noncoupled binuclear copper enzymes) like dopamine β-monooxygenase and peptidylglycine α-hydroxylating monooxygenase, which are hydroxylating enzymes, has not been elucidated. The mechanisms proposed in the literature mainly suggest Cu^{II}−OO•, Cu^{II}−OOH, and Cu^{II}−O• as the species susceptible of C−H bond activation, although the last copper−oxo species has not been identified conclusively in an enzyme or synthetic complex.[10,27,28,44–47] The crystal structure of a precatalytic complex of peptidylglycine α-hydroxylating monooxygenase shows that O_2 binds end-on onto one monocopper center with no indication of its charge.[27] A number of synthetic Cu−O_2 complexes have been characterized.[47,48]

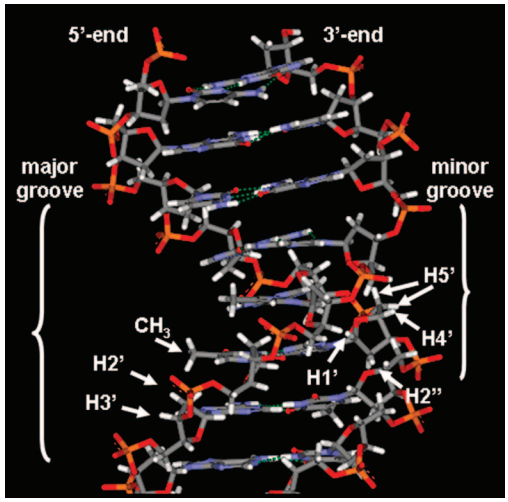

Figure 6. C−H bonds susceptible to activation on B-DNA.

As detailed in the next paragraph, C−H bond activation on DNA will lead to a carbon-centered radical located on deoxyribose units. The fate of this intermediate radical will depend on the nature and the efficiency of the active metal complex. Combination with dioxygen or intramolecular rearrangement will occur in some cases (this involves only one oxidizing equivalent). Further oxidation of the radical intermediate (corresponding to two oxidizing equivalents) will be exemplified by either electron transfer leading to a carbocation, which will be trapped by H_2O, or formation of an alcohol through the oxygen rebound mechanism. The multiple possible products of DNA damage are abundant.

3. Products of DNA C−H Bond Activation

Except for the methyl group of thymidine residues, oxidizable C−H bonds of DNA involving a sp^3 carbon are on deoxyribose (Figure 6). They are designated as H1′ (located on C1′-carbon linked to the nucleobase), H2′ and H2″ (on the only sugar carbon not directly linked to an oxygen atom), H3′ (on one carbon implicated on phosphodiester backbone), H4′ (on the carbon with a hydroxyl residue implicated in hemiacetalic junction of the sugar), and H5′ and H5″ (on the other carbon forming the phosphodiester backbone). All sp^3 carbons may be potentially transformed into a radical by abstraction of a hydrogen atom. According to structures obtained by X-ray crystallography of oligodeoxyribonucleotides (ODN), the 1′-, 2″-, 4′-, and one 5′-hydrogen are accessible from the minor groove on classical B-form duplex DNA, while 2′- and 3′-hydrogens and CH_3-thymine are in the major groove.[15,16] One 5′-hydrogen points directly into the minor groove; the other one is oriented away from the backbone toward solvent. The minor groove 5′- and 4′-hydrogen atoms are the most accessible in a typical B-form double helix. However, the reactivity of a metal complex toward one or another C−H bond does not only depend on the accessibility or the reactivity of these bonds but also on the more or less fine interactions between this metal complex and DNA as illustrated by typical examples in the next paragraphs. Diffusible species will display oxidative damage related to the accessibility of the target sites.[49]

The observation that some metal complexes are able to perform only (or highly preferentially) one type of sugar oxidation like $Cu(phen)_2$ (C1′), rhodium phenanthrenequinonediimine complexes (C3′), iron bleomycin (C4′), or Mn(TMPyP) (C5′) has greatly facilitated the establishment of DNA degradation mechanisms due to the DNA C−H oxidation by metal complexes.[14–17,50,51] This was particularly true when the metal complex shows some sequence selectivity that allows the easy study of one isolated oxidation events on the DNA structure. Additional data were gained from other DNA oxidation agents such as enediyne derivatives that can selectively abstract one H-atom of DNA,[15,16,50,51] synthetic ODNs including modified nucleosides able to generate selectively a radical on each carbon of the DNA under controlled conditions,[52,53] and from the extensive study of the DNA degradation products due to HO• produced by Fe^{II}(EDTA) or γ-irradiation.[14–16,50,54,55] Importantly, each position of H-atom removal leads to the formation of typical DNA oxidation products, allowing unambiguous characterization of the corresponding oxidation pathway. Except for some tandem reactions that are probably only involved as minor reaction pathways, the rate-limiting step is the H-atom abstraction. Therefore, the oxidized site can be determined by kinetic isotope effects measured on selectively deuterated DNA carbons. C1′−C5′ radicals have been characterized by EPR on mononucleosides, but their detection on duplex DNA is difficult.[56] The next paragraphs concern the fate of these radicals due to hydrogen atom abstraction on DNA. When it is possible, we discuss the mechanism pathways on the classical B-DNA structure.

3.1. H1′ Abstraction

Typical redox-active metal complexes able to generate C1′-radical on DNA duplex are copper 1,10-phenanthroline derivatives,[15–17,50,57] cationic manganese porphyrins,[15,17] oxoruthenium complexes,[58] Cr(V)-complexes,[59] and the HO• generators.[50,54,55]

C1′-oxidation via direct H-atom abstraction leads to the C1′-radical **1** (Figure 7). Importantly, the C1′ lies deeply inside the minor groove and is relatively inaccessible to diffusible species such as hydroxyl radical.[16,49] Therefore, in the case of free HO• generating systems like Fe^{II}(EDTA)/H_2O_2/ascorbate, C1′-oxidation is less frequent than C4′- or C5′-oxidation.[60,61]

Once formed, the C1′-radical **1** may undergo different reactions, but all of them produce the same oxidized sugar residue (Figure 7). As proposed in the case of the $Cu^{I}(phen)_2$/H_2O_2 system, the 1′-deoxyribosyl radical **1** is oxidized to cation **2** probably by the metal complex .[62,63] Rate constants for the oxidation of the 2′-deoxyuridin-1′-yl radical with $CuCl_2$ and $FeCl_3$ are reported to be 7.9×10^7 and 1×10^8 M^{-1} s^{-1}, respectively.[64] Nucleophilic attack of a water molecule at the C1′-cation **2** induces nucleobase release associated with the formation of an unstable deoxyribonolactone abasic site **3**. The same product **3** may be obtained by oxygen rebound in the case of Mn^{III}(TMPyP) associated with $KHSO_5$.[65]

Photocleavable modified nucleotides, selectively generating C1′-radical **1**, have been synthesized.[66–68] They can be incorporated into an ODN sequence by phosphoramidite chemistry.[69] They have been used to analyze the addition of O_2 to the C1′-radical **1** leading to C1′-peroxy radical **6**. A rate constant of 1×10^9 M^{-1} s^{-1}, near the diffusion rate, is generally proposed for this addition. Heterolytic fragmentation of the C1′-peroxy radical **6** yields the C1′-carbocation **2** and the release of a molecule of superoxide anion. Superoxide anion was detected spectrometrically thanks to epinephrine oxidation into adrenochrome.[70] Newcomb and

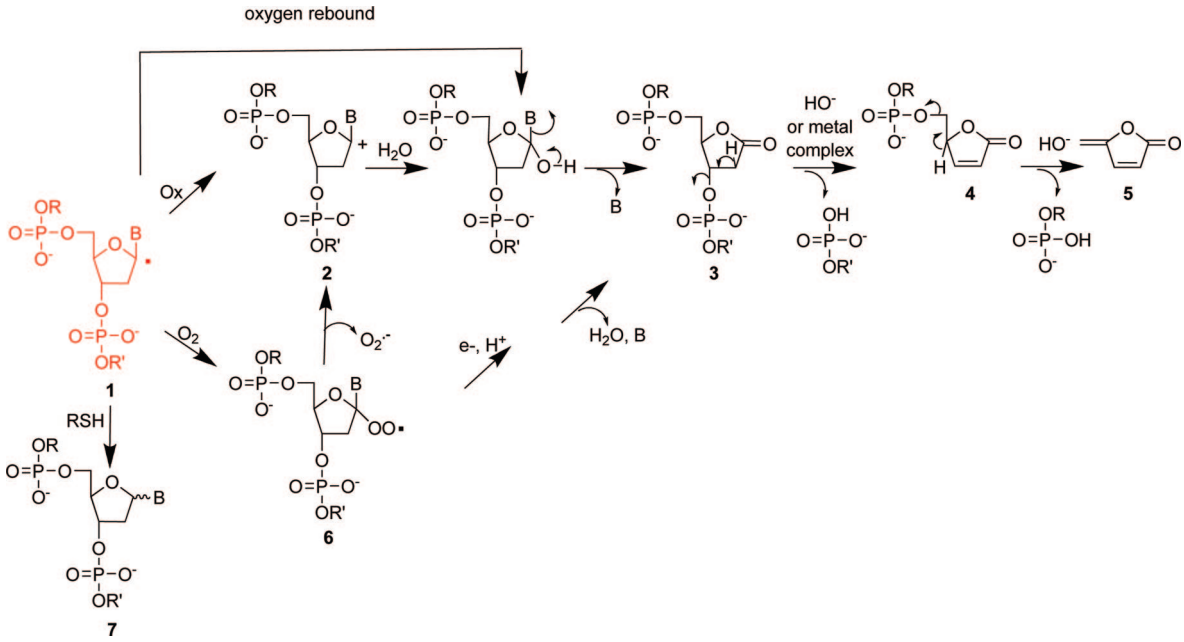

Figure 7. Possible reaction pathways of the C1′-radical. The C1′-radical is shown in red.

Chatgilialoglu reported a rate constant of $\sim 10^4$ s^{-1} for superoxide anion elimination from the C1′-peroxy radical of 2′-deoxyuridine monomer.[53,67] Importantly, this value is too fast to compete with the reduction of the peroxy radical **6** by thiols under physiological conditions (concentration of thiols: ~5 mM). However, the reduction of **6** to deoxyribonolactone **3** has been observed under particular experimental conditions.[16,70]

C1′-radical **1** may also be trapped by thiols with a high degree of stereoselectivity to give **7**. On synthetic models able to generate **1** in duplex DNA, β-2′-deoxyuridine was more than 6-fold favored over the mutagenic α-nucleotide when the radical was trapped by β-mercaptoethanol. The β/α ratio was only 1.3−2 in the case of C1′-radical **1** on mononucleotide and ~4 in single-stranded ODN, showing the structural effect of the duplex DNA for the stereoselectivity of this reduction.[64,68] Moreover, competition studies between β-mercaptoethanol and O_2 indicated that the thiol trapped C1′-radical **1** with a bimolecular rate constant of $\sim 4 \times 10^6$ M^{-1} s^{-1} in single-stranded DNA or on the DNA monomer. This rate constant decreased to $(1.8 \pm 0.6) \times 10^6$ M^{-1} s^{-1} in the case of duplex DNA.[68] This is consistent with the lower accessibility of the C1′-radical **1** in double-stranded DNA. However, the relative rate constants ($k_{O2}/k_{\beta\text{-mercaptoethanol}} = 1100$) for the trapping of the C1′-radical **1** indicate that, in the presence of physiological levels of thiols (~ 5 mM) and O_2 (63 μM), the formation of C1′-peroxy radical **6** will dominate. Therefore, it might be important to consider this reduction by thiols only when DNA oxidation occurs under hypoxic conditions.

An ODN-containing deoxyribonolactone abasic site **3** has been observed by HPLC associated with mass spectrometry[63,71,72] or by polyacrylamide gel electrophoresis (PAGE).[71,73−76] A deoxyribonolactone abasic site **3** induces a destabilization of the duplex DNA as reflected by a decrease of 22 °C of the T_m of an 11-mer when compared to an unmodified sequence.[74] This lesion is relatively unstable. A half-life of 32−54 h has been estimated for a deoxyribonolactone abasic site **3** in duplex DNA under physiological conditions. The half-life was only 20 h in single-stranded DNA, reflecting the double-strand stabilization effect.[73] However, metal complexes such as $Cu(phen)_2$ derivatives[77,78] or metal salts [Zn(II), Cu(II), Ni(II), or Mg(II)][79] catalyze a β-elimination, inducing a rapid strand break and precluding the observation of **3** in some cases. Such metal complexes may behave as Lewis acids and may catalyze the elimination of the phosphate group from the C3′ position.[80] This β-elimination takes place also in the presence of polyamine or upon heating at pH 7 and, more classically, upon heating under alkaline conditions. The reaction yields a DNA fragment with a 5′-phosphate-end and an unstable butenoide intermediate **4**. Compound **4** has been nevertheless observed on ODN by HPLC coupled to electrospray MS by Oyoshi et al.[63] A second β-elimination (or δ-elimination) step releases a DNA fragment with a 3′-phosphate end and a modified sugar characteristic of C1′-oxidation: 5-methylenefuranone **5**. Compound **5** is easily detected by HPLC or GC−MS, although it shows a limited stability that complicates its exact quantification.[81,82] The lactones **3**, **4**, and **5** do not exchange their oxygen atom with solvent. Consequently, the origin of the oxygen atom incorporated during the oxidation process is easy to check by mass spectrometry thanks to the use of ^{18}O-labeled O_2, H_2O, or metal−oxo.[63,65]

The deoxyribonolactone abasic site **3** was characterized by NMR on duplex ODNs. It induced only a small change in the DNA structure. The residue **3** was located in the DNA double-helix, and the opposite nucleobase residue remained intercalated.[83] Interestingly, the high reactivity of the deoxyribonolactone abasic site **3** has allowed the setup of typical reactions (involving addition of piperidine, *N*,*N*′-dimethylethylenediamine, β-mercaptoethanol...) that convert this lesion to a characteristic set of cleavage products that can be readily analyzed by PAGE or mass spectrometry.[71,84] It can also be noted that this high reactivity has been involved in the formation of covalent adducts between **3** and the amino-residues of proteins that could be responsible for a part of the toxicity of C1′-DNA oxidation.[85,86]

Finally, it has been proposed that C1′-radical also formed indirectly during tandem reactions involving, as a first oxidation event, the formation of a radical **8** on the C6 of pyrimidine nucleobase. Radical **8** may originate from classical addition of HO$^{\bullet}$ to the C5−C6 double bond of thymine

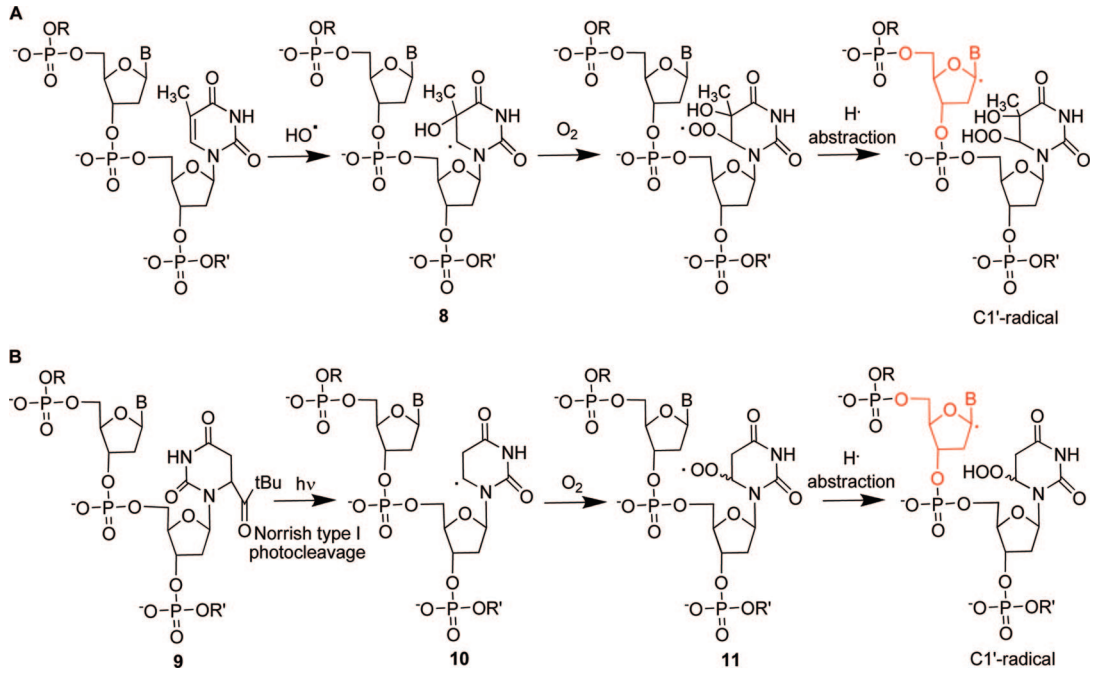

Figure 8. Tandem reactions producing C1′-radical from a C6-radical on pyrimidine. The first radical can be generated by (A) HO• or (B) photocleavage of butylketone precursor. Alkylketone (**9**) and phenylselenide groups are usually chosen to induce, by photocleavage, a carbon radical at specific positions on DNA models.[50,52,53] The proposed mechanism of the HO• reaction is illustrated in the case of thymine. The C1′-radical is shown in red.

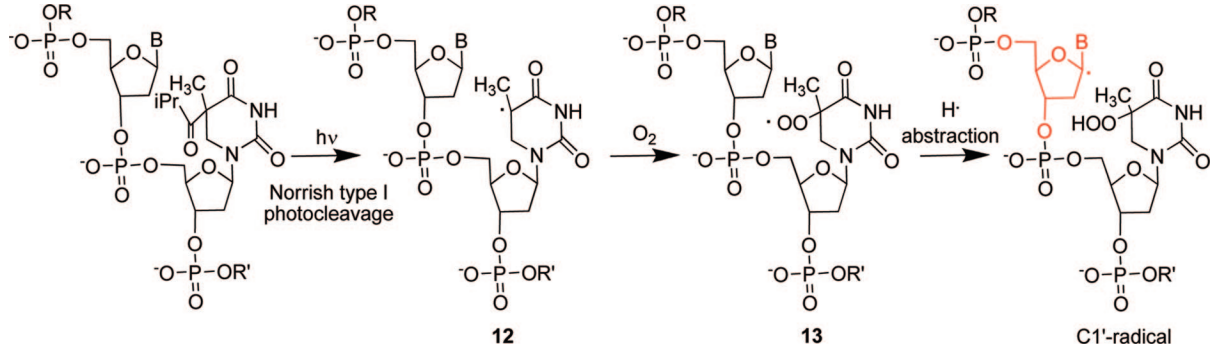

Figure 9. Tandem reactions producing C1′-radical from a C5-radical on pyrimidine. Reaction observed on single-stranded DNA models. The C1′-radical is shown in red.

or cytosine.[87] Figure 8A summarizes this mechanistic pathway.[88] Model **10** of this C6-radical can be produced from pyrimidine analogues **9** by Norrish type I photocleavage of aketylated precursors introduced in oligodeoxyribonucleotidic sequences (Figure 8B). They have been used to establish the proposed mechanism. When generated in the presence of O_2, a diastereomeric mixture of peroxy radical **11** is obtained that can selectively abstract H• at the 1′-position of the 5′-adjacent nucleoside. This was confirmed by the detection of deoxyribonolactone abasic site **3**[84,89] and kinetic isotope effects.[90] Molecular modeling demonstrates that the above observations may be rationalized on the basis of duplex DNA secondary structure. Indeed, the C1′-hydrogen atom is less than 2.5 Å away from the terminal 6R-peroxy oxygen atom when the radical nucleoside is in anti-conformation.[91]

Because the addition of HO• is also possible to the C6 of pyrimidine nucleobases leading to a radical at C5, the radical **12** at C5 (Figure 9) has also been prepared and included in single-stranded ODNs.[90] Dioxygen-dependent direct and alkali-induced strand breaks were observed at the nucleoside located on the 5′-side of the thymidyl radical. A mechanism involving the removal of H• at C1′ by the peroxy radical **13**, derived from O_2 attack on **12**, has been proposed on the basis of significant primary kinetic isotope effects. Interestingly, 5-halouracyl generates also C5-radical when irradiated.[72] In this case, C1′-oxidation is in competition with C2′-oxidation.

3.2. H2′-Abstraction

Hydrogen atom abstraction from the C2′-position of deoxyribose in DNA-damage processes is uncommon. The C2′-position is disfavored on the basis of the relatively high bond strength.[61] To date, no metal complex has been reported to selectively perform this type of oxidation. However, an oxidized abasic site resulting from C2′-oxidation was observed on DNA after γ-irradiation (generation of HO•).[92] The same product has been obtained after photolysis of DNA containing 5-halopyrimidine.[72,93] In another case, a kinetic isotope effect was observed at the C2′-position of selectively deuterated DNA cleavage by Fe^{II}(EDTA)/H_2O_2/ascorbate.[49] Detailed mechanistic data obtained with single- or double-stranded DNA containing 5-bromo- or 5-iodo-uridine **14** are proposed here (Figure 10). C2′-oxidations might arise only from tandem modifications of DNA (the first events being a nucleobase oxidation).

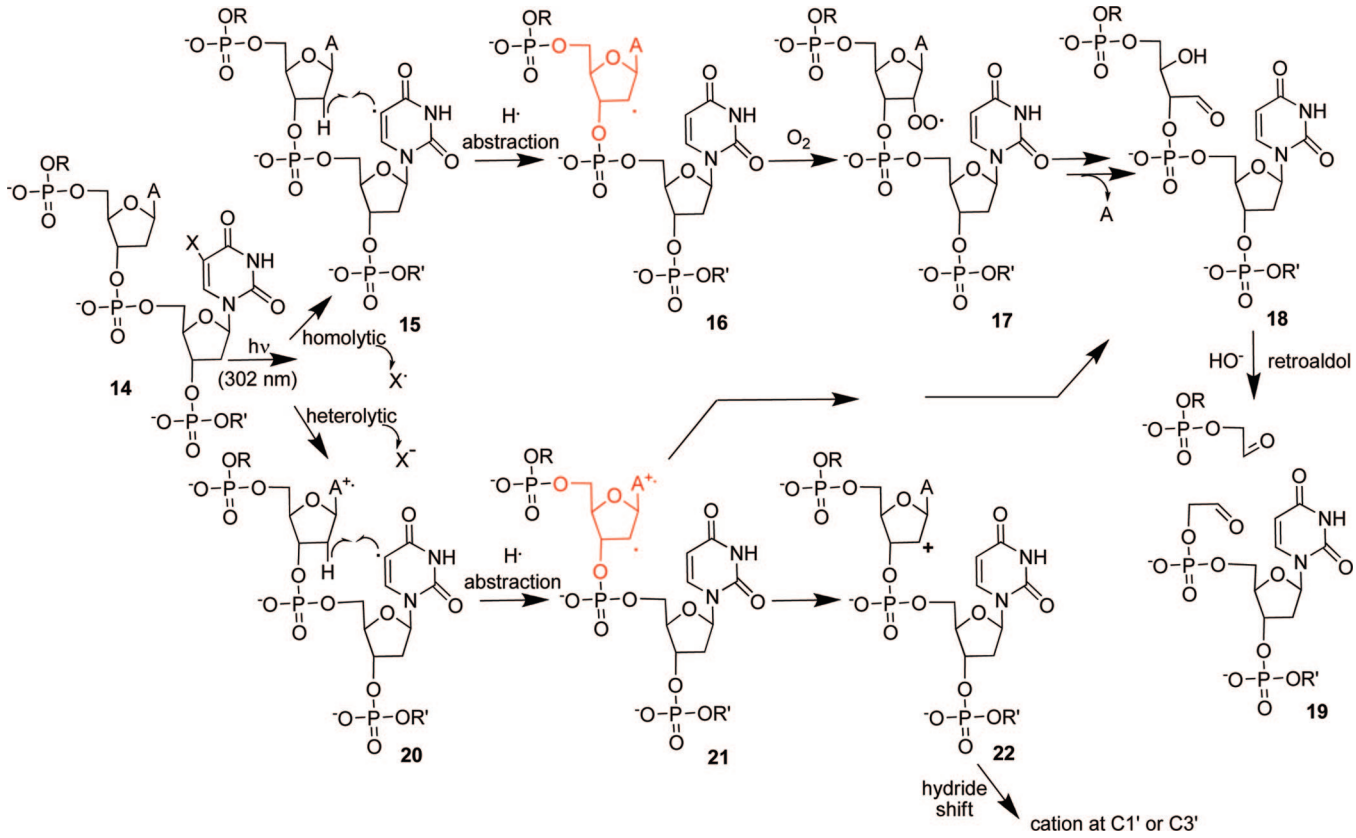

Figure 10. C2′-oxidation observed on B-DNA including a halopyrimidine. Mechanism pathways are proposed with dA at the 5′-position of the halogenated nucleotide. The C2′-radical is shown in red.

5-Bromodeoxyuridine ($d^{Br}U$) mimics thymidine in size and hydrogen-bonding ability, but it is photoreactive. 5-Iododeoxyuridine ($d^{I}U$) shows the same type of reactivity. Irradiation at 302 nm leads to homolytic or heterolytic cleavage of the C5−halogen bond producing a C5-radical **15** and **20**, respectively.[15,94,95] It is associated with the release of $I^{\bullet}$ or $Br^{\bullet}$ in the case of a homolytic cleavage. Heterolytic cleavage is favored for 5-bromodeoxyuridine. It is due to a photoinduced single electron transfer that releases I^- or Br^- and forms a radical cation **20** on the nucleobase on the 5′-side of the halo-uridine.[96] The use of 5-bromodeoxyuridine necessitates the presence of an adenosine on the 5′-side (5′-dA-$d^{Br}U$-3′ sequence). It has been proposed to be due to the involvement of the heterolytic cleavage pathway where a photoinduced electron transfer between adenine and ^{Br}U forms the 5′-$dA^{\bullet+}$-$^{Br}U^{\bullet-}$-3′ intermediate. Elimination of Br^- via heterolytic cleavage gives rise to intermediate **20** (Figure 10).[96,97] In the case of 5-iododeoxyuridine, homolytic cleavage is favored, the oxidative activity is observable for any nucleobase at the 5′-side, and the reaction is more efficient.[72,97]

Importantly, on B-DNA, the uracyl-5-yl radical competitively abstracts C1′- and C′2-hydrogen atoms of the adjacent deoxyribose moiety at the 5′-side. The C1′-oxidation event produces deoxyribonolactone abasic site **3** (Figure 7) as described in the previous paragraph. For the same DNA sequence, the percentage of C2′-oxidation, when compared to C1′-oxidation, is generally more significant when $d^{I}U$ and not $d^{Br}U$ is used. Isotope studies have shown that only H2″, located below the sugar plane, is abstracted.[95] C2′-oxidation is favored under aerated conditions, although the C1′-oxidation dominates under hypoxic conditions.[98]

Homolytic and heterolytic pathways lead to C2′-radicals **16** and **21**, respectively (Figure 10).

Addition of dioxygen to the C2′-radical **16** yields peroxy radical **17**, which may undergo homolytic or heterolytic cleavage to form an erythrose-containing abasic site **18** associated with nucleobase release. The presence of the abasic site **18** destabilizes the DNA-double helix because the T_m of a synthetic 12-mer duplex ODN containing the C2-abasic site **18** in the middle of one strand shows a decrease of ∼16 °C when compared to the unmodified analogue.[99] This abasic site **18** is more resistant to alkali than other DNA oxidized abasic sites, probably because it lacks a leaving group (phosphate) at the β-position of the aldehydic function. No direct DNA cleavage is observed. However, heating under alkaline conditions induces a retroaldol reaction at the abasic site. DNA cleavage results with fragments ending with phosphoglycaldehyde **19**.[72] The products containing aldehydic residues can be reduced with $NaBH_4$ and, when reaction is performed on ODN, can be identified by HPLC or by PAGE. Moreover, the aldehydic abasic site **18** is able to form Schiff bases with the NH_2 groups of proteins that may be correlated to the in vivo toxicity of this oxidized residue.[100,101]

Interestingly, for a dA−$d^{Br}U$ sequence in double-stranded DNA, the adenine radical cation **21** oxidizes the C2′-radical to C2′-cation **22**. In deaerated solutions, 1,2 hydride-shifts from C2′ to either C1′or C3′ have been observed. They give rise to either C1′-cation **2**, which is the precursor of deoxyribonolactone abasic site **3** (Figure 7), or C3′-DNA oxidation product consisting in fragment **23** with an unsaturated ketone on the 3′-end.[97,98] Fragment **23** may be formed as proposed in Figure 11 or through a C3′-cation as proposed in the next paragraph on C3′-DNA oxidation. These hydride shifts were confirmed by ^1H NMR on synthetic nucleosides selectively generating the C2′-radical.[98] The observation of

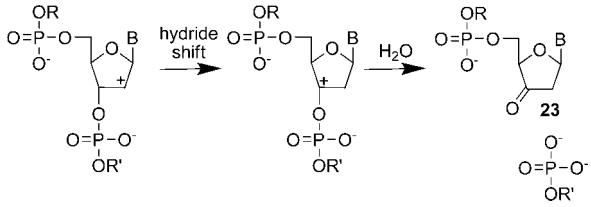

Figure 11. A proposed mechanism for the formation of 3′-ketoenolether fragment from a C2′-cation.

the C3′-oxidation product, from this mechanistic pathway, which does not involve O_2, was favored by hypoxic conditions. In these particular conditions, the addition of O_2 (to form **17** and **18**) is low, thus favoring the oxidation of C2′-radical to C2′-cation **22**.

Another mechanism has been proposed in the case of Z-DNA (Figure 12). Indeed, the irradiation of d(CGCG^{I}UGCG)/d(CXCACXCG), where ^{I}U is 5-iodouracil and X is 8-methylguanine allowing the duplex to adopt a Z-DNA conformation, gave stereospecific 2′-hydroxylation at the 5′ side of ^{I}U.[102] ODN **28** containing ribo-guanosine was formed. The use of stereospecifically deuteriated ODN allowed Kawai et al. to show that stereospecific H2′ abstraction by C5-radical **24** gives rise to C2′-radical **25**. Addition of dioxygen to **25** leads to C2′-peroxy radical **26**, which is reduced to C2′-peroxide **27** and to ribo-derivative **28**. In accordance with the proposed mechanism, the yield of **28** greatly increased upon addition of NaI known as a hydroperoxide reductant. Moreover, when the experiment was carried out under $^{18}O_2$ atmosphere, incorporation of ^{18}O atom into the C2′-hydroxylated derivative **28** was observed. This preferential hydroxylation of the Z-form of DNA has been associated with the structural features of the Z-form of DNA such as C3′-endo sugar puckering and alternative syn−anti conformation.[93] Digestion of the oxidized nucleotide **28** by RNase T1 to d(CGC)rG> (> = cyclic phosphate) confirms the reaction. Importantly, C2′-oxidation is favored on RNA due to the presence of the hydroxyl group on the ribose moiety.[103]

3.3. H3′ Abstraction

C3′-oxidation requires a metal complex able to selectively interact in the DNA major groove where the C3′−H bond is located. It has been reported with photoreactive agents such as $Rh^{III}(phen)_2(phi)$ and more easily with $Rh^{III}(phi)_2(bipy)$ that interact in the DNA major groove through intercalation of the 9,10-phenanthrenequinone (phi).[104] A similar mechanism has also been proposed in the case of $[Rh(en)_2phi]^{3+}$.[105] When irradiated near 310 nm, the rhodium complexes are believed to form a π cation radical via photoinduced ligand-to-metal charge transfer.[15,16,106] This radical can undergo H-atom abstraction at C3′ of deoxyribose.

After the action of the Rh-complex on a duplex ODN, cleavage fragments bearing a 3′-phosphoglycaldehyde-end **31** have been identified by PAGE. They do not migrate like 3′-phosphate-fragments, and their migration is different after $NaBH_4$ reduction (Figure 13). They were associated with the 5′-phosphate fragment and with the release of base propenoic acid **32**. Base propenoic acid **32** was detected by HPLC and GC−MS. Its reduction with $NaBH_4/AlCl_3$ yields base propenol. The formation of 3′-phosphoglycaldehyde-fragment **31** and base propenoic acid **32** is dioxygen dependent, according to a proposed mechanism involving the addition of O_2 to the C3′-radical **29** followed by a reduction step to yield a hydroperoxide **30** on the C3′. A Criegee-type rearrangement followed by the addition of a molecule of water leads to the release of 3′-phosphoglycaldehyde- (**31**), 5′-phosphate-fragments, and base propenoic acid **32**.[104] Interestingly, irradiation in the presence of glutathione of single-stranded ODN including a C3′-pivaloyl-3′-xylothymidine residue (a photoreactive precursor of the C3′-radical) produces also 3′-phosphoglycaldehyde-fragment **31**. This confirms the first part of this mechanism consisting of the generation of the C3′-radical **29**.[107] For the last steps of the reaction, the involvement of a Criegee-type rearrangement is only a proposal.

The 3′-phosphoglycaldehyde-fragment **31** can be considered as a selective product of C3′-oxidation of DNA. Indeed, if it is possible to observe it after C2′-oxidation as summarized in Figure 10, it is only after a particular treatment allowing retroaldol reaction. Fragment **31** is relatively stable to alkali because it is not destroyed by a 30 min at 90 °C heating step in 1 M aqueous piperidine,[104] while it is sensitive to more drastic alkaline conditions such as NaOH 0.66 M, 40 °C, 1.5 h.[107] Nuclease P1 digestion of the 3′-phospho-

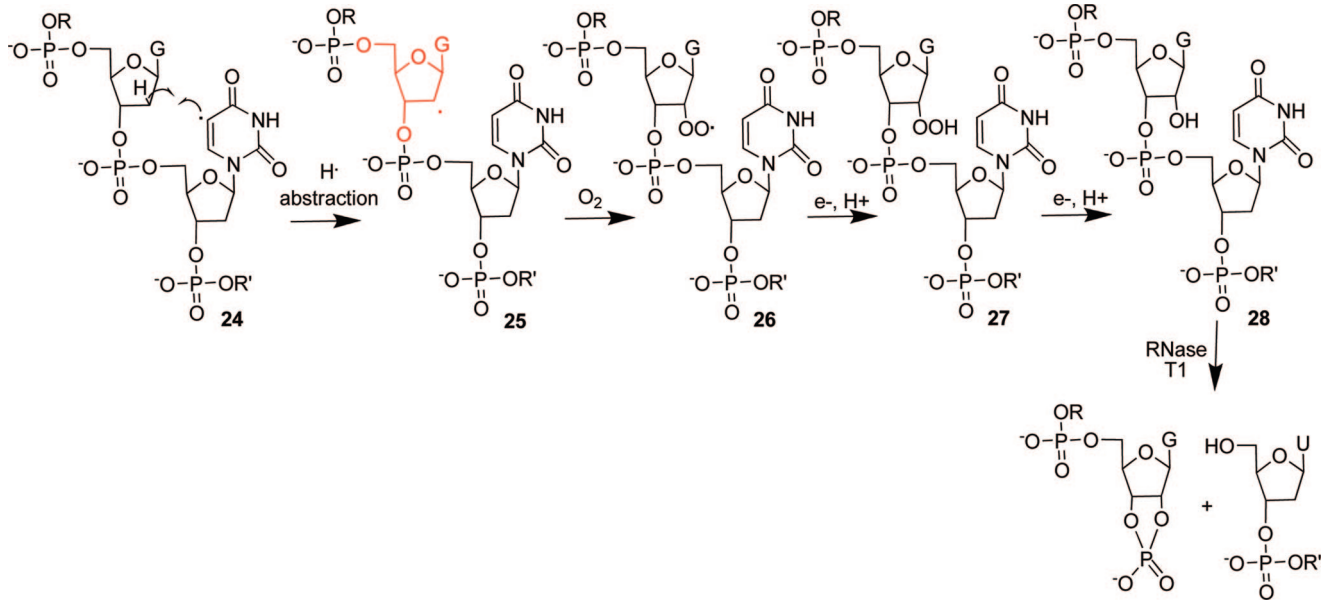

Figure 12. Proposed reaction pathway of the C2′-radical in Z-DNA. The C2′-radical is shown in red.

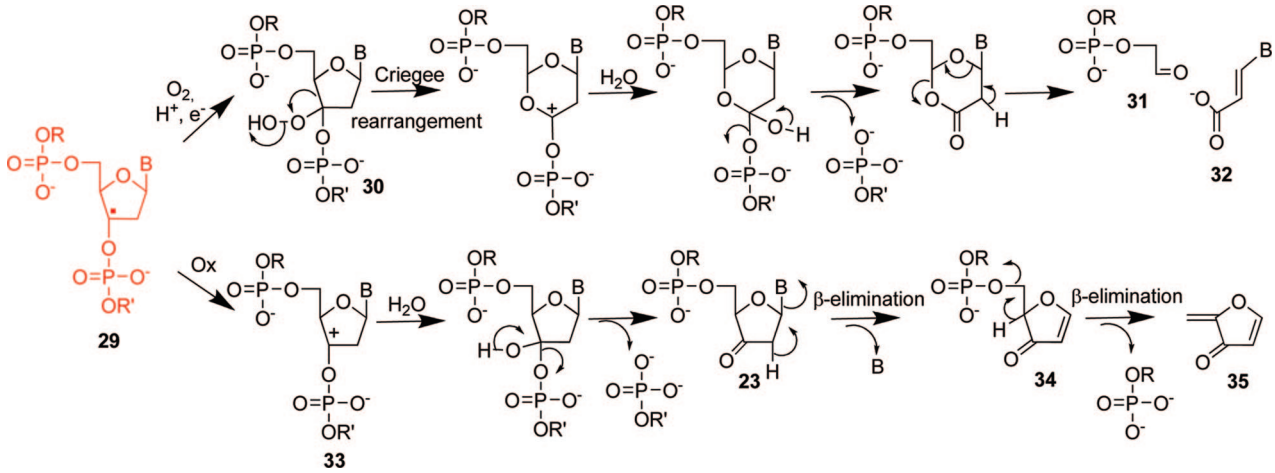

Figure 13. Possible reaction pathways of the C3′-radical. The C3′-radical is shown in red.

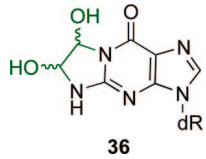

36

Figure 14. Addition of glyoxal to dG (glyoxal shown in green).

glycaldehyde-fragment **31** releases 3′-phosphoglycaldehyde. This last compound forms a stable oxime with pentafluorobenzylhydroxylamide. This oxime is detected by GC−MS after a silylization step.[108] It has been proposed that 3′-phosphoglycaldehyde-fragment **31** could release glyoxal after a phosphate−phosphonate rearrangement as observed on the phosphoglycaldehyde model.[109] This glyoxal can form diastereomeric 1,*N*2-glyoxal adducts **36** to guanines of DNA (Figure 14). This reactivity could explain the detection of glyoxal adducts to dG when DNA is oxidized with the Fe^{II}(EDTA) complex.[110] However, kinetic isotope effect measurement for duplex DNA cleavage by the Fe^{II}(EDTA)/H_2O_2/ascorbate system (production of HO•) suggests that hydrogen abstraction from this C3′-position with the non-selective diffusible oxidizing species HO• is a minor contribution to strand-break formation in B-form duplex DNA by HO•. This is probably due to the poor accessibility of this DNA position to solvent.[49]

A second mechanism has been proposed to explain the non-oxygen-dependent formation of 3′- and 5′-phosphate fragments and nucleobase release by the Rh-complexes (Figure 13).[14,104] In this anaerobic pathway, the oxidation of the C3′-radical **29** produces C3′-cation **33**. Addition of H_2O induces a strand break associated with the release of a 5′-phosphate fragment and a poorly stable 3′-keto-2′-deoxyribonucleoside-fragment **23**. A first β-elimination involving hydrogen at C2′ induces nucleobase release and the formation of a 3′-ketoenolether fragment **34**. A second β-elimination yields 3′-phosphate fragment and a putative 2-methylene-3′(2H)-furanone **35**. The 3′-keto-2′-deoxyribonucleoside-fragment **23** has been identified by HPLC and mass spectrometry after irradiation of photoreactive single-stranded ODNs containing precursors of C3′-radicals.[107,111] The 3′-ketoenolether fragment **34** was also observed and was associated with the decomposition of the previous fragment **23**.[107] The 3′-ketoenolether fragment **34** is reduced by $NaBH_4$ to a stable DNA fragment that has been characterized by PAGE. Besides, fragments **23** and **34** have been observed in experiments involving duplex DNA containing 5-bromouridine, and they have also been proposed to be generated from C2′-oxidation events and hydride transfer.[97]

Both aerobic and anaerobic mechanisms involving C3′-radical **29** induce direct strand cleavage on DNA. Because of the special organization of B-DNA duplex, when DNA cleavage is performed by a major-groove binder in the case of sequence selective cleavage, a 5′-shift between the cleavage sites on both strands of DNA is observed. On the opposite, a 3′-shift is due to minor groove binders that oxidize C1′-, C4′-, or C5′-carbons in the minor groove.[104,112]

Furthermore, 3′-phosphoglycolate **37** and 5′-aldehyde fragments **38** have also been characterized during the analysis of the degradation of C3′-radical selectively generated by irradiation of a C3′-pivaloyl-3′-xylothymidine precursor included in single-stranded ODNs (Figure 15). They are typical products of the oxidation of C4′ and C5′, respectively. Two orientations of attack of O_2 at the prochiral C3′-radical **29** to produce a C3′-peroxy radical were proposed to explain the formation of these unexpected fragments.[107] In the first orientation, the C3′-peroxy radical abstracts H• from the C4′ of the same nucleotide to yield **37**. In the other orientation, the C3′-peroxy radical abstracts H• from the C5′ of the next downstream nucleoside to yield **38**. This type of reactivity necessitates a proper spatial orientation of the involved substituents. It might not be possible on more constrained duplex DNA.

3.4. H4′-Abstraction

The observation of 3′-phosphoglycolate fragments **37**, migrating faster than the corresponding 3′-phosphate fragments, is frequent during the analysis of DNA-oxidation products by PAGE. It is a marker of C4′-oxidation of deoxyribose.[14−16,50,51,55] This C4′-oxidation can be observed with many agents able to abstract a hydrogen atom on deoxyribose and is particularly well documented in the case of iron bleomycin, $Cu(phen)_2$, Fe(EDTA), or γ-irradiation (the two last conditions generating HO•). Dioxygen is always involved in the formation of fragment **37**. Different chemical pathways have been proposed to account for the formation of **37**.

In the case of DNA oxidation by iron bleomycin, phosphoglycolate fragments **37** are always associated with the release of base propenals **45**. Kinetic isotope effects are in accordance with the abstraction of H4′-atom to produce C4′-radical **39** as the rate-determining step of the reaction. The origin of the oxygen atoms involved in the reaction was

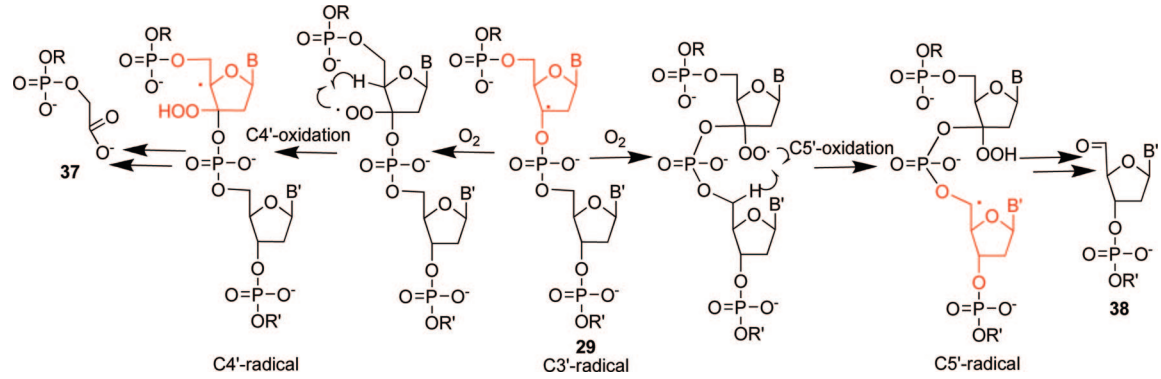

Figure 15. Tandem reaction from a C3′-radical: proposed mechanism for the formation of a secondary radical at C4′ or C5′.[107] The C3′-, C4′-, and C5′-radicals are shown in red.

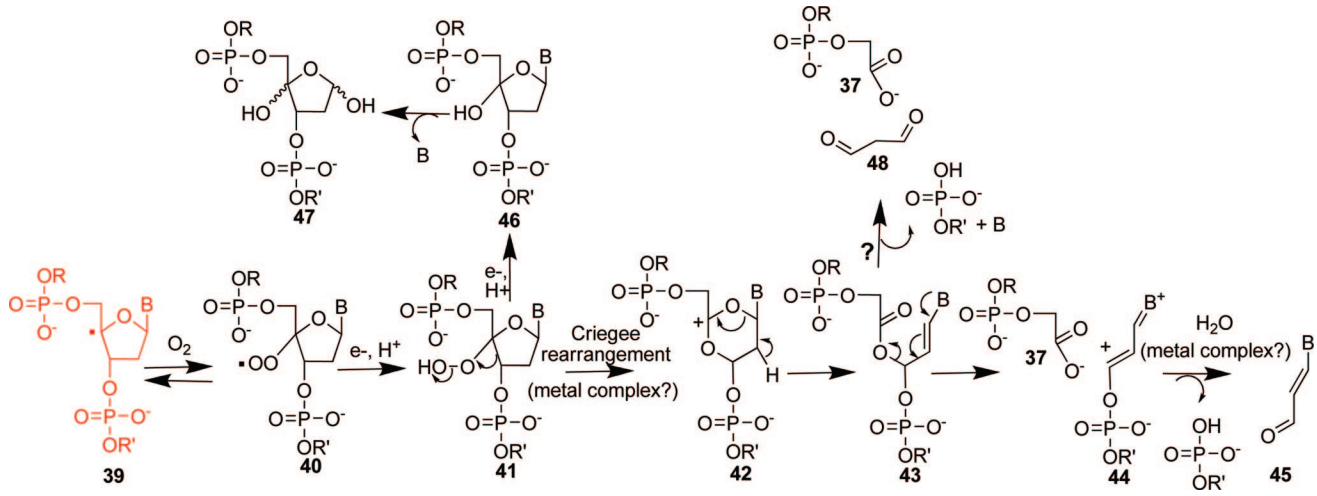

Figure 16. "Peroxide **41** reaction pathways" of the C4′-radical in the presence of dioxygen. The base propenal (**45**) route has been proposed from studies of DNA oxidation by iron bleomycin. The presence of question marks reflects that, for not well understood reasons, different metal complexes do not induce base propenal (**45**) release, although 3′-phosphoglycolate fragments (**37**) are clearly observed. It has been proposed that these last systems induce malondialdehyde (**48**) release instead of base propenal (**45**). The C4′-radical is shown in red.

determined from experiments with $H_2{}^{18}O$ or $^{18}O_2$. From kinetic measurements and labeling studies, a mechanism involving a C4′-hydroperoxide **41** (Figure 16) has been proposed to account for the following observations:[14–16,51,113,114] (i) strand breakage and C2′-hydrogen abstraction (specific 2′-*pro-R*-hydrogen H2″)[115,116] occur 1 order of magnitude faster than base propenal release;[116,117] (ii) one oxygen atom of the glycolate carboxyl group is derived from dioxygen, apparently the oxygen forming the C4′-hydroperoxide **41**, and the other one from the original deoxyribose-ring oxygen;[116,118] (iii) the oxygen atom of the aldehyde of base propenal **45** originates from the solvent (H_2O);[116] and (iv) the C3′ carbon−oxygen bond is broken during the release of the 5′-phosphate fragment.

In this mechanistic pathway,[15,16,55,113,114] the metal complex abstracts H4′-atom from deoxyribose to form an initial C4′-radical **39** that combines with dioxygen and produces the peroxy radical **40**, which is then reduced to hydroperoxide **41**. The hydroperoxide **41** undergoes a Criegee-type rearrangement resulting in oxygen insertion between the C4′ and C3′ carbons of the deoxyribose target and the formation of a C4′-cation **42**. Criegee-type rearrangement is generally an acid-catalyzed mechanism, but it has been proposed, in the case of iron bleomycin, that the metal complex may act as a Lewis acid.[15,113,114] Intermediate **42** promotes specific 2′-*pro-R*-proton elimination and C1′−O bond rupture, giving rise to a new intermediate **43**. Subsequently, DNA strand scission occurs with the release of a new DNA terminus bearing a 3′-phosphoglycolate moiety **37**. The remaining fragment **44**, connected to the new 5′-terminus formed at the site of strand-scission, is then hydrolyzed through the addition of water to the 3′-carbon, leading to the release of base propenal **45** and a new 5′-phosphorylated DNA terminus.

However, other mechanisms have also been proposed, particularly when the fate of the C4′-radical is independent of a metal complex.

One of these alternative pathways involves tetraoxide formation (Figure 17).[55,119] Peroxy radical **40** may react with another peroxy radical to form a tetraoxide, which decomposes homolytically to give a C4′-alkoxy radical **49** (Figure 18, path A). Intermediate **49** undergoes a β-cleavage of the C4′−C3′ bond to give a C3′-radical **50**. This radical is then trapped by O_2 to form intermediate **51**, which again bimolecularly forms a tetraoxide, and decays via a Russel fragmentation giving hemiketal **52** (Figure 18, path B). The later could decompose into dicarbonyl compound **53**. Further β-elimination leads to a 3′-phosphoglycolate **37** and base propenal **45**. Alternatively, von Sonntag et al. have proposed that **53** does not produce base propenal, but decomposes in 3′-phosphoglycolate **37**, nucleobase, and malondialdehyde **48**.[119] However, this "tetraoxide pathway" requires the proximity of two well-oriented peroxy radicals, both based presumably on DNA, and thus seems unlikely in the case of a poorly sequence-selective single-strand DNA breaker. On the other hand, this pathway may be favored with bimetallic

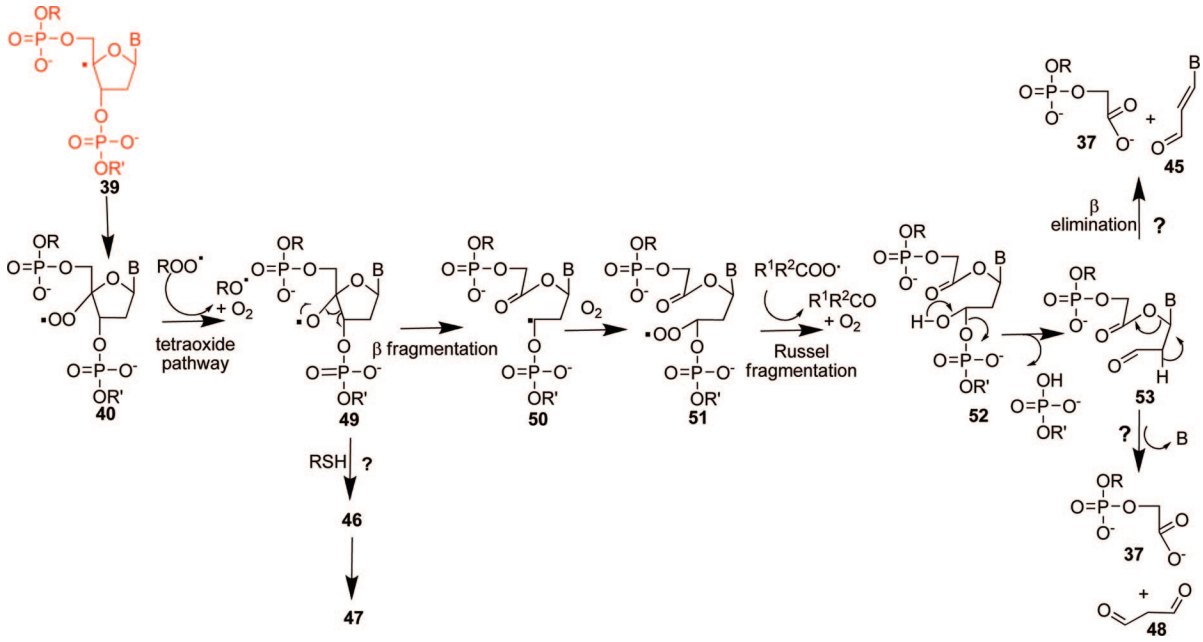

Figure 17. "Tetraoxide reaction pathway" of the C4′-radical in the presence of dioxygen. This reaction pathway was established in the case of DNA oxidation by neocarzinostatin or HO• generators and from the analysis of C4′-radical models. The presence of question marks reflects that, for not well understood reasons, different metal complexes do not induce base propenal (**45**) release, although 3′-phosphoglycolate fragments (**37**) are clearly observed. It has been proposed that these last systems induce malondialdehyde (**48**) release instead of base propenal (**45**). The C4′-radical is shown in red.

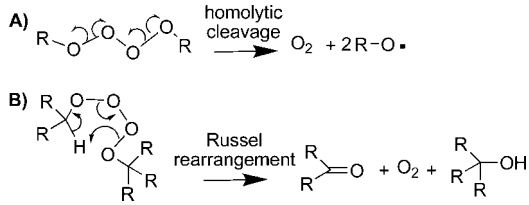

Figure 18. Tetraoxide cleavage pathways.

complexes: each metal center may provide a radical center on a DNA sugar. These radicals might react through the tetraoxide pathway if they are well oriented. This later case has not been described up to now for metal complexes, but it was proposed in the case of double-strand cleavage of DNA by enediynes.[51]

A third proposed reaction pathway for the formation of phosphoglycolate **37** involves a heterolytic cleavage of the C4′-radical **39** (Figure 19). In this pathway, the C4′-radical **39** breaks the secondary C−O bond of the phosphate linkage at the 3′-position in a heterolytic reaction. This releases a 5′-phosphorylated DNA fragment and a radical cation **54** where both charge and radical are stabilized by the oxygen lone pair. This radical cation reacts with H_2O to generate a new C4′ DNA-radical **55**, which forms a hydroperoxide **56** by reaction with O_2. Hydroperoxide **56** then undergoes a Grob fragmentation (base-catalyzed) that generates the dicarbonyl compound **53** (this intermediate **53** is also proposed to be formed in the tetraoxide pathway, Figure 17). Finally, a subsequent β-elimination leads to the 3′-phosphoglycolate fragment **37** and the base propenal **45**.[120,121]

Giese et al. have selectively generated C4′-radicals **39** on ODNs. They have shown that **39** can be transformed into hydroperoxides **41** and **56** that have been characterized by MALDI-MS.[121] An analogue of the peroxy radical **40** was also observed by EPR on mononucleoside.[120] Compounds **41** and **56**, or their precursors, can lead to 3′-phosphoglycolate fragments **37**.[120,121] The outcome of the C4′-radical **39** through the pathway involving the C4′-hydroperoxide **41** (Figure 16) or the heterolytic cleavage of this C4′-radical **39** (Figure 19) has been correlated to its accessibility to intermolecular reaction. A good accessibility favors the "hydroperoxide **41** pathway".[121] O_2 concentration is another significant parameter: a poorly oxygenated medium favors the "heterolytic cleavage pathway", while high concentration of O_2 favors the "C4′-hydroperoxide **41** pathway".[122] Kinetic constants were measured with these models. Experiments were conducted in the presence of glutathione as a source of electrons and hydrogen. Heterolytic cleavage of the C4′-radical **39** gives rise to 5′-phosphate fragment and radical-cation **54** (Figure 19). For this unimolecular process, a rate constant of $\sim 10^3$ s^{-1} was measured for a single-stranded ODN. The reaction was about 10 times slower in the case of duplex DNA.[123] In the presence of O_2, the C4′-radical **39** is trapped rapidly (2×10^9 M^{-1} s^{-1}) to give peroxy radical **40**. However, this reaction is reversible. The rate constant of dioxygen release from single-stranded DNA C4′-peroxy radical is 1.0 s^{-1} at ambient temperature. Peroxy radical **40** abstracts hydrogen atom from glutathione with a rate constant of 1.6×10^6 M^{-1} s^{-1} to produce the hydroperoxide **41**. Therefore, in these model reactions, performed without any metal complex, the strand cleavage mechanism depends on the concentration of the hydrogen donor. At low concentration of glutathione, the "heterolytic cleavage pathway" is favored even under aerobic conditions. The result of this analysis is that for 250 μM O_2 and 0.1 mM of glutathione, which are classical concentrations to study DNA cleavage with metal complexes, the pathways involving the C4′-peroxide **41** and the heterolytic cleavage forming **56** can be in competition (except if the metal complex favors one pathway). Other data obtained on these models concern the reduction of the C4′-radical **39** by glutathione (a rate constant of 1.9×10^6 M^{-1} s^{-1} was determined) to give predominantly the natural 2′-deoxyribonucleotide in the case of duplex

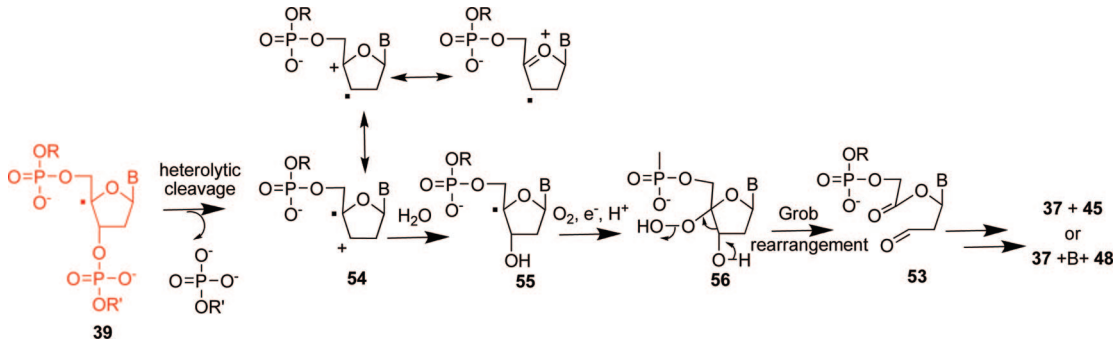

Figure 19. "Heterolytic cleavage reaction pathways" of the C4′-radical in the presence of dioxygen. This reaction pathway was established in the case of DNA oxidation by HO• generators and from the analysis of C4′-radical models. The C4′-radical is shown in red.

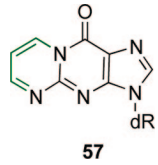

Figure 20. Addition of malondialdehyde adduct to dG (M1dG) (adduct is shown in green).

DNA, although a single-stranded ODN reacts in an unselective way.[54,123]

All of these proposed pathways give 5′-phosphate- and 3′-phosphoglycolate-fragments. 2D-NMR study and molecular modeling have been performed on duplex ODNs containing these two lesions, mimicking C4′-oxidation in the middle of the sequence.[124] The studies revealed that the lesioned DNAs were in B-form and that the 3′-phosphoglycolate and 5′-phosphate were extra-helical. The base opposite the gap and the base pairs adjacent to the gap remained well stacked in the DNA duplex.

Alternatively, although base propenals **45** are easily observable by HPLC when DNA is oxidized by iron bleomycin, they have not been observed in the case of DNA oxidations by $Cu(phen)_2$ or Fe(EDTA) that induce also the formation of 3′-phosphoglycolate fragments **37**. For $Cu(phen)_2$, Sigman et al. failed to trap them or malondialdehyde **48** (their hydrolysis product) with thiobarbituric acid or $NaBH_4$, dimedone, hydroxylamine, or carbodiimide.[125] An explanation could be that base propenal **45**, known to be reactive, and in particular sensitive to thiols,[126] decomposed in the reaction medium. On another hand, Cu(3-Clip-Phen), which is similar to $Cu(phen)_2$, generates "malondialdehyde-like" products, which react characteristically with thiobarbituric acid, but does not produce any base propenal, although the later are stable under the used experimental conditions.[127] In the same way, base propenal **45** has not been detected upon the attack of HO• on DNA[119] (γ-irradiation or $Fe^{II}(EDTA)/O_2$) even though malondialdehyde **48** has been observed.[128] To explain the production of base propenal **45** in the case of DNA oxidation by iron bleomycin, von Sonntag has proposed that after the formation of the C4′-radical, the metal complex stays on DNA and participates in the following steps of the reaction.[50,119] Importantly, base propenal−nucleobase adducts can form, in particular with guanine. Pyrimido[1,2-α]purin-10-(3H)-one adduct **57**, Figure 20, often referred to as M1dG, is the most frequent. Malondialdehyde **48** is less efficient to form the same adduct that is toxic for cells.[128] It has also been suggested that base propenal **45** or malondialdehyde **48** are involved in the formation of DNA−DNA and DNA−protein cross-links.[129]

Furthermore, the C4′-hydroperoxide **41** can be reduced to the C4′-hydroxyl intermediate **46** (Figure 16). A reduction of the C4′-alkoxy radical **49** by thiols seems also reasonable and could lead to the same intermediate **46** (Figure 17). The subsequent elimination of the nucleobase yields C4′-oxidized abasic site **47** containing a 2-deoxypentos-4-ulose residue (that may be in equilibrium between an open and a closed form).[51,130] However, compound **47** is more generally proposed to originate from the C4′-radical **39** in the absence of O_2 (Figure 21). When DNA was oxidized by Fe(BLM), it was demonstrated that the oxygen atom incorporated at C4′ of **47** originated from water,[131] allowing the proposal that the C4′-radical **39** was oxidized to a C4′-carbonium ion **58**, which produces the C4′-hydroxylated intermediate **46** (then **47**) upon addition of H_2O. The C4′-oxidized abasic site **47** is unstable with a half-life of 8−26 h at pH 7 on duplex ODNs.[132,133] It is an alkali-labile lesion. Therefore, in the presence of base, a β-elimination step releases a 5′-phosphate fragment and a 4′-ketodeoxyribose fragment **59**, which reacts again with alkali to produce 3′-phosphate fragment (Figure 21). Importantly, when NaOH was used, fragments 3′-terminated by a 3-hydroxy-5-oxo-1-cyclopenten-1-yl can be obtained by rearrangement of the 4′-ketodeoxyribose fragment **59**.[134,135] The C4′-oxidized abasic site **47** or the 4′-ketodeoxyribose fragment **59** can be trapped as stable alcohols by reduction with $NaBH_4$. A reaction with hydrazine produces another stable and characteristic fragment 4′-terminated by a typical 3-pyridazinylmethyl residue.[136] The NMR analysis of a duplex ODN including the C4′-oxidized abasic site **47** showed only the α-anomer of the cyclic form, and the structure of the duplex was globally in B-form with the base opposite the abasic site intrahelical.[137] The C4′-oxidized abasic site **47** destabilizes the DNA double-helix with respect to the unmodified sequence. A decrease of 17 °C has been observed for the T_m of a 12-base pairs duplex where the modification was included in the middle of the sequence.[133] Interestingly, the 4′-ketodeoxyribose fragment **59** can form 6-(2-deoxy-β-D-erythro-pentafuranosyl)-2-hydro-3(3-hydro-2-oxopropyl)2,6-dihydroimidazo[1.2,*c*]-pyrimidin-5(^{3}H)-one adducts **60** on proximate cytosine base (Figure 22).[138]

When B-DNA is oxidized by HO• (generated by γ-radiation) yet in the absence of O_2, other DNA oxidation products are observed: 2,5-dideoxypentose **64**, 2,3-dideoxypentose-5′-phosphato DNA fragment **68**, 2-deoxypentos-4-ulose **63**, 2-deoxypentos-4-ulose-3′/5′-phosphato DNA fragments **67** and **72**, and, as minor products, 2,3-dideoxypentose **70** and 2,5-dideoxypentose-3′-phosphato DNA fragment **71**.[139,140] They can be explained by mechanistic pathways proposed in Figure 23, and they might be observed when metal

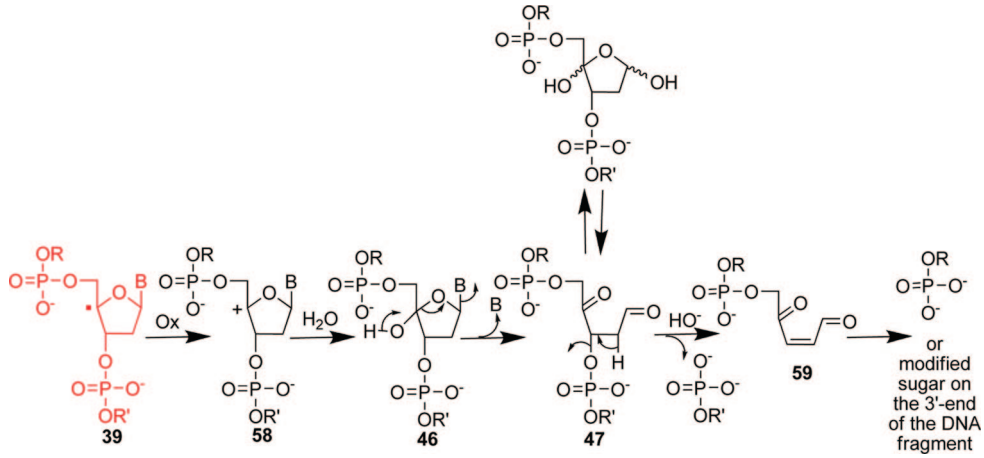

Figure 21. Possible reaction pathways of the C4′-radical in the absence of dioxygen. The C4′-radical is shown in red.

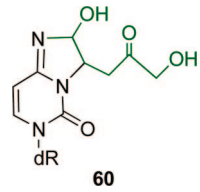

60

Figure 22. Addition of 4-ketodeoxyribose to dC (adduct is shown in green).

complexes are able to generate only a species able to remove H• from the DNA-deoxyribose. A strand cleavage occurs through the heterolytic cleavage of the neighboring phosphate group of the C4′-radical **39**. Cleavage at C3′ giving **54** (major pathway, Figure 23) strongly dominates over cleavage at C5′ giving **69** (minor pathway, Figure 23). Description of the major pathway of Figure 23 is as follows. Radical cation **54** reacts with H_2O (preferential addition at C3′) leading to a new neutral radical **61** that can be reduced to **65**. The secondary C4′-radical **61** can either be oxidized in **66** (giving **67**) or eliminate the second phosphate group to give **62**. A second set of analogous reactions leads from **62** to **63** and **64**. Similar processes apply to the minor pathway in Figure 23.

When Giese's group generated C4′-radical **39** by photoirradiation of modified single-stranded ODNs in the presence of reductant (glutathione) but in the absence of O_2, the C4′-oxidized abasic site **47** (Figure 21) was not observed. Strand cleavage occurred.[120] This cleavage led to 5′- and 3′-

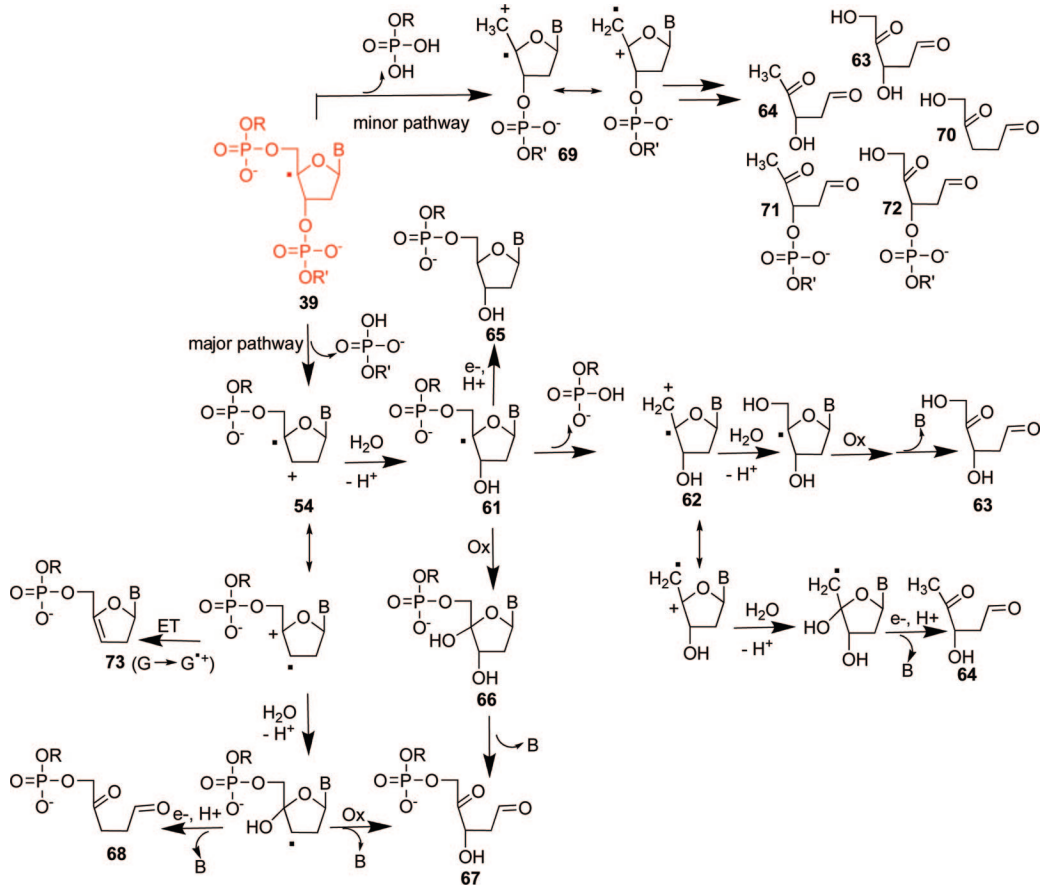

Figure 23. Possible reaction pathways of the C4′-radical in DNA in the absence of dioxygen proposed for DNA oxidation by the HO• diffusible species. Only the major pathway is described. The C4′-radical is shown in red. ET stands for electron transfer.

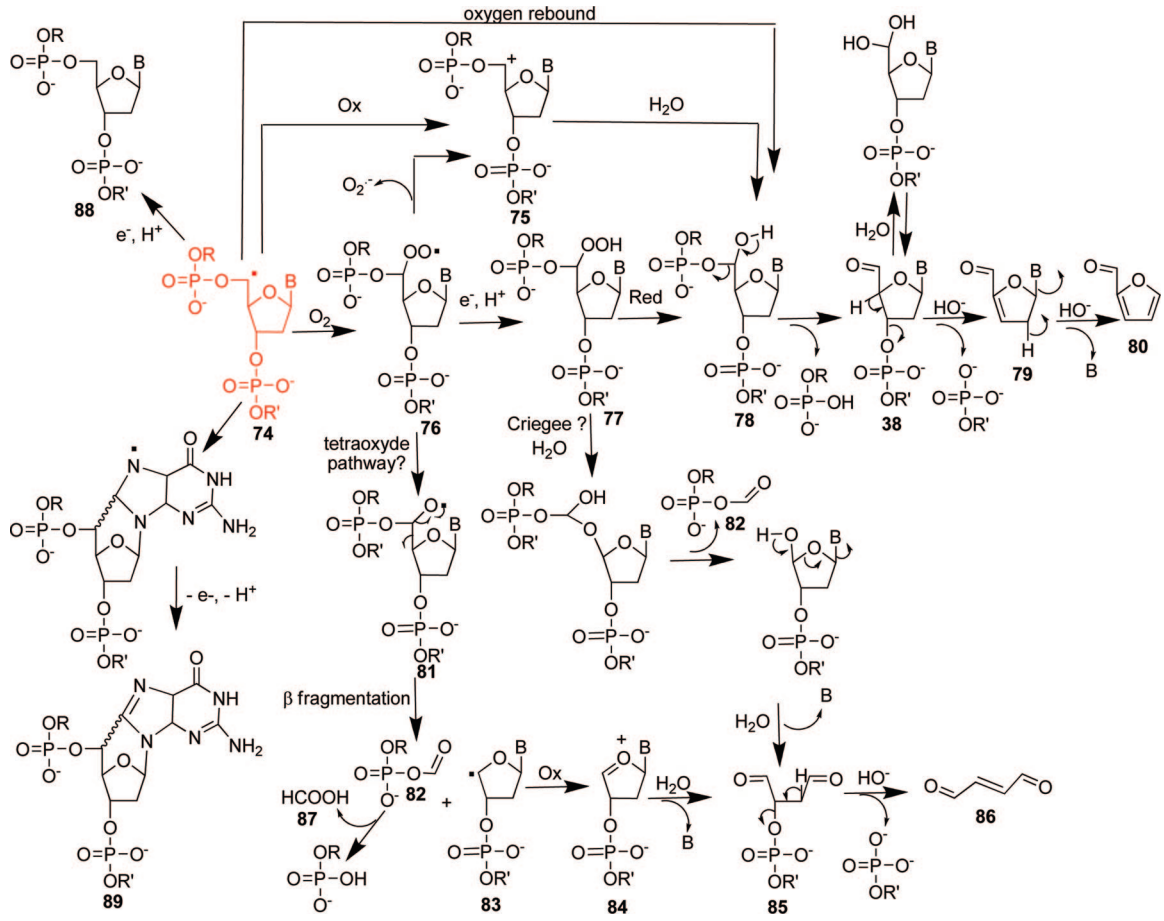

Figure 24. Possible reaction pathways of the C5′-radical.

phosphate fragments associated with the loss of the modified nucleoside but also to fragments including a deoxyribonucleotide **65** at the 3′-end. Compound **65** was due to the reduction of intermediate **54** by glutathione. However, when single- or double-stranded ODNs contained a neighboring guanine, the C4′-radical **39** was shown to be reduced to fragment **73** including an enolether at the 3′-end. This reaction probably resulted from an electron transfer from guanine (the more oxidizable nucleobase) to the radical cation **54**.[141,142]

3.5. H5′-Abstraction

The C5′-hydrogens are the most accessible on B-DNA. This is why the Fe^{II}(EDTA)/H_2O_2/ascorbate system (that produces diffusible HO•) preferentially oxidizes C5′ site as observed with selectively deuterated DNA-deoxyriboses.[49] In addition, this site of oxidation has also been well characterized with other metal complexes that do not seem to produce diffusive oxidative species such as the Mn(TMPyP)/$KHSO_5$ system[17,143–146] or Cu(phen)$_2$ derivatives.[17,63,127] Enediyne derivatives also produce this type of oxidation with some sequence selectivity, and a part of the mechanisms that can be involved in this oxidation pathway has been first studied with these molecules, in particular with neocarzinostatin.[51,147] Additionally, HOO• (that can be produce by many metal complexes) seems also able to produce C5′-radicals on DNA.[148]

Typical products of the C5′-oxidation pathway are 5′-aldehyde-terminated DNA fragments (Figure 24). They are easily seen by PAGE after a 3′-end labeling of DNA. Their mobility is slower than the same-length 5′-phosphate fragments. With the Mn(TMPyP)/$KHSO_5$ system, they are probably obtained by the oxygen rebound reaction at the C5′-radical **74** to form a 5-hydroxyl-species **78** that spontaneously releases a 3′-phosphate and the 5′-aldehyde fragment **38**.[65,143,145,149] Same fragments are probably also formed by oxidation of the C5′-radical **74** to C5′-cation **75** followed by addition of a molecule of water as observed on C5′-radical of monodeoxyribonucleosides.[150] This oxidation can be catalyzed by metal complexes. Different metal salts have been tested on mononucleoside models. $K_3Fe(CN)_6$ was the most active (with a rate constant of $(4.2 \pm 0.4) \times 10^9$ M^{-1} s^{-1}), but the reaction has been proposed to be also possible with $FeCl_3$, $CuCl_2$, and CuCl by Chatgilialoglu et al.

The C5′-radical **74** may also react with dioxygen to form a C5′-peroxy radical **76** (rate constant 2×10^9 M^{-1} s^{-1}). It has been proposed that this radical loses $O_2^{\bullet -}$ to form the C5′-cation **75**.[150] However, the analysis of DNA oxidation by neocarzinostatin has shown that the C5′-peroxy radical **76** can be also reduced to the hydroperoxide **77** and into compound **78** to produce the 5′-aldehyde fragment **38**. In this later case, it has been demonstrated that the origin of the oxygen atom incorporated on the 5′-aldehyde residue **38** is from O_2 thanks to experiments performed in the presence of $NaBD_4$ to trap the aldehyde as a stable alcohol as soon as it was produced.[151] This precaution was necessary because the C5′-aldehyde **38** oxygen atom exchanges rapidly with water. It is generally observed as a hydrated form that prevents the determination of the origin of the C5′-aldehydic oxygen.[65,152]

The 5′-aldehyde-fragment **38** is relatively stable; this facilitates its characterization. A half-life of ~100 h at 37 °C (pH 7.2) has been estimated for its cleavage. The same

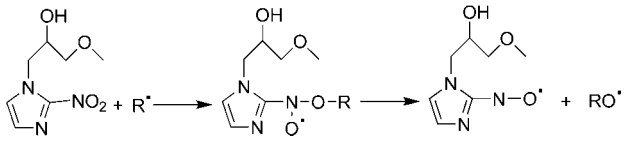

Figure 25. Formation of an alkoxy-radical with misonidazole.

cleavage can be also observed by heating under mild alkaline conditions.[153] An initial β-elimination releases a 5′-phosphate fragment and an unstable 5′-aldehyde-3′,4′-unsaturated nucleoside **79**. A second β-elimination gives rise to the nucleobase and furfural **80**. Furfural is easily detected by HPLC or mass spectrometry, and it is a marker of the C5′-oxidation. The 5′-aldehyde-3′,4′-unsaturated nucleoside **79** can be trapped by reduction with $NaBH_4$ as a 5′-hydroxyl-nucleoside. A subsequent hydrogenation with palladium on charcoal leads to a 2′,3′-dideoxyribonucleoside having the natural β-configuration at C4′ as confirmed by comparison with synthetic references.[154] The 5′-aldehyde-fragment **38** can also be reduced with $NaBH_4$ or oxidized in acid with alkaline NaOI.[155] It is also easily transformed into oxime ether by reaction with carboxymethoxylamine.[152] The oxidation of the aldehydic group of **38** to acid can be also performed by a metal complex such as the Mn(TMPyP)/$KHSO_5$ system.[145,149]

The C5′-peroxy radical **76** or the C5′-hydroperoxide **77** can react by a divergent way that does not lead to **38** but to 3′-formyl-phosphate- and 5′(2-phosphoryl-1,4-dioxobutane)-terminated DNA fragments **82** and **85**, respectively, and spontaneous release of nucleobase. Fragments **82** and **85** have been observed in the case of DNA oxidation by neocarzinostatin, although they accounted for very few materials as compared to the 5′-aldehyde fragment **38**. A Criegee-type rearrangement of the C5′-hydroperoxide **77** has been proposed to explain the formation of **82** and **85**,[156] but the fact that the divergent pathway is favored by misonidazole in the case of DNA oxidation by neocarzinostatin seems more in accordance with the formation of an oxy-radical **81** (Figure 25).[157] As discussed for C4′-DNA oxidation, a tetraoxide pathway might be involved. A β-fragmentation of the 5′-oxy-radical **81** may release the 3′-formyl-phosphate-terminated fragment **82** and a C4′-radical **83**. Further oxidation of **83** leads to intermediate **84**.[147,157] The trapping of **84** by a molecule of water releases the nucleobase and the 5′(2-phosphoryl-1,4-dioxobutane)-terminated fragment **85**.[55,158] The 3′-formyl-phosphate-fragment **82** spontaneously hydrolyzes to formic acid **87** and a 3′-phosphate-fragment. The 5′(2-phosphoryl-1,4-dioxobutane)-terminated fragment **85** is also unstable. Its half-life was estimated to be only 11 h at 37 °C (pH 7.2).[153] Indeed, a β-elimination step releases a 5′-phosphate-fragment and *trans*-1,4-dioxo-2-butene **86**.[159] However, the 5′(2-phosphoryl-1,4-dioxobutane)-terminated fragment **85** can be reduced by $NaBH_4$ to a stable 5′(1,2,4-trihydroxybutane)-terminated fragment.[156,159] The fragment **85** can also react with hydrazine, giving a 5′-phosphate-fragment and a typical pyridazine.[153,159] *trans*-1,4-Dioxo-2-butene **86** has been detected in the case of DNA oxidation by Fe^{II}(EDTA).[159] This compound **86** can form stable oxadiaazabicyclo(3.3.0)octaimine adducts **90** and **91** on dA and dC of DNA (Figure 26), respectively, that may be mutagenic.[160] Adducts **92** and **93** on dG have been also observed on nucleosides, but they have not been found on DNA. In another way, the formyl moiety of 3′-formylphosphate residues **82** has been proposed to acylate the *N*6-amino groups of lysine side chains of the chromatin.[161] Importantly, the 5′-aldehyde- and 5′-(2-phosphoryl-1,4-dioxobutane)-terminated fragments **38** and **85** can form adducts with Tris, an usual component of buffers.[152,153]

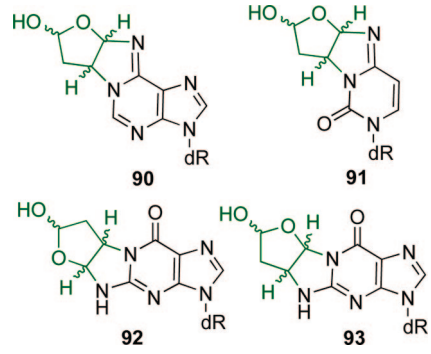

Figure 26. Addition of *trans*-dioxobutene to dA (**90**), dC (**91**), and dG (**92** and **93**) (adduct is shown in green).

Finally, the C5′-radical **74** can be reduced by thiols to give undamaged DNA **88** (Figure 24). This corresponds to a repair process. Rate constants for the reactions of the monomeric 2′-deoxyadenosin-5′-yl radical with cysteine and gluthatione in water have been determined to be $\sim 2 \times 10^7$ and 5×10^7 M^{-1} s^{-1} at 22 °C, respectively, but the value on duplex DNA is unknown.[150] In deaerated solution, the C5′-radical **74** may also add to the C8-position of a purine base on the same deoxyribose unit. This intramolecular cyclization followed by oxidation yields 8,5′-cyclo-2′-deoxyguanosine (cyclo-dG **89** shown in Figure 24) and 8,5′-cyclo-2′-deoxyadenosine (cyclo-dA) with both possible 5′*R*- and 5′*S*-diastereoisomers within DNA.[162] This reaction has been reported in the case of DNA oxidation by $HO^{\bullet}$ (generated by γ-irradiation). The yield of cyclopurine nucleoside was higher in single-stranded DNA as compared to double-stranded DNA. In double-stranded DNA, (5′*R*):(5′*S*) ratios of approximately 2 and 0.3 were reported for cyclo-dA and cyclo-dG, respectively.[163] This poor reactivity of the duplex DNA can be correlated to the fact that the attack of the C5′-centered radical at C8 of the purine nucleobase requires the base to rotate around the glycosidic bond into the syn conformation. When this occurs, it results in substantial perturbation of the DNA double-helix near the lesion for both *R*- and *S*-diastereoisomers.[164] A noticeable decrease in the melting temperature of 14-mer ODN duplex containing (5′-*S*)-cyclo-dA was observed when compared to the unmodified sequence ($\Delta T_m = 6$ °C).[165] On mononucleoside models, the rate constant for cyclization was estimated at 1.6×10^5 and $\sim 1 \times 10^5$ s^{-1} for cyclo-dA[166] and cyclo-dG,[167] respectively.

3.6. H-Abstraction from the Methyl Group of Thymine

Many metal complexes oxidize DNA nucleobases. Generally, the reactions do not involve $H^{\bullet}$ abstraction as a primary event. Therefore, they are out of the scope of the present Review. Information is available in excellent reviews.[50,87,168–170] An exception is the oxidation of the methyl group of DNA thymine, although it is important to first note that it is probably always a minor mechanism of DNA oxidation. It has been principally described in the case of metal complexes that produce $HO^{\bullet}$ through the Fenton reaction. Indeed, the hydroxyl radical is able to perform H-atom abstraction at the methyl group at C5 of thymine to produce 5-(2′-deoxyuridinyl)methyl radical **94** (Figure 27).[50,87] On the

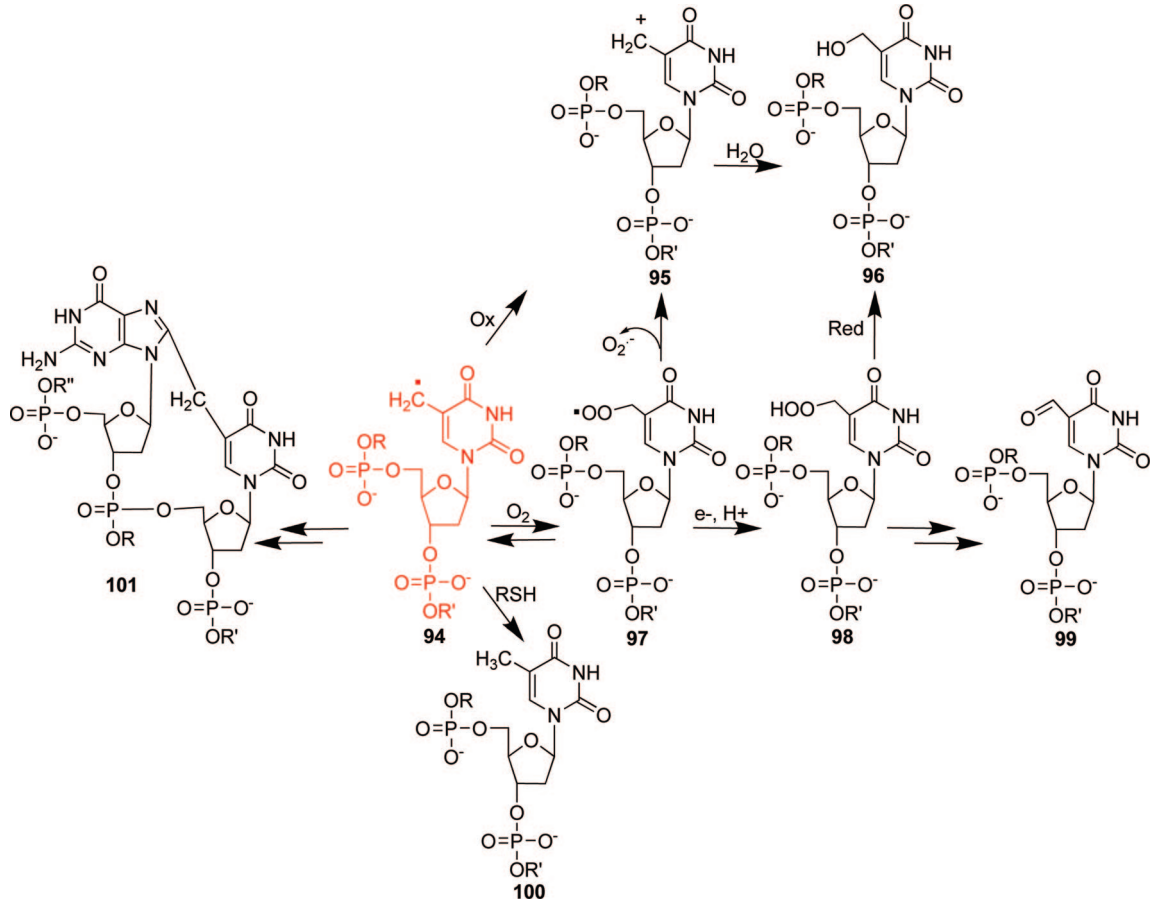

Figure 27. Possible reaction pathways of the methyl-radical of thymine. The radical on the methyl group of thymine is shown in red.

B-DNA duplex, the methyl group is accessible from the major groove.

In the absence of dioxygen, oxidation of radical **94** leads to cation **95**, which, after hydration, gives a 5-hydroxymethyluracyl residue **96** on DNA.[55,80,171] In aerated solution, it has been proposed that addition of O_2 to the radical **94** at a diffusion-controlled rate ($K = 2 \times 10^9$ M^{-1} s^{-1}) generates a peroxy radical **97**, reduced to hydroperoxide **98**. The later may decompose into 5-hydroxymethyluracyl- or 5-formyluracyl-residues **96** and **99**, respectively.[172] Importantly, metal ions and some metal complexes or metallo-proteins accelerate the degradation of the 5-hydroperoxymethyl-2′-deoxyuridine into 5-hydroxymethyluracyl or 5-formyluracyl.[173,174] These residues **96** and **99** pair with adenine in Watson−Crick geometry[175,176] with the OH-group of 5-hydroxymethyluracyl **96** laying on the 3′-side of the base plane.[177,178] Interestingly, the electron-withdrawing 5-substituent destabilizes the *N*-glycosidic bond and makes the 5-formyluracyl residue **99** highly susceptible to hydrolysis. Therefore, a heat treatment in alkaline conditions (0.1 M piperidine, 90 °C, 30 min) induces strand cleavage at this site.[179]

Kinetic parameters have been measured on monomeric 5-(2′-deoxyuridinyl)methyl radical independently generated from photochemical precursors.[180] It appeared that the trapping of O_2 was reversible ($k_{O2} = 3.4$ s^{-1}) and that the rate constant of the reduction of the peroxy radical to the peroxide was 2×10^2 M^{-1} s^{-1} when glutathione was used as reductant. The rate constant for reduction of peroxide **98** into 5-hydroxymethyluracyl or 5-formyluracyl was 0.08 s^{-1}. Reduction of the 5-(2′-deoxyuridinyl)methyl radical to thymidine occurred with a rate constant of 6.9×10^6 M^{-1} s^{-1} in the presence of glutathione.

The 5-(2′-deoxyuridinyl)methyl radical **94** can also add to the C8 of adjacent purine to produce G^T (**101**, Figure 27), T^G, A^T, or T^A tandem lesions after an oxidation step.[181,182] The reaction is predominant in the absence of dioxygen. G^T intrastrand cross-link with guanine located on the 5′-side of the oxidized thymine is favored. A theoretical study proposed that this is due to local geometric and tuning preference.[183] G^T has been observed when calf thymus DNA was oxidized by the $CuCl_2/H_2O_2$/ascorbate system in aerated solution. However, this lesion was approximately 3 orders of magnitude lower than the commonly observed single base-lesions (8-oxo-7,8-dihydro-2′-deoxyguanosine, 5-(hydroxymethyl)-2′-deoxyuridine, and 5-formyl-2′-deoxyuridine).[184] Because Cu(II) and Cu(I) salts form stable complexes with the *N*7 of guanine, the reaction could be facilitated during these experiments. The 5-methylcytosine residue is able to form similar adducts with guanine.[185]

Reaction of 5-(2′-deoxyuridinyl)methyl radical **94** with chromatin tyrosine has also been seen.[186] Interstrand cross-linking with the opposing 2′-deoxyadenosine has also been observed on synthetic duplex ODNs where the 5-(2′-deoxyuridinyl)methyl radical **94** was generated from photochemical precursor.[53,180,187,188] However, in this type of cross-linking, the thymine residue needs to be in a syn-configuration, which is considered as an unfavorable constraint in the case of classical B-DNA.

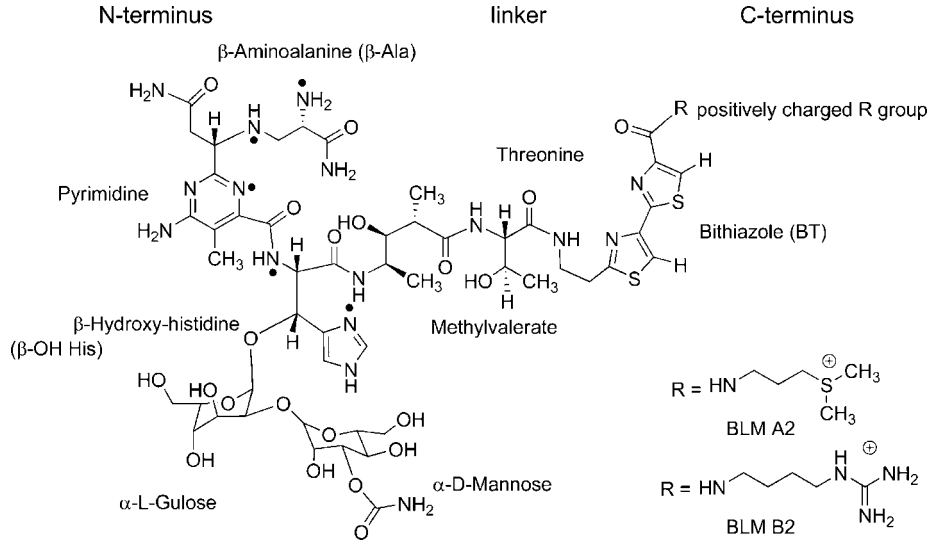

Figure 28. Bleomycin structure. Bleomycins differ by the R groups. The nitrogen atoms involved in metal chelation are indicated.

4. Examples of Metal Complexes as Chemical Nucleases

4.1. Fenton Chemistry and DNA Damage

Hydroxyl radical can be produced by Fenton chemistry, in which a transition metal complex delivers an electron to H_2O_2 (Figure 1). Many redox-active metal complexes are able to promote Fenton chemistry. Because DNA is sensitive to HO• radicals, redox-active metal complexes in the presence of O_2 or H_2O_2 are able to induce oxidative DNA damage. If the transition metal complex does not approach DNA closely enough, the only way by which DNA can be oxidatively damaged is through the attack of diffusing HO•, which is possible within a reasonable distance. In the absence of detailed studies ruling out the production of diffusing HO•, Fenton chemistry is the most probable mode of action of redox-active metal complexes with DNA. The efficiency of the Fenton reaction mediated by a metal complex toward DNA will be the result of the ratio between the ability to produce active oxidative species as compared to the protection against self-degradation. For the diffusible HO•, a critical point will be the distance at which the radicals are produced with respect to the nucleic acid target. Because the hydroxyl radical is an extremely reactive and nondiscriminating free radical, the sites of attack have no dependence on the base sequence of the nucleic acid and are multiple.

A common method for generating hydroxyl radical makes use of $[Fe^{II}(EDTA)]^{2-}$ and H_2O_2. Tullius et al. showed that Fe(EDTA) behaves in a manner identical to that of radiation-generated hydroxyl radicals.[189] The iron complex is able to promote oxidative DNA damage despite the fact that it is negatively charged and does not approach DNA. Therefore, the production of HO• at a certain distance from DNA does not preclude DNA damage provided the concentration of the metal complex is high and the complex is able to generate hydroxyl radicals with high yield. However, the covalent attachment of a Fenton reagent to a DNA binding entity drastically increases the efficiency of oxidative DNA damage and decreases the concentration of reagent at which DNA damage is observed.[190] Diffuse damage, but restricted to the vicinity of the site of interaction of the DNA interacting moiety, is the signature of HO• reaction in these cases.[191,192]

Hydroxyl radicals are able to abstract H• from a backbone sugar C−H bond and/or to react with the aromatic double bonds of nucleic acid bases.[50,87,168−170] Pulse radiolysis studies have indicated that 80−90% of the DNA damage is associated with nucleic acid bases, while 10−20% is associated with modified deoxyribose moieties. As detailed in this Review, sugar radicals lead either to oxidized DNA strands where the nucleic acid strand is not cleaved (but contains alkali-labile sites) or to direct DNA breaks. Most of the time, and for convenience, only direct DNA breaks are analyzed. The alkali-labile lesions can be cleaved with alkali (piperidine treatment), and also reagents such as hydrazine and *n*-butylamine.[135,193] Hydroxyl radical cleavage of DNA (or RNA) is a useful method for mapping nucleic acids structures or protein/DNA interactions because hydroxyl radicals react primarily at the most accessible regions of nucleic acids.[194,195]

Various experiments can be designed to determine the involvement of freely diffusing hydroxyl radicals during DNA oxidation. Catalase and superoxide dismutase avoid the production of H_2O_2, which is at the origin of hydroxyl radical by Fenton and Haber−Weiss chemistry. Hydroxyl radicals can be trapped by alcohols (ethanol, mannitol, glycerol), or by dimethylsulfoxide, or rhodamine B.

4.2. Iron−Bleomycin

The bleomycins (Figure 28) are a clinically useful family of natural glycopeptide antibiotics with antitumoral activity. They were isolated from *Streptomyces verticillus* more than 40 years ago.[196] The clinically administered form of the drug is predominantly composed of two forms, 60% BLM A_2 and 30% BLM B_2. The cytotoxicity of BLMs results from oxidative cleavage/damage of DNA in the presence of a redox-active metal ion cofactor (copper or most probably iron), O_2, and a reducing agent. The active species of the drug is a metal-centered oxidant, an oxygenated BLM, whose formation requires the binding of O_2 at a vacant coordination site on the metal. The oxidative degradation of DNA always involves C4′−H abstraction from deoxyribose units by the active species of the drug. The major site of DNA cleavage is the pyrimidine nucleoside of a 5′-GPyr-3′ sequence. DNA double-strand breaks, although formed in a much lower amount as compared to single-strand breaks, are considered as the most relevant cytotoxic damage of BLM.[197] However, oxidative RNA damage has been also implicated as a

potential target contributing to BLM cytotoxicity.[198,199] Additionally, BLM is able to mediate lipid peroxidation.[200]

The unique structure and properties of iron BLMs in mediating dioxygen activation and its remarkably efficient DNA degradation associated with its clinical use have attracted the interest of many laboratories.[14,113,114,197,198,201–206] Despite extensive studies over the past 40 years, fundamental aspects of BLM activity are still not completely clear including the nature of activated bleomycin, DNA binding and recognition, and the mechanism of double-strand breaks.

4.2.1. Structure of Metallo−Bleomycin

Although BLMs were isolated as Cu^{II} complexes, the clinically administered drug is the metal-free form. The nature of the in vivo metal cofactor, Fe^{II} or Cu^{I}, responsible for BLM's activity is difficult to know with certainty. Iron seems more likely.[201,207,208] The BLM−Cu^{II} and BLM−Fe^{III} complexes are highly stable with affinity constants at pH 7.0 such as $\log K = 18.1$ and 16, respectively.[201] On the other hand, the stability of the reduced forms of copper and iron BLM is lower than that of their oxidized forms. Cuprous ion binds weakly to BLM, and, from competition experiments, the affinity constant of BLM−Fe^{II} was found lower than that determined for BLM−Zn^{II} ($\log K = 9.7$). In blood, apo-BLM can rapidly transform into a stable BLM−Cu^{II} complex. BLM may enter the cells as a metal-free form or as a BLM−Cu^{II} complex. Inside cells, any iron or copper BLM complex will exist in the reduced state. Cysteine and glutathione readily reduce BLM−Fe^{III} into BLM−Fe^{II}, while the reduction of BLM−Cu^{II} into BLM−Cu^{I} is slower.[201,209]

Both metal complexes are able to mediate DNA single-strand breaks in vitro in the presence of O_2 and reductant with about the same efficiency and sometimes at different sequence sites.[209] The mechanism of DNA damage by copper BLM was not studied in detail as compared to iron BLM and will not be discussed in the present Review.

Although cobalt BLM is inactive as a cytotoxic agent, cobalt complexes of BLM proved particularly useful for structural studies, especially the BLM−Co^{III}−OOH form. Under aerobic conditions, BLM−Co^{II} transforms into BLM−Co^{III}−OOH and BLM−Co^{III}. These two species can be isolated separately. Both cobalt species are diamagnetic and can be examined in detail by NMR spectroscopy. The "green complex" BLM−Co^{III}−OOH is a stable analogue of activated BLM with a hydrogen peroxide anion coordinated at one apical position on the metal ion and mimicking O_2 activation. Under the conditions of photochemical activation, BLM−Co^{III}−OOH cleaves DNA with the same sequence specificity as activated BLM and with the same exclusive C4′−H abstraction.[210] Thus, BLM−Co^{III}−OOH is the closest model available for structural studies of iron-based activated species of BLM.[211,212]

The ligand and chiral organization of iron and copper BLM has remained controversial due to lack of structural information. However, recent crystal structures showed the same structure for BLM−Co^{III}−OOH[213] and BLM−Cu^{II}.[214,215] The BLMs are composed of four distinct domains remarkably optimized for oxidative DNA damage. Except for a few examples, chemical modifications described thus far decrease the efficiency of the drug.[113,197,203,204,206,216,217] It seems that the structure of BLM is not simply the juxtaposition of four independent domains, each of which is devoted to a special role. As an emerging picture, optimization of each domain and cooperation between them gives rise to this fascinating DNA cleaving agent whose complexity may rival with that of biological enzymatic active sites.

The four domains of BLM are the metal binding domain (N-terminal part), the bithiazole tail (C-terminal), the linker region between the two previous ones, and finally the sugar domain (Figure 28). The C-terminus domain of BLM is exclusively devoted to DNA binding. The bithiazole moiety binds to double-stranded DNA by intercalation or through interactions in the minor groove as will be detailed later. The positively charged tail of the C-terminus domain enhances DNA affinity by electrostatic interactions. The metal binding domain has been shown to be important in the recognition of the 5′-GPyr-3′ sequence in DNA. The linker domain is not just a simple linker, as believed previously, yet seems to play a role in the formation/stabilization of activated BLM, in the compaction of the structure for the fitting in the minor groove, and in DNA binding. The disaccharide moiety containing a gulose and a carbamoyl mannose is important for cell penetration in cancer cells[218] and is also considered to participate in the positioning of the metal binding domain with respect to DNA.

For many years, the crystal structure of a simplified model of BLM, the Cu^{II} complex of P-3A, was the closest crystal reference for the metal binding domain of BLM (**c** in Figure 29).[219] Cu(P-3A) is a biosynthetic intermediate of BLM lacking the disaccharide and the structure beyond the hydroxyhistidine group. Since the reports of the crystal structure of BLM A_2−Cu^{II} complexed with the bleomycin-binding protein (BLMA),[214] or protein MRDP[215] and BLM B_2−Co^{III}−OOH bound to DNA,[213] two complete structures for metallo−BLM are now available. Their metal binding domains are similar (**a** and **d** in Figure 29). They are different from Cu(P-3A).

Most of the knowledge on the structure of various metallo−BLM complexes in solution is derived from spectroscopic data and particularly from studies combining multinuclear NMR experiments and molecular dynamic simulations. It is generally accepted, and recently confirmed by the two metallo−BLM crystals,[213–215] that the ligands on the equatorial positions are the N (δ) of imidazole, the β-hydroxyhistidine (β-OH His) amidate nitrogen (deprotonated amide), the N1 intracyclic nitrogen of pyrimidine, and the primary amine of β-aminoalanine (β-Ala). The metal-binding domain in the N-terminus domain of BLM is able to stabilize octahedral transition metal complexes, but five-coordinated square pyramidal arrangement is also possible (Figure 29). The fifth ligand, in the axial position, is most of the time found to be the primary amine nitrogen atom of β-Ala. This is also confirmed by the crystal structures of BLM−Co^{III}−OOH[213] and BLM−Cu^{II}.[214,215] The sixth site is either vacant or labile to be available for O_2 binding in the perspective of the formation of activated BLM, as in BLM−Co^{III}−OOH, where the sixth position is occupied by the peroxide. The BLM ligand is thus described as a mono anion (deprotonated amide).

However, the studies of various metallo−BLM in the literature[113] do not agree in general with the recent crystal structures.[213–215] This is due to the complexity of the BLM ligand. The chelation of a metal ion in the metal binding domain of BLM can be organized with two different chiralities. The screw sense adopted by the metal binding domain appears to be different depending on the metallo−BLMs studied. Screw sense 1 and 2 depend on the face upon which the axial ligand is positioned on the square plane

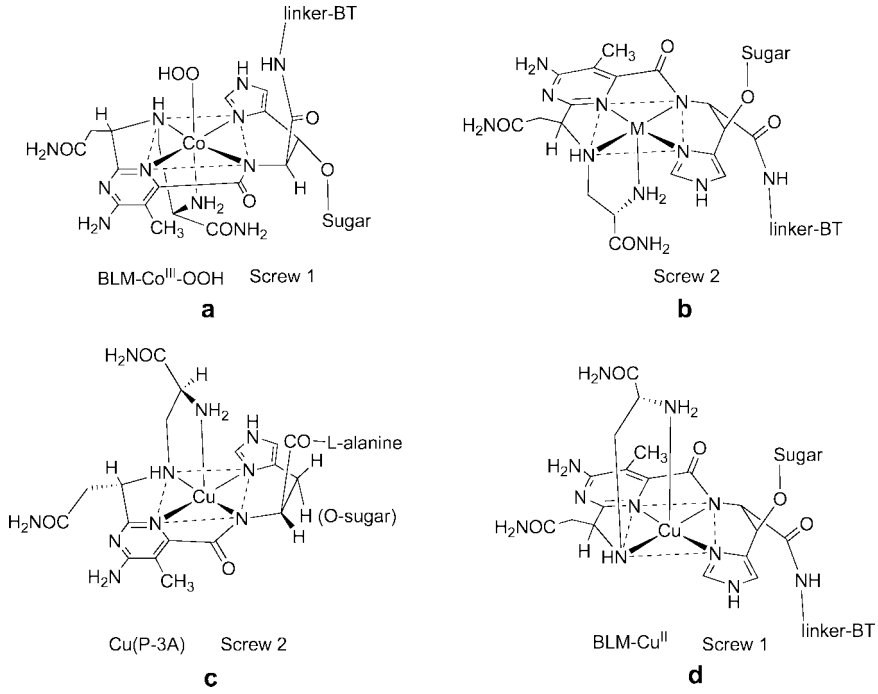

Figure 29. Structure of metallo−bleomycin and domain organization. M stands for metal ion. Linker, bithiazole tail, and sugar are omitted for clarity. Screws 1 and 2 correspond to the geometry of BLM−Cu^{II} and BLM−Co^{III}−OOH[213–215] and to Cu^{II}(P-3A) crystal structures, respectively.[219]

(Figure 29). Changing the face of the coordination of axial primary amine of β-Ala (Figure 29, pathways **a** to **c**, and **b** to **d**) reverses the chirality. Similarly, reversing the rotation sense of the four equatorial ligands (Figure 29, pathways **a** to **b**, and **c** to **d**), but not the face of β-Ala, changes the screw sense of the complex. In either case, the linker-bithiazole tail and the sugar moiety are located on opposite sides with respect to the equatorial plane of the coordination complex. The β-Ala primary amine and the sugar moiety are located on opposite faces in screw 2 and on the same side in screw 1. The two chiral organizations do not represent solution structures in rapid equilibrium with one another. They can only be converted after metal bond dissociation.

To date, BLM−Co^{III}−OOH is the best characterized metallo−BLM. The determination of its structure in interaction within the minor groove of DNA by NMR[197,206,211,220–228] or by X-rays[213] is one important piece in the understanding of the mechanism of action of BLM. Additionally, the binding affinity of BLM−Co^{III}−OOH for the 5′-GPyr-3′ sequence in DNA is one of the highest among the metallo−BLMs.[114,211,229] NMR studies on BLM−Co^{III}−OOH as a free complex or in interaction with DNA have concluded that it adopts the screw 1 structure (compound **a**, Figure 29) with the bithiazole folded over the metal binding domain.[197,206,211,220–228] This was confirmed by the recent crystal structure of a DNA bound complex.[213]

However, various screw senses and different axial ligands organizations were reported. Concerning copper BLM, BLM−Cu^{II} adopts screw sense 1 (compound **d**, Figure 29) in the crystal when bound to protein BLMA or protein MRDP.[214,215] The complex of nonmetalated BLM with another BLM-binding protein, BLMT, shows the same compaction of BLM metal binding domain with a prescrew 1 conformation.[230] On the opposite, the crystal structure of Cu(P-3A) accommodates screw sense 2 (compound **c**, Figure 29).[219] From NMR studies, BLM−Cu^{I} seems to adopt a prescrew 2 conformation[231] with exclusion of the amide nitrogen of β-OH His as ligand.[209,231] NMR studies of BLM−Fe^{II},[232,233] BLM−Co^{III},[220] and BLM−Co^{II} seem also to favor screw sense 2 orientation in solution,[232] while BLM−Fe^{II}−CO shows screw sense 1.[234]

The axial coordination of the primary amine of β-Ala has sometimes been proposed to be replaced by the coordination of the nitrogen atom of the carbamoyl amide group of α-D-mannose, for instance, in the case of pepleomycin−Co^{III},[223] bleomycin A_2−Zn^{II},[235] and BLM A_2−Fe^{II}−CO.[234] The axial ligation of carbamoyl for BLM−Fe^{II}−CO was questioned.[211] Nevertheless, when the sugar domain is absent, the primary amine of β-Ala is found as an axial ligand as in Co^{III}(deglyco pepleomycin)[223] and Zn^{II}(deglyco BLM).[236] Additionally, both groups (primary amine of β-Ala and carbamoyl NH_2) were also described as axially coordinated on the two opposite faces of the metal coordination plane in the case of BLM A_2−Zn^{II}, BLM A_5−Zn^{II},[237–239] BLM−Fe^{II},[233] and BLM−Co^{II}, which implies a screw 2 sense organization.[232,240]

Concerning BLM−Fe^{II}, magnetic circular dichroism has provided an electronic structural probe of the BLM−Fe^{II} site.[241] X-ray absorption spectroscopy studies provided complementary geometric structure insights.[242] In the case of BLM−Fe^{II}, the primary amine of β-Ala was demonstrated to be an axial ligand, and the carbamoyl group of mannose either provided a weaker sixth endogenous ligand or contributed significantly to the coordination environment of the Fe(II) site through second sphere effects.[241,242] Support for second sphere effects comes from the BLM−Co^{III}−OOH and BLM−Cu^{II} crystal structures with hydrogen bonds between the carbamoyl group of mannose and the primary amine of β-Ala in screw 1 configuration, especially when the drug is compacted when interacting with a protein or DNA.[213–215] On the other hand, direct yet weak coordination of carbamoyl group at the axial position (opposite β-Ala) may be possible in screw 2. Both alternatives leave an open access for exogenous O_2 binding at the sixth apical position on the metal center for iron BLM.

The BLM−Co^{III}−OOH structure in solution shows that the bithiazole tail is folded underneath the metal binding domain on the same face as the hydroperoxide ligand. The linker peptide is in a well-defined conformation that brings the bithiazole into close proximity with the pyrimidyl.[211,220,221] This conformation is almost identical when bound to DNA. Metal-free BLM displays an extended conformation as well as BLM−Cu^{II} bound to bleomycin-binding proteins.[214,215]

Various metal complexes of BLM are described with screw 2, while BLM−Co^{III}−OOH and BLM−Fe^{II}−CO are with screw 1. These complexes are the closest models of BLM activation for DNA cleavage because they both exhibit an octahedral metal coordination arising from the coordination of a sixth exogenous small axial ligand instead of O_2. Although the chiral and ligand organization of the metallo−BLMs, especially iron BLM, has not been unambiguously identified, it is noticeable that the two metal complexes of BLM that are available as crystals (BLM−Co^{III}−OOH and BLM−Cu^{II}) show exactly the same structure, suggesting that iron BLM might also have a similar structure (screw 1).

4.2.2. Interaction of Bleomycin with DNA

Specific and "unspecific" binding sites are usually considered. Binding of BLM to specific sites consisting of 5′-GPyr-3′ (5′-GC-3′ or 5′-GT-3′), which are the sites of most single-strand breaks and the unique sites of double-strand breaks mediated by BLM, is the best documented. However, although emphasis was put on this sequence context of cleavage, it appears that other sequences such as 5′-GA-3′ or even 5′-AT-3′ are cleaved efficiently by BLM.[114,243,244]

The affinity binding constant of different BLMs spans 2 orders of magnitude depending on the nature of the chelated metal and the sequence of DNA.[211,229,245,246] In specific sites, free BLM interacts with DNA with a binding constant of $\sim 10^4$ M^{-1}, while BLM−Cu^{II}, BLM−Zn^{II}, BLM−Co^{III}, and BLM−Fe^{III} interact with binding constants equal to $\sim 10^5$ M^{-1}. The strongest binding affinity of BLM−Co^{III}−OOH reaches a $K_{aff} \approx 10^6-10^7$ M^{-1}. In nonspecific DNA sequences, the binding constants of all BLM complexes are similar $\sim 10^5$ M^{-1}, and the binding constant of free BLM remains at $\sim 10^4$ M^{-1}. Metal-free BLM displays an extended conformation, which is thought to interact with DNA through its bithiazole tail. In contrast, all of the metal complexes contain additional conformational determinants resulting from metal ion coordination such that they could interact with DNA through an organized folding in addition to the bithiazole (and probably some differences in the mode of binding of the bithiazole). When associated with DNA, the metal binding domain, the linker region, and the disaccharide moiety are located in the minor groove. The position of the bithiazole moiety with respect to DNA (intercalation versus minor groove binding) depends on the DNA sequence that metallo−BLM interacts with and may depend also on the structure of the metal binding domain of BLM.

While in interaction with the specific site, iron BLM specifically abstracts the C4′−H hydrogen atom at the pyrimidine nucleoside of the 5′-GPyr-3′ site. BLM−Co^{III}−OOH is a stable analogue of the so-called activated BLM, BLM−Fe^{III}−OOH. BLM−Co^{III}−OOH affords a convenient model for the study of activated BLM in interaction with DNA. As demonstrated in the recent crystal structure of BLM−Co^{III}−OOH in complex with a double-stranded ODN containing a 5′-GT-3′ site,[213] and in accordance with previous NMR studies,[211,220,221,225,227] the binding of BLM in the specific site is ideally positioned for C4′−H activation (Figure 30). The involvement of the metal binding domain in the specific binding of BLM with the 5′-GPyr-3′ site is crucial. Two hydrogen bonds between the pyrimidine moiety of BLM (intracyclic nitrogen and 4-amino) and guanine base (NH_2 and N3) participate in the formation of the DNA/BLM complex and define the sequence specific cleavage site 5′-GPyr-3′.[213,247] This provides a molecular basis for the preference of G (rather than A) at the 5′-position of the cleavage site. The recognition of G is possible from the minor groove without denaturation of the DNA double helix and creates a "three base pair" system (Figure 30). The precise positioning of the metal binding domain at this 5′-G base is associated with the intercalation of the bithiazole moiety one base pair downstream of the sequence 5′-GPyr-3′ with the bulky charged tail located in the major groove.[211,213,221,222,225,227] As a consequence, the deoxyribose target of the Pyr-3′ residue is located between the metal coordination plane and the bithiazole and close to the activated metal center. The distal oxygen atom of a modeled hydroperoxide is positioned 2.5 Å from the C4′ atom of the deoxyribose unit of the Pyr-3′ nucleoside in the crystal. The proximal oxygen atom is 4.7 Å from the same C4′.[213] These distances are evaluated with a modeled peroxide ligand because the hydroperoxide was not seen in the crystal of BLM−Co^{III}−OOH. Similarly, in NMR structures, the distance between the distal oxygen of the hydroperoxide and the H4′ hydrogen atom of the cleavage site is short, ∼2.2−2.5 Å.[225,227] The proximal oxygen, which would be at about the same position as the activated oxygen of a putative iron−oxo species, is measured in the case of BLM−Co^{III}−OOH at 3.5 Å from the H4′-atom target.[225]

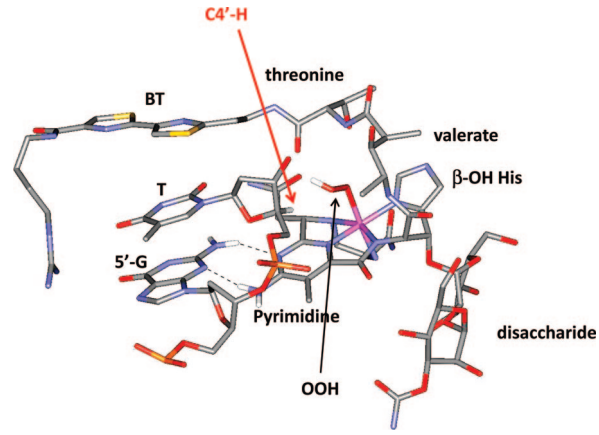

Figure 30. BLM−Co^{III}−OOH, in interaction with a 5′-GT-3′ site on double-stranded DNA[225] (PDB file 1GJ2). Hydrogen atoms are omitted for clarity except for those involved in hydrogen bonding between the pyrimidine moiety of BLM and guanine of 5′-GPyr-3′ site and the C4′−H target.

Importantly, the establishment of hydrogen bonds between the pyrimidine moiety of the metal domain and the guanine base in the minor groove is dependent on the screw sense of the ligand groups wrapping around the metal ion. As such, BLM metal complexes in screw sense 2 cannot form the two specific hydrogen bonds between pyrimidyl group and guanine.

The linker region covers the coordinated hydroperoxide. This folded structure of the metal-linker domain exists already in solution for BLM−Co^{III}−OOH. Thus, preorganization of the linker region together with the metal binding domain in a rigid form is proposed to be determinant in DNA

binding.[206,222,225] Although the rigid metal binding domain and bithiazole seem to be preorganized in solution, an induced fit takes place upon interaction of BLM with DNA, and especially with the specific sequence, with the formation of several hydrogen bonds between the two partners (drug/DNA) and compaction of the drug.

The positioning of the linker region may give an opportunity to the establishment of appropriate hydrogen bonds or acid and base catalysts precisely situated to stabilize oxygenated species or to assist in the heterolytic O−O bond scission. Unfortunately, these groups are not identified thus far. In recent DFT calculations, groups of the linker region were found to donate hydrogen bonds to the distal O-atom of the peroxide. One hydrogen bonding was donated by the NH group of the side-chain methylvalerate moiety and the other by the NH moiety of the threonine side-chain.[248] In the crystal, the linker groups did not interact with the peroxide. Some of them rather exhibited H-bonds to DNA groups.

The conformationally stable metal binding domain and linker establish a closed-packed adduct with the minor groove in which the hydroperoxide occupies a sterically constrained pocket, which has limited access to the solvent. The nuclear magnetic resonance of the hydroperoxide proton of BLM−Co^{III}−OOH, observed at 8.38[227] or 8.89 ppm,[221] indicates that it is shielded from the solvent when interaction with specific DNA takes place, whereas in the free drug or when bound to nonspecific sites it is not detected due to its rapid exchange with solvent. Although no structural role for the disaccharide domain could be clearly assigned, it seems that its presence in the minor groove serves as a "space-filling" unit, helping the metal binding domain to reach its target.[213]

The 5′-GPyr-3′ is the hot spot for a double-strand break, which is considered as the crucial cytotoxic event. This structure of BLM−Co^{III}−OOH/DNA interaction inspired a model for the mechanism by which a single BLM complex may effect double-strand damage without dissociation from the DNA.[197,206,222,247] Although BLM can mediate single-strand cleavage through multiple binding modes, the double-strand damage event was proposed to involve partial intercalation of the bithiazole moiety within the DNA double helix. The rigidity of the metal binding domain associated with a rotation around the C−C bond connecting the two thiazolium rings followed by repositioning of the metal binding domain toward the second DNA strand were proposed to be the keys for the possible attack of a single bound BLM molecule on both strands. The active site of the drug, the metal center, could thus be located on suitable distances with respect to the two C4′−H targets on both strands. However, recent data using BLM analogues tethered to a bulky entity, which are no longer capable of intercalation, indicate that intercalation of the bithiazole may not be necessary for double-strand cleavage.[249,250] Cooperative binding of two BLM molecules can be hypothesized. A second molecule of BLM would bind at the first damage place on DNA; yet the structural basis for this cooperative binding site remains unknown. On the other hand, it seems that there are not yet any identified hot spots in supercoiled plasmid that allow cyclodextrine-modified BLM to mediate efficient direct double-strand cleavage. Double-strand cleavage of DNA by BLM is certainly not trivial and is still not fully understood. Cooperative binding of two BLM molecules at the same site is difficult to imagine in vivo.

Concerning iron BLM, which is considered as the most probable biologically relevant BLM derivative, no precise structure of this BLM derivative free or in complex with DNA is available. The study of the interaction of iron BLM with DNA is not simple. BLM−Fe^{II} is unstable in the presence of O_2, BLM−Fe^{III} is not the probable oxidation state of the drug inside cells, and BLM−Fe^{III}−OOH is not stable. Furthermore, the paramagnetic nature of iron precludes detailed NMR analyses. Nevertheless, some information on the interaction of iron BLM and DNA was gained from a number of spectroscopic studies.[113]

The metal binding domain of BLM−Fe^{III} binds to an oligomer DNA containing the specific 5′-GC-3′ site, differently than it does to an oligomer, which has no preferential binding site. ESR studies indicate that the BLM−Fe^{II}−NO spectrum is not perturbed by interaction with nonspecific DNA sequence on the opposite to what is observed with the specific DNA site. The iron center of BLM−Fe^{III} is high-spin when BLM−Fe^{III} interacts with a nonspecific DNA and low-spin when it is bound to an ODN bearing the specific site.

BLM−Fe^{III} binds to specific DNA in slow exchange on the NMR time scale, whereas it binds in fast exchange to nonspecific DNA. The same behavior is observed for BLM−Co^{III}−OOH. A strong argument for these two metallo−BLM to form closely similar interaction with the specific 5′-GPyr-3′ site comes from the finding that substitution of guanine for inosine in the specific site converted the BLM−Fe^{III}/DNA and BLM−Co^{III}−OOH/DNA interaction into a fast exchange process.[227,246]

ESR studies with iron BLMs bound to calf thymus DNA fibers show that the NO of BLM−Fe^{II}−NO was held rigidly in place, suggesting that the NO group is structurally oriented by hydrogen bonding in a way reminiscent of the peroxide of BLM−Co^{III}−OOH. The metal binding domain of BLM−Fe^{III}, BLM−Fe^{II}−NO, binds with almost the same orientation as compared to DNA helix axis as that of BLM−Co^{III}−OOH.[251] Additionally, circular dichroism spectra of ODNs in complex with BLM−Fe^{III} show perturbation of the double helix structure only in the case of an ODN carrying a specific site. This was correlated to the intercalation of the bithiazole moiety between base pairs for the specific interaction.[246] An intercalated bithiazole was also observed for BLM−Co^{III}−OOH in interaction with the specific 5′-GT-3′.

The steric availability for axial ligand binding was also recently addressed for iron BLM. CTPO (3-carbamoyl-2,2,5,5-tetramethyl-3-pyrrolin-1-yloxy) was used to probe the nitroxide to the metal center of BLM−Fe^{III} in the absence and presence of an ODN carrying a specific interaction site.[227] The nitroxide has greatly reduced accessibility to the BLM−Fe^{III} center once bound to specific site. Similarly, BLM−Fe^{III} was found relatively unreactive with ascorbate while interacting with specific DNA as compared to free BLM−Fe^{III} or BLM−Fe^{III} in interaction with a nonspecific DNA, consistently with the conclusions of poor solvent accessibility to the metal center described for BLM−Co^{III}−OOH in the specific site. The rates of ascorbate reduction of free BLM−Fe^{III} or bound to specific and unspecific DNA were compared. Nonspecific DNA has no effect on the rate of reduction of free BLM−Fe^{III}. In contrast, BLM−Fe^{III} was reduced with a 10-fold lower rate in the case of the specific interaction with DNA.[227] As in the adduct of BLM−Co^{III}−OOH with specific sites on DNA, the metal center of

BLM−Fe^{III} in the specific interaction is buried from solvent, but not completely inaccessible.

However, the reaction of BLM−Fe^{III} with O_2 and ascorbate, in the presence of specific or nonspecific DNA, leads in either case to activated BLM and to the release of base propenals (**45**, Figure 16), one of the typical products of DNA damage by C4′−H activation. The concentration of BLM−Fe^{III}−OOH declined more rapidly with specific DNA in comparison with that in the presence of the nonspecific DNA.[229] The activated species of iron BLM is readily detected with either DNA.[227,229,245,246] Thus, although the interaction of the metal binding domain of BLM−Fe^{III} is different in specific versus nonspecific sites, the same chemistry can take place yet at different rates. The iron center can reach in any case a proper position to be activated for the typical C4′−H abstraction reaction.

Magnetic circular dichroism and X-ray absorption spectroscopies have also been used to assess the binding of the biologically relevant BLM−Fe^{II} with DNA.[241,252] The Fe^{II} center is perturbed regardless of DNA sequence. BLM−Fe^{II} bound to nonspecific or specific DNA sequence has the same affinity for azide.[252]

In summary, BLM−Fe^{III} binds to DNA in a different way in a specific site as compared to a nonspecific site. The metal binding domain of BLM−Fe^{III} in the specific site resembles that of the BLM−Co^{III}−OOH (H bondings with the 5′-G, intercalation of the bithiazole moiety between DNA base pairs). An induced fit of the metal binding domain seems to occur upon binding at the specific site as compared to the unspecific site or the drug in solution. The accessibility of the metal to the solvent is lower in the specific site although not prohibited. In either situation, interaction with a specific or an unspecific oligomer DNA, activation of BLM−Fe^{III} with O_2 and ascorbate is possible and leads to C4′−H activation. From the data on BLM−Fe^{III}/DNA interaction in addition to the similar chemistry of the two compounds toward DNA, it seems that the structure of the BLM−Co^{III}−OOH/DNA adduct can be taken as a credible model for BLM−Fe^{III}−OOH/DNA.

Studies of variations of the metal binding domain properties upon binding to DNA at specific site 5′-GPyr-3′ or at nonspecific sites provided some clues in understanding the DNA binding mechanism of BLM. Slow exchange on an NMR time scale, bithiazole intercalation, two hydrogen bonding contacts between guanine, and the pyrimidine moiety of BLM are generally observed features for BLM−Co^{III}−OOH and BLM−Fe^{III} interacting in the specific site 5′-GPyr-3′. On the other hand, fast exchange, minor groove location of bithiazole, and absence of NOEs of the pyrimidine moiety with DNA protons are observed for BLM−Co^{III}−OOH and BLM−Fe^{III} at nonspecific sites and for BLM−Cu^{II}, BLM−Zn^{II}, and BLM−Co^{III} at any sites of DNA.

From the examination of the properties of binding of several metallo−BLMs to duplex ODN, bearing or not a specific site, by circular dichroism spectroscopy, it is concluded that in the absence of the capacity of the metal binding domain to associate through specific hydrogen bonds with guanine at the interaction site, minor groove binding of bithiazole becomes more significant.[246] It is suggested that intercalation of the bithiazole requires a specific metal domain configuration in the minor groove.

Thus, one may propose that preorganization of the metal binding domain of iron BLM in solution (screw sense 1, Figure 29) predisposes the drug to recognize the specific site. DNA binding would start by an interaction of the bithiazole tail and the metal domain in the minor groove. Moving along the DNA minor groove to a specific site containing a guanine nucleoside would anchor the whole molecule at that site followed by an induced fit between the drug and DNA. The conformation of the metal binding domain would be somehow different in the situations of specific versus nonspecific interaction with DNA. The metal center seems more accessible to solvent in the minor groove of nonspecific sites. The reaction between O_2 and reductants with the iron center seems easier in a nonspecific interaction context.[227]

The structures of BLM−Zn^{II} interacting with $d(CGCTAGCG)_2$[236,238,239] and $d(CGCGAATTCGCG)_2$[235] may illustrate this general scheme. It gives an example of a metallo−BLM with an alternative metal binding domain folding in interaction with DNA and shows that even within this unspecific-like interaction the metal center can be close to H4′-atoms. The structure of BLM−Zn^{II} in interaction with DNA is clearly different from that of BLM−Co^{III}−OOH. BLM−Zn^{II} has a ligand coordination environment different from those of BLM−Fe^{II}−CO and BLM−Co^{III}−OOH. Modeling of the drug−DNA complex from NMR data indicated a preferred orientation of the metal binding domain in minor groove with no strong clue for the recognition of the 5′G residue of the specific 5′-GPyr-3′ site.[235,239] The bithiazole binding mode appeared as multiple[235] including partial intercalation[239] and minor groove binding.[236] The $d(CGCGAATTCGCG)_2$ duplex afforded unanticipated DNA cleavage at two major sites by BLM−Fe^{II} + O_2 that occurred at the A5 and C11 residues. The activation of the C4′−H of C11 corresponds to the typical target of specific cleavage site, whereas reaction at the C4′−H of A5 is unusual. In the Dickerson's crystal structure, these two target C4′−H's are located toward each other in the minor groove, leading to the hypothesis that one single bound molecule of iron BLM may be able to reach either strand in this special sequence context. In the BLM−Zn^{II} complex with $d(CGCGAATTCGCG)_2$, the metal ion is at 6.4 and 5.4 Å from the C4′−H of C11 and A5 residues, respectively.[235]

4.2.3. Activation of Iron Bleomycin

While BLM−Cu^{II} is capable of effecting DNA cleavage in the presence of O_2 and dithiothreitol, much less is known about its mechanism of activation and DNA strand scission.[209] The most interesting discussion in the context of C−H bond activation comes from the extensively investigated yet still controversial activation of iron BLM.[113,114,205,206] The different routes of BLM activation have been delineated;[18] however, the ultimate species responsible for DNA oxidation is an issue of debate.

DNA degradation by iron BLM is dioxygen and reductant dependent. BLM−Fe^{II} binds O_2 at one vacant coordination site to produce a ferric superoxide intermediate, BLM−Fe^{III}−$OO^{\bullet}$, which accepts one electron and one H^+ and transforms into a ferric hydroperoxide, BLM−Fe^{III}−OOH, referred to as "activated" BLM (Figure 31). Alternatively, BLM−Fe^{III}−OOH species can be obtained directly (in the absence of reducing agent) from BLM−Fe^{III} in the presence of H_2O_2. These initial steps leading to BLM−Fe^{III}−OOH correspond to the general mechanism previously depicted in Figure 3. Activated BLM displays an EPR spectrum characterized by sharp features at g = 2.26, 2.17, and 1.94.[253] It has been identified as a low-spin ferric hydroperoxide.[205,253–258] Re-

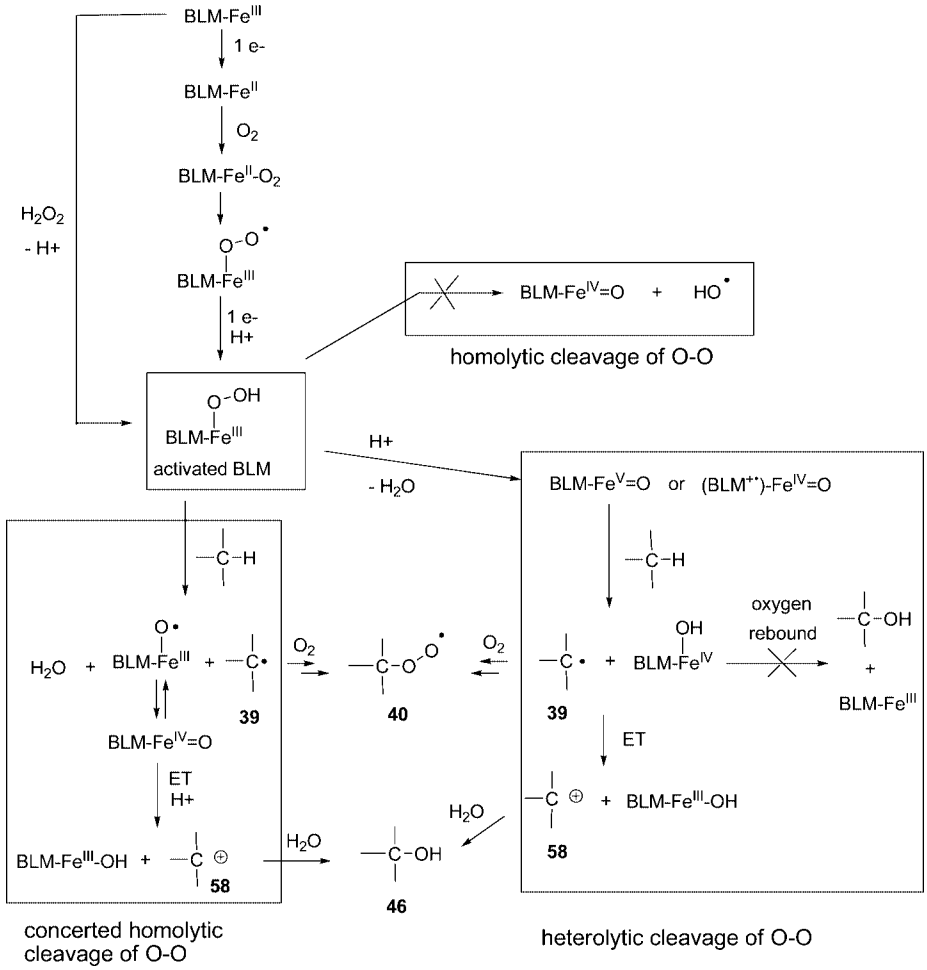

Figure 31. Proposed pathways for BLM−Fe^{II} activation. Homolytic cleavage of the O−O bond of Fe^{III}−OOH species was discarded. Heterolytic cleavage of the O−O bond of Fe^{III}−OOH better fits experimental data but awaits definitive evidence. ET stands for electron transfer.

markably, BLM−Fe^{III}−OOH has a half-life of 2 min at 4 °C[253] (which in solution at 37 °C is estimated to be 15 s). It does not exchange O-atoms with water.[254,259]

Activated BLM is kinetically competent to initiate DNA degradation.[205] It is the last detectable intermediate prior to DNA strand scission. The BLM O−O bond scission is the rate-limiting step in its decay reaction in the presence or in the absence of DNA, and the rate-limiting step in DNA attack.[205] BLM−Fe^{III}−OOH is relatively stable, but its conversion to low-spin BLM−Fe^{III}, which is first-order, is poorly characterized because no observable intermediate product accumulates. Ferric BLM obtained from activated BLM carries a hydroxyl anion or a water molecule as axial ligand, whose O-atom originates from the previously coordinated hydroperoxide.[260]

It is clear that BLM−Fe^{III}−OOH exists as an intermediate in the cycle of BLM. A doubt remains whether this ferric hydroperoxide is indeed the final species responsible of H-atom abstraction. A high-valent ferryl species may rather be the final active species, as discussed in section 2. In theory, BLM−Fe^{III}−OOH could be the precursor of three types of other forms of activated oxo-ferryl BLM, BLM−Fe^{V}═O, BLM$^{+\bullet}$−Fe^{IV}═O, or BLM−Fe^{IV}═O associated with one equivalent of OH$^{\bullet}$ radical, depending on the mechanism of O−O bond cleavage (heterolytic or homolytic cleavage) (Figure 31). These three alternative pathways respect the two oxidizing equivalents of BLM−Fe^{III}−OOH above BLM−Fe^{III}.

The arguments in favor of BLM−Fe^{III}−OOH as being the activated species of BLM rely on its characterization and on the fact that it is kinetically competent in mediating DNA damage. DFT calculations compatible with BLM−Fe^{III}−OOH being thermodynamically and kinetically competent for H-atom abstraction were reported.[261,262] On the opposite, both homolytic and heterolytic cleavage were found energetically unfavorable.[263] Therefore, a proposed hypothesis for the reactivity of activated BLM, BLM−Fe^{III}−OOH, is a concerted homolytic cleavage of the O−O bond with C4′−H abstraction, also referred to as direct hydrogen abstraction (Figure 31). It is reminiscent of the "second electrophilic oxidant" proposed for cytochrome P450.[18–20] This mechanism is questioned for BLM, nonheme iron systems, and cytochrome P450.[2,4,21,23,24,248]

H-abstraction through the concerted mechanism implies that the decay rate of activated BLM should be faster in the presence of DNA. Although the decay rate of activated BLM was reported initially to be independent of DNA,[253] recent reinvestigation of the kinetics of activated BLM decay in the presence of DNA showed that its decay proceeded 2.5 times faster when iron BLM is in interaction with an ODN containing the specific site as compared to the decay rate in solution.[264,265] These data should support the concerted mechanism. However, things do not seem simple. Other recent experiments on activated BLM decay were conducted at low temperature. As in the case of the stable BLM−Co^{III}−OOH, BLM−Fe^{III}−OOH, which is stable at

low temperature, can undergo photolysis when irradiated at its ligand-to-metal charge transfer wavelength (~350 nm) at 77 K and promotes DNA cleavage with concomitant formation of low-spin BLM−Fe^{III}.[260] The decay of activated BLM, generated under light irradiation, proved also DNA dependent.[260] The low temperature photolysis of activated BLM increased over 1 order of magnitude with DNA whatever the sequence (DNA containing a specific site or not). However, the same rate enhancement was observed even though the DNA C4′−H target was absent on a modified double-stranded ODN, which consisted of a modified C residue 3′ to a G, in the form of a 2′*O*-4′-methylene-bridged locked ribocytidine.[260] Thus, the most recent data are not in favor of the concerted mechanism because the interaction of the metal binding domain with DNA assists the decay of BLM−Fe^{III}−OOH, in a way independent of the presence of C4′−H.

Furthermore, the rate of BLM−Fe^{III}−OOH decay (in the absence of DNA) was shown to be slower in D_2O than in H_2O. The KIE was $k_H/k_D \approx 3.6$[263] or 2.6.[205] A lower KIE, $k_H/k_D \approx 1.7$, was also observed for the decay of activated BLM in the presence of an ODN containing the specific site of BLM.[264] In the concerted mechanism context, this KIE was calculated to be consistent with a secondary KIE involving the proton of the hydroperoxide.[265] However, these experimental solvent kinetic isotope effects rather support a heterolytic cleavage of the O−O bond of BLM−Fe^{III}−OOH through the protonation (or hydrogen bonding) at the distal O-atom by a H-donor group (solvent or BLM group).[29,266] In the absence of DNA, the BLM decay would be more dependent upon the solvent.

Heterolytic cleavage of the O−O bond of BLM−Fe^{III}−OOH might lead to a BLM−Fe^{V}=O species (Figures 3 and 31). Iron cannot easily sustain the Fe(V) oxidation state.[267] In heme enzymes and in model porphyrin systems, the two oxidizing equivalents are partitioned so that one resides in iron(IV) and the other either in the porphyrin cation radical[1,12] or in the protein.[268] Consequently, a formal BLM−Fe^{V}=O might be rather envisioned as a $BLM^{+\bullet}$−Fe^{IV}=O. Recent DFT calculation[248] reinvestigated the heterolytic modes of O−O bond cleavage of a BLM−Fe^{III}−OOH complex, taking into account the hydrogen bonds network that may be involved in the process of BLM activation starting, from the known structure of BLM−Co^{III}−OOH bound to DNA at the 5′-GT-3′ specific site.[225] In this structure, the linker region wraps around the hydroperoxide. In support of a proton transfer to the distal O-atom, the formation of a high-valent iron−oxo species was found possible thanks to BLM side chains in the linker region (valerate and threonine functionalities) assisting an acid−base proton reshuffle. An active species of BLM in the form of a Compound I like intermediate was found energetically accessible. The calculations found a stabilization of the generated formal Fe^{V}=O species as a Fe^{IV}=O associated with a $BLM^{+\bullet}$ cation radical located on the valerate residue. The rate-determining step was the heterolytic cleavage of the O−O bond in agreement with experimental data. The authors further suggest that this mechanism is compatible with ^{18}O kinetic isotope effects measured during BLM−Fe^{III}−OOH decay.[255]

It is tempting to hypothesize that DNA binding might help the process of proton reshuffle and promote the formation of iron−oxo BLM. However, DNA interaction is not absolutely necessary for iron BLM activation. Indeed, iron BLM can be activated in the absence of DNA and was used as a catalyst for small molecule oxidation.[269–272] Furthermore, DNA cleavage is observed in specific and nonspecific sites that seem to involve different metal binding domain conformations. This mechanism would be compatible with DNA interaction, helping in some way the folding of the linker region in the proper vicinity of the hydroperoxide and participating in a more efficient heterolytic cleavage. It would explain a relative stability of BLM−Fe^{III}−OOH before activation in situ. However, this mechanism remains to be tested experimentally. The hydrogen bondings between the linker groups and the hydroperoxide of the BLM−Co^{III}−OOH in interaction with DNA were observed in the NMR[225] but not in the crystal structure.[213]

Finally, as discussed previously in section 2, the last possible pathway of BLM activation (Figure 31) consists of homolytic cleavage of the O−O bond of BLM−Fe^{III}−OOH. It should lead to the production of $HO^{\bullet}$. In the case of BLM, it was excluded on the basis of two points, KIE and exquisite specificity of DNA reaction. The kinetic isotope effect $k_H/k_D \approx 2-7$ in H-atom abstraction, determined for the reaction of activated BLM with deuteriated DNA,[273] is different from the KIE measured for free $HO^{\bullet}$ radicals ($k_H/k_D \approx 1-2$).[274,275] BLM's KIE is nevertheless smaller than that observed for cytochrome P450, $k_H/k_D \approx 3-5$[276] or $k_H/k_D \approx 11$.[277] Moreover, because $HO^{\bullet}$ are diffusible radicals, it is likely that they would escape to some extent and reach diverse targets different from the unique C4′−H bond observed in BLM's DNA damage. Nevertheless, homolytic cleavage of the O−O bond is not impossible with BLM and was indeed reported to be the major mechanism of BLM activation when BLM−Fe^{III} was activated with a suitable hydroperoxide, 10-hydroperoxy-8,12-octadecadienoic acid, which gives evidence for homolytic versus heterolytic cleavage.[278] This activation mechanism of BLM was established in oxidation reactions of low molecular weight compounds and may not be relevant to DNA damage.[270]

In conclusion, despite the efforts made toward the elucidation of the real active species of BLM, and in the absence of any characterization of an unstable high-valent iron−oxo species, which would be generated from BLM−Fe^{III}−OOH by a relatively slow process (rate-determining step, kinetic bottleneck)[260] yet would react quickly in H-atom abstraction, the question of the nature of the active species of BLM remains open.

4.2.4. DNA Oxidation by Iron Bleomycin

The oxidative chemistry of BLM in the context of DNA damage is not exactly similar to the cytochrome P450 paradigm. Although the active species of iron BLM is formally at the same oxidation state as Compound I of heme enzymes, it behaves like cytochrome P450 in the first oxidation step and like peroxidases in the second one (Figure 31). It resembles cytochrome P450 in the fact that the metal-centered oxygenated species is capable of performing the homolytic cleavage of the C4′−H bond of a deoxyribose unit. This first step generates a carbon-centered radical at C4′ (**39**). However, the typical oxygen rebound mechanism described for cytochrome P450 or model compounds does not occur with BLM in the context of DNA oxidation. The carbon-centered radical (**39**) does not end as an alcohol carrying the oxygen atom from the putative iron−oxo entity (Figure 5). Instead, two reaction pathways have been evidenced. The process of C−H bond activation by iron

BLM either stops after the formation of **39** or proceeds further to the formation of a carbocation (**58** Figure 21).

The C4′-radical may combine with O_2 to give an intermediate C4′−OO• (**40**). The 3′-phosphoglycolate (**37**) and base-propenal (**45**) products result together with concomitant direct strand cleavage (Figure 16). The oxygen atom incorporated in the 3′-phosphoglycolate originates from O_2.[118] In this pathway, only one oxidizing equivalent of activated BLM is consumed, and BLM should end up as BLM−Fe^{IV}−OH, or as its deprotonated form BLM−Fe^{IV}=O (both species being at the same oxidation state as Compound II of heme enzymes) (Figure 31).

Alternatively, the C4′-radical may be oxidized. This second oxidation step is proposed to proceed by electron transfer between the BLM−Fe^{IV}−OH (or BLM−Fe^{IV}=O) entity and the C4′-radical (Figure 31). It leads to a carbocation at C4′ (**58**), which would ultimately be trapped by H_2O to give a 4′-hydroxylated abasic site (alkali-labile lesion) (**47**) (Figure 21). This mechanism is consistent with a 100% incorporation of an oxygen atom from water in the C4′-hydroxylated product generated by iron BLM.[136] This pathway is a typical two-redox equivalent oxidation and ends up with a stoichiometric conversion of activated BLM to the starting BLM−Fe^{III}. The fact that the hydroxylated product (4′-hydroxylated abasic site, **47**) generated by BLM on DNA does not carry any oxygen atom originating from dioxygen (or from H_2O_2 when BLM−Fe^{III} is activated through the peroxide shunt) is a strong argument against an oxygen rebound mechanism (Figure 5).

The C4′-radical (**39**) was demonstrated to be the common intermediate between the two pathways leading to the 3′-phosphoglycolate fragment (**37**) and the 4′-hydroxylated abasic site (**47**), respectively. Identical KIEs are observed on the formation of both products with C4′-deuteriated DNA.[247,279] The partitioning between these two pathways depends on the concentration of O_2. Under anaerobic conditions, 98% of 4′-hydroxylated abasic sites are formed.[14] Under 1 atm of O_2, ∼30% of BLM-induced damage consists of 4′-hydroxylated abasic sites and ∼70% of 3′-phosphoglycolate fragment.[280] Thus, the trapping of the carbon-centered radical **39** by O_2 competes efficiently with the electron transfer oxidation of the radical. In the case of iron BLM DNA oxidation, this radical **39** does not evolve to a C3′ cation radical (**54**, Figure 19) as reported for the C4′ radical generated by other DNA oxidation routes.

The trapping of the C4′ radical by a molecule of O_2 (in addition to that required for BLM−Fe^{II} activation) is at the origin of direct single-strand break and might be a mechanistic key for double-strand cleavage of DNA by BLM. When oxidation of a C−H bond by the active species of iron BLM stops at the step of radical **39**, one oxidative equivalent still remains on the metal center of BLM for a putative attack on the other strand. Alternatively, it has been speculated that the C4′−OO• may be able to oxidize the proximal BLM−Fe^{IV}−OH intermediate to form a formal BLM−Fe^{V}=O species that would in turn be able to mediate oxidation of the complementary strand.[114] The concomitant reduction of C4′−OO• (**40**) into C4′−OOH (**41**) (Figure 16) would initiate the process of single-strand scission of the first oxidized strand. Double-stranded DNA lesions mediated by BLM always include a cleavage event with a 3′-phosphoglycolate-terminated fragment (**37**). One may note that the relatively long half-life of the carbon-centered radical generated by the active species of BLM on DNA and its subsequent trapping by dioxygen may have an interesting consequence regarding the biological activity of the drug. It might be at the origin of the capability of this drug to mediate a double-strand break from a single molecule of activated BLM. This, of course, still awaits experimental evidence.

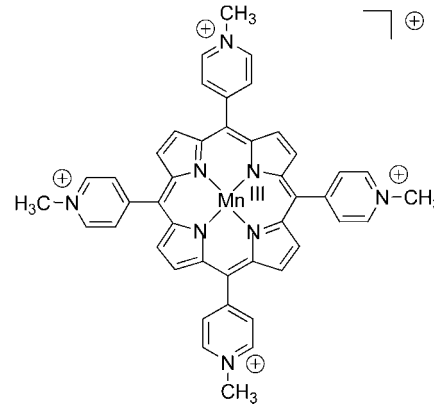

Figure 32. Structure of the cationic manganese porphyrin used for oxidative DNA damage: Mn^{III}-bis(aqua)*meso*-tetrakis(4-*N*-methylpyridiniumyl)-porphyrin, Mn(TMPyP). This complex has overall five positive charges. Axial ligands (two water molecules) were omitted for clarity.

4.3. Manganese−Porphyrin

4.3.1. Structure and Activation

Mn^{III}-bis(aqua)*meso*-tetrakis(4-*N*-methylpyridiniumyl)-porphyrin, Mn(TMPyP), is a water-soluble manganese porphyrin with four cationic substituents (Figure 32). With deprotonated pyrroles, the porphyrin core is a dianionic strong ligand. When a manganese(III) ion is inserted in the center of the porphyrin macrocycle, the metal complex does not dissociate. As other iron or manganese porphyrins, it is able to mimic the chemistry of the heme enzymes, cytochrome P450, and peroxidases in association with oxygen atom donors. It is capable of hydroxylation reaction through C−H bond activation, olefin epoxidation, and electron transfer reactions.[12] This chemistry takes place in water. The active species of this catalyst is a high-valent manganese−oxo species that contains the two oxidizing equivalents required to oxidize the substrate. It is an oxomanganese(IV) porphyrin cation radical, ($P^{+\bullet}$)Mn^{IV}=O, formally referred to as Mn^{V}=O.

The active species can be generated, from the Mn^{III} starting state, with O_2 in the presence of a reducing agent or with H_2O_2 as for heme enzymes under physiological conditions. On the other hand, as for biomimetic iron porpyrins, it can be generated with oxygen atom donors such as iodosyl benzene, magnesium monoperphtalate, potassium monopersulfate ($KHSO_5$), also referred to as oxone, or peroxynitrite ($ONOO^-$). $KHSO_5$ can be replaced by a more biocompatible reactant, consisting of the association of sulfite (Na_2SO_3) and O_2.[12,13,17] Importantly, $KHSO_5$, which is associated with Mn(TMPyP) in most of the studies of DNA damage, is soluble in water at physiological pH. The first detection of a Mn^{V}−oxo porphyrin intermediate under catalytic conditions was achieved by using rapid-mixing stopped-flow techniques with Mn(TMPyP) and *meta*-chloroperbenzoic acid or $KHSO_5$.[281] Furthermore, the Mn^{V}=O derivative of the *meso*-tetrakis-(2-*N*-methylpyridiniumyl)-porphyrin isomer was surprisingly stable (a few minutes), allowing its characterization by ^{1}H NMR.[282]

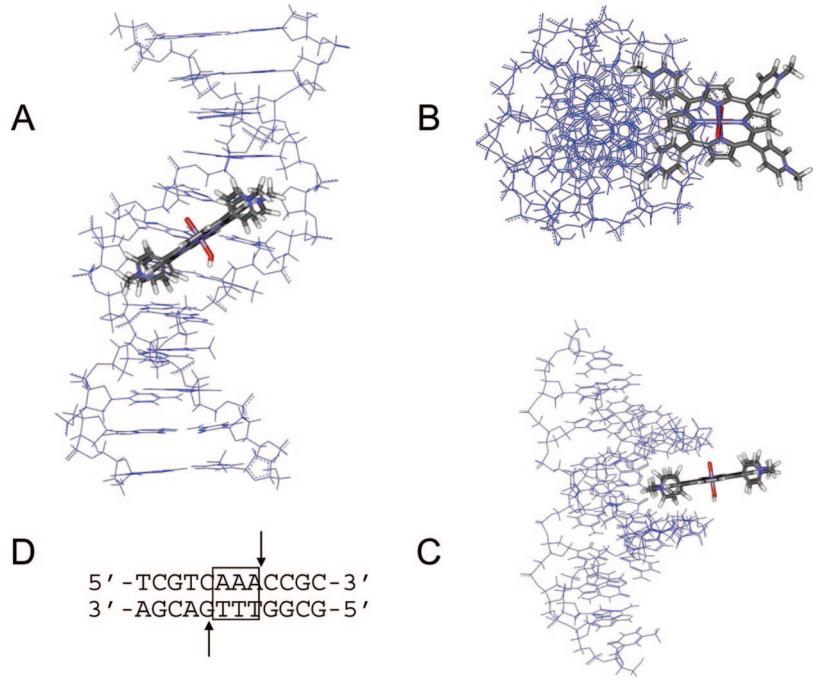

Figure 33. Modeling of the interaction of a high-valent manganese−oxo porphyrin (with a *trans* hydroxo ligand) with the minor groove of the three consecutive A·T base pairs of 5′-TCGTCAAACCGC/5′-GCGGTTTGACGA duplex. (A) Side view; (B) top view; (C) side view, rotation by 90° as compared to (A); and (D) sequence of the duplex; the cleavage site is indicated by arrows.[286]

The dissymmetric peroxide $KHSO_5$ used for DNA cleavage with Mn(TMPyP) contains a good leaving group (SO_4^{2-}). Its coordination to the Mn^{III} porphyrin is followed by rapid heterolytic cleavage of the O−O bond of the peroxide and ensures the formation of the two oxidizing equivalent entity Mn^{V}=O (X = OSO_3^-, Figure 4c). The oxidizing system based on Mn(TMPyP) associated with $KHSO_5$ does not produce hydroxyl radicals. It can be considered as a "clean" reagent as compared to many metal complexes with regards to the nature of the active species involved in oxidative DNA damage.

Furthermore, the Mn^{V}=O activated species of Mn(TMPyP)/$KHSO_5$ system is a powerful oxidant. Hydroxylation reaction of aliphatic C−H bond occurs by the so-called oxygen rebound mechanism (Figure 5). Because of the possible coordination of a water molecule (in the form of hydroxo ligand) on one face of the porphyrin ring in aqueous medium, this catalyst was shown to transfer an oxygen atom originating either from the peroxide or from $H_2{}^{18}O$ in a 1:1 ratio.[35,36,65] Because the exchange of the oxo−oxygen atom with water is slow, this result correlated with an oxo−hydroxo tautomerism along the vertical axis of the high-valent metal−oxo porphyrin, which is proof of oxygen rebound mechanism (Figure 5).

For the C−H bond activation to occur through an oxygen rebound mechanism, the C−H bond target must be within chemical bonding distance with respect to the oxo group. The interaction between the substrate and the catalyst must be strong enough so that intermediate species such as the carbon-centered radical does not dissociate from the metallo−porphyrin. This would eventually lead to a rearrangement of the radical, and to a non stereoselective reaction, or to its trapping by O_2. Thus, the strict interaction of the metal catalyst with DNA is critical to position and maintain the activated high-valent entity toward C−H bonds of DNA. Furthermore, the reaction must be rapid. A slow oxygen rebound process would have the same consequences as a loose contact. The high reactivity of the activated species of Mn(TMPyP) together with its special and strong interaction with DNA are the clues of the DNA C−H bond activation chemistry of this chemical nuclease. The interaction of Mn(TMPyP) with DNA is dependent on the sequence of DNA. Thus, the Mn(TMPyP)/$KHSO_5$ system will shift from the hydroxylation of DNA C−H bonds to electron transfer reactions when the high-valent metal−oxo entity will be unable to reach the C−H bonds of deoxyriboses.

4.3.2. Interaction with DNA and DNA Oxidation

Because of the presence of two molecules of water as axial ligands on the manganese ion, Mn(TMPyP)[283] does not intercalate between the DNA base pairs like other aromatic and positively charged DNA ligands. Nevertheless, it is endowed with a high affinity for DNA due to the five positive charges. Binding constants are in the range of $\sim 10^6-10^7$ and $\sim 10^4-10^5$ for AT-rich and GC-rich regions of DNA, respectively.[12,17] The interaction of Mn(TMPyP) in the minor groove of B-DNA is at the origin of its stronger binding in AT-rich regions of DNA. The binding of Mn(TMPyP) in the minor groove is unfortunately not supported by structural data. Interaction in the minor groove of DNA for metalated *meso*-tetrakis-(4-*N*-methylpyridiniumyl)-porphyrins bearing axial ligands was deduced from circular or linear dichroism studies. Zn(TMPyP)[284] and Co(TMPyP)[285] lie at an angle of 62−67° and 42−45°, respectively, relative to the helix axis. This is compatible with groove binding outside of the helix without groove attribution. As will be detailed, the strongest argument in favor of the minor groove location of Mn(TMPyP) comes from its precise and nonambiguous chemical reactivity.[143,145] Molecular modeling studies of the interaction of the oxo−hydroxo−manganese active species with a duplex ODN of 5′-TCGTCAAACCGC/5′-GCGTTTGACGA sequence confirmed that minor groove interaction is possible for a diaxially liganded porphyrin (Figure 33A).[286] The

maganese−oxo porphyrin was docked within the minor groove of B DNA duplex. It can be seen on this model that the shape of the porphyrin ligand edge fits the form of the minor groove (Figure 33B). The porphyrin interface with the minor groove is devoid of any hydrogen-bond donor or acceptor groups but presents two methylpyridiniumyl positive substituents. The negative potential of the minor groove of DNA is known to attract positively charged molecules that are able to adopt the curvature of the groove (examples of these molecules are spermine, distamycin, netropsin, and polyamides).[287] The methylpyridiniumyl porphyrin belongs to this category of crescent-shaped DNA ligands. Three consecutive A·T base pairs constitute the minimum site of interaction of Mn(TMPyP). The binding constant of Mn(TMPyP) for a DNA site composed of at least three consecutive A·T base pairs was reported as high as 10^7 M^{-1}.[288]

While in interaction with DNA, the metal in the center of the porphyrin macrocycle is still accessible from the solvent and available for coordination by $KHSO_5$ (Figure 33C). Consequently, activation of the manganese porphyrin may take place at the site of reaction on DNA. Because the manganese−oxo entity may be located on either side of the porphyrin plane, the oxidation chemistry is possible on either strand of DNA. On the model, the distance between the oxo O-atom and the deoxyribose C−H bonds (C4′−H or C5′−H of both strands) is ∼3 Å. The chemical reactivity of $Mn(TMPyP)/KHSO_5$ has shown conclusively that the manganese porphyrin is able to attack the two strands of DNA, from the minor groove, at the minimum binding site of three consecutive A·T base pairs.[143,145] For convenience, it is referred to as an $(AT)_3$-box.

The striking point when looking at DNA cleavage by $Mn(TMPyP)/KHSO_5$ is that a cleavage event always occurs at the nucleoside located immediately at the 3′-position of an $(AT)_3$-box (Figure 33D).[146,288] This is observed on the two strands of DNA. DNA cleavage is not double-stranded. The attack of the manganese−oxo porphyrin takes place on a statistic basis on either strand from one binding interaction site. The 3′-shift of the cleavage on the two DNA strands is the signature of the minor groove location of the cleaving reagent. The mechanism of DNA cleavage is exclusively due to C5′−H hydroxylation of the deoxyribose unit located on the 3′-side of an $(AT)_3$-box, on both strands. The hydroxylated sugar corresponds to intermediate **78** in Figure 24. Radical species **74** together with the classical products derived from its trapping with O_2 are not observed with $Mn(TMPyP)/KHSO_5$. Intermediate **78** is the precursor of a direct strand break at ambient temperature and physiological pH. It is evidenced by the formation of two DNA fragments ending by a 5′-aldehyde nucleoside (**38**, Figure 24) and a 3′-phosphate DNA fragment, respectively. The aldehyde oxygen atom exchanges rapidly with water (Figure 24). C5′-oxidized product of the sugar, intermediate oxidized nucleoside (**79**) and furfural (**80**) (Figure 24), could be observed after a heating step at 90 °C and at pH 8, which induces two successive β-eliminations.[17,143,154]

An interesting extension of this sequence-specific reaction on DNA by $Mn(TMPyP)/KHSO_5$ is the possible reduction of the aldehyde function (**38**, Figure 24) into an alcohol so that the released DNA fragments end by a 5′-OH and a 3′-phosphate, respectively. This one-pot reaction (oxidation followed by a reduction step) is thus equivalent to a sequence selective hydrolysis of a phosphodiester bond of DNA.[145]

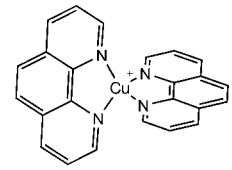

Figure 34. Structure of $Cu^I(phen)_2$.

Hydroxylation of the C1′−H bond of DNA deoxyriboses was first reported for $Mn(TMPyP)/KHSO_5$.[17] The resulting DNA products can be found in Figure 7. The C1′−H bond is located so deeply inside the double helix of DNA that it seems difficult to envision a direct access of the manganese−oxo entity to that bond without partial denaturation of DNA. Indeed, this chemistry takes place when the porphyrin reacts with single-stranded regions of DNA or under drastic conditions of double-stranded DNA damage. The C1′ chemistry could not be related to any particular site of interaction of the metallo−porphyrin. The typical product of C1′−H activation is 5-methylene-2-furanone (**5**, Figure 7). This C1′−H reaction allowed the analysis of the reactivity of the activated species of $Mn(TMPyP)/KHSO_5$ system. From labeling experiments in $H_2{}^{18}O$, it was found that the oxygen atom inserted in the C1′−H bond in **5** originated from the oxo−manganese entity.[65] Hydroxylation of the C1′−H bond is unambiguously due to an oxygen rebound mechanism from a formal Mn^V=O species (or oxomanganese^{IV} porphyrin cation radical) into the C1′−H bond.

The chemistry of this manganese porphyrin toward DNA is a clear example of the oxygen rebound chemistry for C−H bond activation by a biomimetic model of cytochrome P450. However, this incorporation of an oxygen atom from a metal−oxo into a C−H bond is only possible when the metal−oxo activated species can have access to a C−H bond. In DNA sequences devoid of $(AT)_3$-boxes[144,289] or when the porphyrin was covalently attached to an ODN,[17,290] the Mn^V=O undergoes an outer sphere electron transfer reaction with the guanine bases of DNA that are the sites of higher electron density on DNA.[17,291] In that case, the Mn^V=O porphyrin (or oxomanganese(IV) porphyrin cation radical) behaves like a biomimetic model of peroxidase and reacts by a two-electron transfer mechanism. The reaction is possible simply through electrostatic interaction between the positively charged porphyrin and the double helix of DNA. The active species of $Mn(TMPyP)/KHSO_5$, a unique Mn^V=O entity, never generates carbon-centered radicals at deoxyriboses.

4.4. Copper Phenanthroline

4.4.1. Structure and Activation

The DNA cleavage activity of Cu^I complexes of 1,10-phenanthroline (phen) with H_2O_2 as coreactant was initially observed by Sigman et al. in 1979.[292] They mediate principally single-strand cleavage on DNA through sugar oxidation. Two types of complexes are able to oxidize nucleic acids, $Cu^I(phen)$ and $Cu^I(phen)_2$, but the latter is clearly more efficient and is generally used (Figure 34).[15,16,55,57,293–295] Phen binds Cu^I ions with equilibrium constants log K_1 and log K_2 of 10.3 and 5.5, for $Cu^I(phen)$ and $Cu^I(phen)_2$ species, respectively.[296] These constants are 8.8 and 6.6 in the case of Cu^{II}.[297] Because of the small value of the second affinity constant, an excess of phen, with respect to copper, is often used to favor the $Cu(phen)_2$ species in diluted conditions. Analysis by X-ray diffraction of single-crystals showed that

Figure 35. DFT-optimized structures of $Cu^{I}(phen)_2$ and $Cu^{II}(phen)_2H_2O$.[300] The Cu^{II} complex appears here in trigonal bipyramid geometry. The oxidation of Cu^{I} to Cu^{II} induces large variation in the complex geometry. Reprinted with permission from ref 300. Copyright 2007 American Chemical Society.

the geometrical environment of the metal ion in $Cu^{I}(phen)_2$ is tetrahedral,[298] but the $Cu^{II}(phen)_2$ complex adopts different coordination geometries such as trigonal bipyramid or octahedron with one or two additional ligand(s) as H_2O or chloride.[299] Figure 35 shows examples of these structures and the large variation of the position of phen ligand around the copper center as a function the oxidation state.[300]

Early studies have established the reactants involved in DNA oxidation.[301] They were performed in the presence or the absence of O_2, H_2O_2, $HO^{\bullet}$ trap (alcohol), enzymes such as catalase, and superoxide dismutase or superoxide generator (the xantine/xantine oxidase system). According to the results, a succession of redox events has been proposed for the generation of the active species. The first step is the reduction of the initial Cu^{II}-complex into Cu^{I}-complex, which further reacts with dioxygen to form superoxide anion. In the following step, the Cu^{I}-complex undergoes an electron transfer reaction with superoxide anion, which produces H_2O_2. Finally, $Cu^{I}(phen)_2$ reacts with H_2O_2 and forms the active species that is able to cleave DNA. Only Cu^{I}-complex and H_2O_2 are necessary for DNA oxidation. The other reactants are merely involved in the generation of H_2O_2.

Despite the frequent use of $Cu(phen)_2$ as a cleaving agent, the exact nature of the reactive species involved in DNA cleavage is still unknown. According to reports on the detailed chemistry of the cleavage reaction, freely diffusible hydroxyl radicals are not responsible for the strand scission.[301,302] A copper bound oxidant, such as $Cu^{III}-OH$ (which is equivalent to a hydroxyl radical coordinated to a Cu^{II} ion) or $Cu^{I}-OOH$, is more likely, but $Cu^{III}=O$ species was also proposed (Figure 2). However, steric exclusion and close proximity between sugar residues and the copper center may explain that hydroxyl trapping agents could not inhibit the $Cu(phen)_2$-mediated reactions. Therefore, the involvement of free $HO^{\bullet}$ cannot be totally excluded.

4.4.2. Interaction with Nucleic Acids

Kinetic studies demonstrated that the nuclease activity of $Cu^{II}(phen)_2$ proceeds by an ordered mechanism: $Cu^{II}(phen)_2$ is first reduced to $Cu^{I}(phen)_2$, which binds reversibly to DNA. Oxidation of the noncovalently bound Cu^{I}-complex with hydrogen peroxide generates the reactive species responsible for DNA strand scission.[303] The association constant for DNA binding of $Cu^{I}(phen)_2$ was determined to be 4.7×10^4 M^{-1} (DNA base pairs).[304] However, $Cu^{II}(phen)_2$ also binds to DNA, but the direct reduction of the $Cu^{II}(phen)_2$/DNA complex by $O_2^{\bullet-}$ is very slow and can be neglected.[125]

The unsubstituted aromatic phenanthroline ligands of $Cu(phen)_2$ preclude hydrogen-bonding interactions with nucleobases as determinants of specificity. The inhibition of cleavage by intercalators suggested that the reaction might proceed through an intercalative complex.[301] DNA binding by intercalation was also strongly suggested by: (i) DNA-induced changes in the $Cu^{I}(phen)_2$ visible absorption spectrum and the induction of a strong $Cu^{I}(phen)_2$ circular dichroism spectrum; (ii) significant increase in DNA solution viscosity upon addition of $Cu^{I}(phen)_2$; and (iii) a binding-site size consistent with the neighbor-exclusion parameter $n \approx 2$ base pairs.[304] Protection of a cleavage zone by netropsin (a minor groove binder) or the lack of cleavage protection by *Eco*RI (which interacts with the major groove of the DNA) suggests a minor groove interaction of $Cu(phen)_2$.[125] The reaction mechanisms involving hydrogen atom abstraction at C1′, C4′, and C5′ of the deoxyriboses (which are located within the minor groove) as the main targets of the oxidative attack also support this positioning of the cleaver.

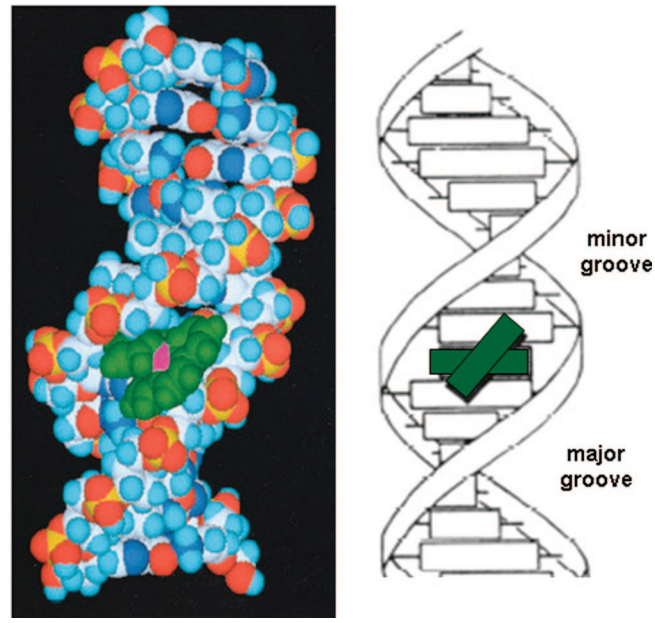

Figure 36. Modeling of the interaction of $Cu^{I}(phen)_2$ in the minor groove of DNA.[308,309] Phenanthroline and copper center appear in green and pink, respectively. Reprinted with permission from refs 308 and 309. Copyright 1996 and 1989 Elsevier.

$Cu^{I}(phen)_2$ is precluded by its tetrahedral geometry from full intercalation, but modeling of its interaction with double-stranded DNA has been performed from crystallographic values of $[Cu^{I}(phen)_2]ClO_4$. In this plausible model, one phen ligand partially intercalates at a 5′-TA-3′ step, and the angle of 50° between the two phen entities of the complex allows the other phen to favorably interact in the minor groove of DNA (Figure 36).[57,304–309] Unfortunately, the nature and therefore the geometry of the activated $Cu(phen)_2$ species being unknown, its interaction with DNA is not established.

The DNA cleavage activity of $Cu(phen)_2$ is sequence-dependent, but not nucleotide specific.[306,310] The only observed selectivity is related to a preference for minor groove binding at 5′-TAT-3′ triplets, which were cleaved intensively at the deoxyadenosine sugar ring. The related sequences 5′-TGT-3′, 5′-TAAT-3′, 5′-TAGPyr-3′, and 5′-CAGT-3′ were less cleaved, while 5′-CAT-3′ and 5′-TAC-3′ triplets, polypurine, and polypyrimidine sequences were cleaved at an even lower frequency.[306] This selectivity was correlated with local variation of base stacking free energy and minor groove size that favor the binding step.[308]

The B-DNA structure is the most easily cleaved DNA. A-DNA is less efficiently cleaved presumably because of fewer favorable contacts between the complex and the

widened minor groove of the A-form double helix. The A-structure, formed by RNA-DNA hybrids, is cleaved on both strands at roughly one-third of the rate observed for B-DNA under comparable conditions. In contrast, the left-handed Z-structure, with its deep narrow minor groove, is completely resistant to $Cu(phen)_2$ degradation.[311] Single-stranded DNA is a poor substrate.[301,312] The $Cu(phen)_2$ system is also able to cleave RNA with a preference for single-stranded loops relative to double-stranded A-structures present in RNA, but the detailed mechanism of cleavage is still unknown.[313]

4.4.3. DNA Oxidation

As expected for a minor groove binder, C−H bonds at C1′, C4′, and C5′ of deoxyriboses are the main targets of activated $Cu^I(phen)_2$.[15,16,55] Oxidation of polydA-dT first allowed the characterization of released nucleobases, and,[314] after a heating step or by freezing, an oxidized sugar residue, 5-methylene furanone **5** (5-MF), specific of C1′-oxidation, was observed by HPLC and GC−MS.[81] Using ^{18}O-enriched hydrogen peroxide and water, the carbonyl oxygen of 5-MF was found to derive from H_2O.[62] Control experiments in the presence of $Cu^I(phen)_2$, H_2O_2, and a reductant under anaerobic conditions showed that O_2 is not involved in the reaction. Fragments with 3′- and 5′-phosphate ends were characterized through enzymatic reactions and confirmed by PAGE analysis of cleavage products of 5′- or 3′-^{32}P-labeled double-stranded ODNs or restriction DNA fragments.[125] To accommodate these observations, the mechanism involving the successive compounds **1**, **2**, and **3** in Figure 7 was proposed. Use of mononucleotide model led Greenberg et al. to propose that $Cu(phen)_2$ itself catalyzes the first β-elimination on **3** producing strand breakage.[78] It was confirmed in the case of an activated Cu(3-Clip-Phen) derivative, which performs also direct strand cleavage from C1′-oxidation of DNA.[77] Deoxyribonolactone abasic sites **3** were nevertheless observed by Sugiyama et al. during HPLC coupled to electrospray MS analysis of oxidation products of a hexanucleotide duplex generated by activated $Cu(phen)_2$.[63] In this case, the resistance of the oxidized abasic site to the $Cu(phen)_2$-promoted direct strand cleavage was associated with the melting of the short duplex after its oxidation because **3** decreases the melting temperature of duplex DNA.[74,77]

Other sugar oxidation mechanisms were less studied. The frequent observation of 3′-phosphoglycolate fragments **37** with $Cu(phen)_2$ indicates C4′ oxidation of deoxyribose.[125] Although no detailed mechanistic study was performed with $Cu(phen)_2$, Figures 16, 17, and 19 propose different reaction pathways for its formation and were previously discussed. However, the observation of base propenal **45** has never been reported in the case of DNA oxidations by activated $Cu(phen)_2$. Sigman et al. failed to trap them (as well as malondialdehyde **48**, their hydrolysis product) with thiobarbituric acid, $NaBH_4$, dimedone, hydroxylamine, or carbodiimide.[125]

Two other oxidation pathways were characterized by Sugiyama et al. during HPLC coupled to electrospray MS analysis of a hexanucleotide duplex oxidized by $Cu(phen)_2$. From the observation of 4′-hydroxylated abasic site **47**, a C4′-carbocation **58** was proposed to be involved as an intermediate in the reaction, in analogy to C1′-DNA oxidation performed by activated $Cu(phen)_2$.[63] This corresponds to the mechanism depicted in Figure 21. However, in the case of DNA oxidation by activated $Cu(phen)_2$, this oxidation pathway seemed minor when compared to the pathway leading to the formation of 3′-phosphoglycolate fragment **37**. During the same experiment, the characterization of C5′-aldehydic fragment **38**, which yielded a 5′-hydroxyl-terminated fragment upon reduction with $NaBH_4$, proved C5′-oxidation (Figure 24). For $Cu(phen)_2$, this pathway seemed also a minor oxidative event. Because the oxidation of the initial radical to a carbocation was often involved in the case of DNA oxidation by activated $Cu(phen)_2$, we may propose that compound **38** arises also from oxidation of C5′-radical **74** to C5′-carbocation **75**, as the first steps of the reaction (Figure 24).

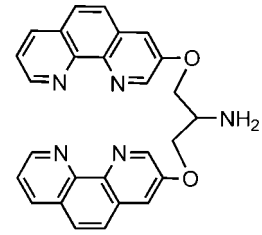

Figure 37. Structure of 3-Clip-Phen.

The C1′-oxidation pathway accounts for 80−90% of the scission events induced by $Cu^I(phen)_2$ (the other 10−20% are essentially related to a cleavage chemistry at C4′ producing 3′-phosphoglygolate fragments).[293,314] The relative importance of the two pathways depends on DNA sequence.[125] However, Monte Carlo simulation or cleavage of DNA duplex by diffusible species showed poor probability of H1′-abstraction, on the floor of the DNA minor groove, when compared to H4′ or H5′, which are clearly more exposed to solvent.[49,57,61,315] Deoxyribose oxidation results are thus in accordance with an activated $Cu(phen)_2$ species interacting in the minor groove floor (by intercalation), and with nondiffusible species (indeed, in the case of diffusible species such as HO•, a 3′-phosphoglycolate/3′-phosphate ratio of 1/1 has been observed).[16] Surprisingly, no kinetic isotope effect was found upon cleavage of DNA deuterated at either C1′, C2′−2″, or C4′ of thymidines residues, all positions from which hydrogen is lost during the course of the reaction, by either the 1:2 or the 1:1 cuprous:phenanthroline complexes.[316]

DNA base oxidations have been also reported for phenanthroline−copper complexes (unfortunately the use of Cu(phen) or $Cu(phen)_2$ is not clear from experimental data).[303,317] The importance of these oxidation events was not clearly compared to deoxyribose oxidation but seems minor.

4.4.4. Copper Clip-Phen

A solution to favor the 2 phen/Cu stoichiometry is to link the two phen entities by a bridge.[17] The position and the nature of the linker greatly influence the reactivity. A serinol bridge between the C3 carbon of phen, as in Cu(3-Clip-Phen) (Figure 37), is particularly efficient, and, in the presence of reductant and air, a significant increase (60 times) of the cleavage of supercoiled DNA was observed when compared to Cu(phen).[318,319] Single-strand cleavage was observed. Interestingly, DFT-optimization showed that the high reactivity of $Cu^{I/II}$(3-Clip-Phen) correlated to a weaker geometrical change during redox activity when compared to $Cu^{I/II}(phen)_2$ (Figure 38 to be compared with Figure 35 optimized in the same conditions).[300,320] $Cu^{I/II}$(3-Clip-Phen) appeared fairly planar during these analyses.

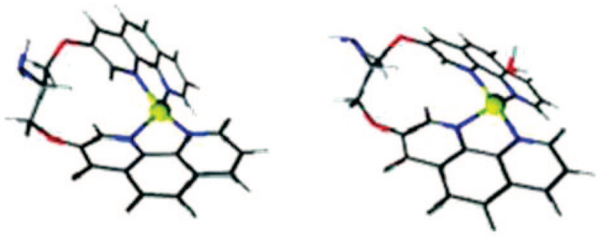

Figure 38. DFT-optimized structures of Cu^{I}(3-Clip-Phen) and Cu^{II}(3-Clip-Phen)H_2O.[300] At the difference of $Cu(phen)_2$ (Figure 35), the oxidation of the Cu^{I} to Cu^{II} induces poor variation in the complex geometry. Reprinted with permission from ref 300. Copyright 2007 American Chemical Society.

Quantifications of the number of single-strand breaks at different concentrations of complexes were in accordance with a system having no or poor DNA sequence selectivity as confirmed by PAGE analysis of ODNs cleaved Cu(3-Clip-Phen). Analysis of DNA oxidation products showed that Cu(3-Clip-Phen) interacts with the minor groove of the double-stranded DNA.[321] HPLC characterization of nucleobases, 5-MF (**5**, Figure 7) and furfural (**80**, Figure 24), showed that it performs C1′- and C5′-DNA oxidation. Quantification of released nucleobases showed that the system was catalytic. Characterization of 3′-phosphoglycolate fragments **37** indicated that this copper complex performed also C4′-oxidation (Figure 16), but this pathway was not associated with base-propenal release, although malondialdehyde (their hydrolysis product) was probably characterized through the chromophore that it forms with thiobarbituric acid. PAGE analysis of cleavage fragments of a 35-mer double-stranded ODN confirmed these data and showed that the system, similarly to activated $Cu(phen)_2$, performed direct strand breaks; 5′-phosphate, 3′-phosphate, and 3′-phosphoglycolate ends were observed. To detect nucleobase oxidation, if any, a heating step in piperidine 1 M was also performed, but no clear modification of the cleavage patterns was observed in accordance with a system preferentially mediating deoxyribose oxidation. It was proposed that Cu(3-Clip-Phen) produces >50% C1′-oxidation, ~15 ± 5% C4′-oxidation, and ~15 ± 5% C5′-oxidation of 2′-deoxyribose on double-stranded DNA.

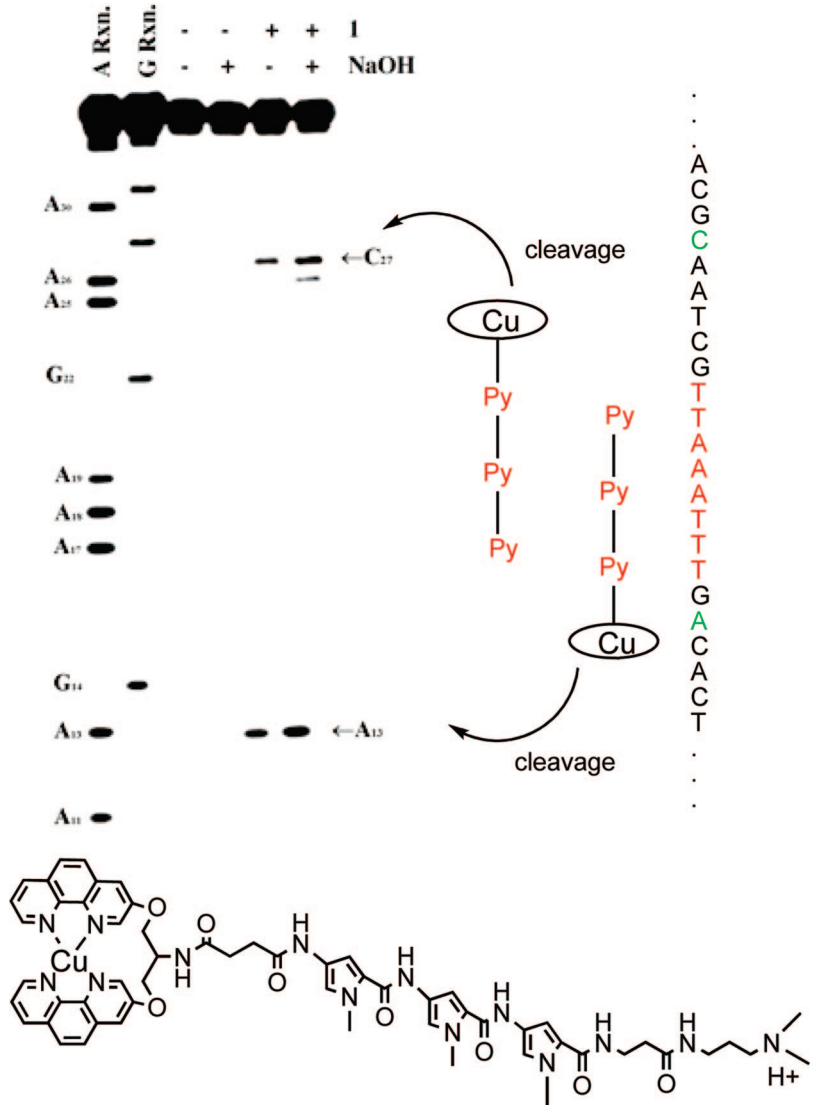

Figure 39. Sequence-selective DNA cleavage observed when Cu(3-clip-phen) is covalently linked to a distamycin analogue.[323] Trimethylpyrole (Py) part is an analogue of distamycin and interacts specifically with the A•T-rich region (in red). The minimum site contains at least 5 AT. This type of structure can interact as monomer or as head-to-tail dimer in the minor groove of DNA. This locates the copper DNA cleavage entity in proper orientation, which subsequently performs selective DNA oxidation on nucleoside highlighted in green. Reprinted with permission from ref 322. Copyright 2005 American Chemical Society.

Activated Cu(3-Clip-Phen) cleaves DNA without clear sequence selectivity, but the copper complex of a conjugate of 3-Clip-Phen with a distamycin analogue performs highly selective cleavage at sequences consisting of a succession of a minimum of 5 A·T base pairs (Figure 39).[322] This allowed an easier confirmation of these mechanisms of DNA oxidation by PAGE. Remarkably, the evolution of a 5′-aldehyde-fragment **38** was followed by its reduction with $NaBH_4$ or its transformation into a 5′-phosphate fragment upon alkaline heating (Figure 24).[321] Kinetic comparison with a DNA duplex including a deoxyribonolactone abasic site **3** at the specific cleavage site allowed Greenberg et al. to demonstrate that the system performs direct strand breakage from C1′-oxidation as proposed for activated $Cu(phen)_2$.[77,323] Clean cleavage patterns were also observed in accordance with the fact that the copper complex forms a nondiffusible active species responsible for the oxidation of duplex DNA.

5. Seeking Selective DNA Damage

Molecular recognition of DNA takes place in different ways: sugar−phosphate backbone binding, intercalation between the base pairs, selective interaction with nucleobases by hydrogen bonds, covalent binding, or metal coordination to these nucleobases. In B-DNA, interactions may arise from the major or the minor groove with consequences on the C−H bonds that are accessible to the oxidation by metal complexes. Finally, DNA can adopt other conformations such as A- or Z-forms, triple-helix, quadruplex DNA. It may also display not only Holliday, single−double, or double-triple strand junctions, but also bending, hairpin, bugles, or mismatches. All of these DNA organizations may be more or less selectively targeted by metal complexes. Selectivity may be due to the structure of the metal ligand, or it may be achieved through vectorization with a selective DNA binder[287,324,325] (a selective binding to RNA is also possible through the judicious choice of vector).[326] Many metal complexes able to abstract hydrogen atom from C−H bond of DNA have been optimized for better DNA interaction. Many interesting results have been obtained, but their number is too large. We have restricted the discussion on general rules and typical examples. Importantly, if an increase of activity or selectivity has always been clearly described, the influence of the metal complex modifications on the mechanisms of DNA oxidation (sugar versus nucleobases) has unfortunately been rarely reported.

Many metal complexes show special design allowing particularly selective DNA interactions. For instance, a Mn-porphyrin including four cationic flexible arms targets quadruplex DNA,[327] Λ-$Ru^{III}(DIP)_3$ or Λ-$Co^{III}(phen)_3$ complexes interact with Z-DNA,[328,329] and dinuclear copper complexes coordinate guanines at single/double-strand junction.[330,331] However, different chemical modifications may be envisioned on a pre-existing redox-active metal complex to increase DNA affinity or to make interaction with DNA more selective. Cationic charges on the metal complexes allow electrostatic attraction for the negatively charged DNA and constitute a major contribution to the binding process. The probably simplest modification that can be done on the metal ligand is the incorporation of amino residues that can be protonated at physiological pH (Figure 40). An additional advantage is to increase the water solubility of the metal complex where necessary. A slightly more sophisticated modification consists of addition of guanidinium residues (guanidinium group is responsible for the

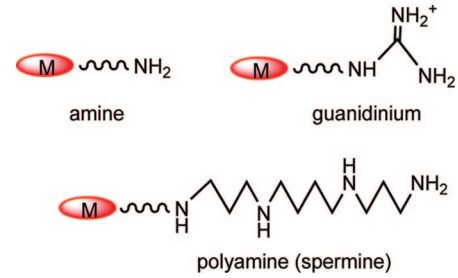

Figure 40. Small modifications increasing DNA affinity: incorporation of amines on the ligand. Red balloons represent the redox-active metal complex.

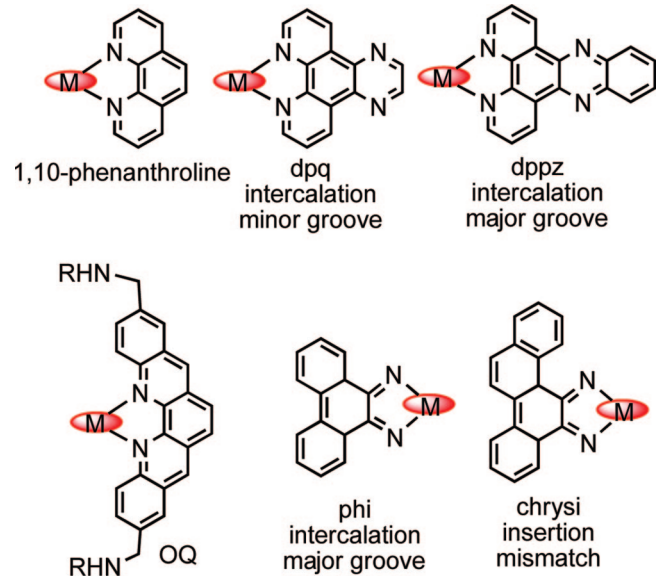

Figure 41. Some typical examples of the extension of the macrocyclic metal ligand to increase or change the affinity or site selectivity of DNA dammage. Only the macrocycle directing the interaction with DNA is shown. Red balloons stand for the other parts of the redox-active metal complex. Macrocycle DNA interactions are indicated.

binding of histones to DNA through arginine residues, and a guanidinium group is found in BLM B2).[332] The guanidinium group interacts electrostatically with phosphate oxygens. Besides, hydrogen bondings with N7 and O6 of guanine (in the DNA major groove) or O2 of thymine (in the minor groove) are often observed for DNA binders. The type of interaction (phosphate or nucleobases) will depend on the other parts of the metal complex that are endowed with their own possibilities of interaction. The linkage of natural polyamines, such as spermine or spermidine, that interact with DNA in vivo have also increased the DNA affinity and the activity of various metal complexes (Cu(Clip-Phen),[333,334] Mn(TMPyP)[335] derivatives...). Interestingly, polyamines can be used as linker for the preparation of conjugates between a metal complex and a DNA binding moiety, therefore increasing the efficiency of DNA damage.[336]

Change in the interaction site of the metal complex with DNA or increase of this interaction can be achieved, in the case of aromatic metal ligand, by extension of the ligand. Indeed, increasing the surface area of the aromatic ligand leads to a substantial enhancement of the intercalative binding affinity. However, the size of the ligand can also induce a change in the site of intercalation. This strategy was first developed by Barton's group.[106,337] The optimization was performed with different octahedral metal complexes and in

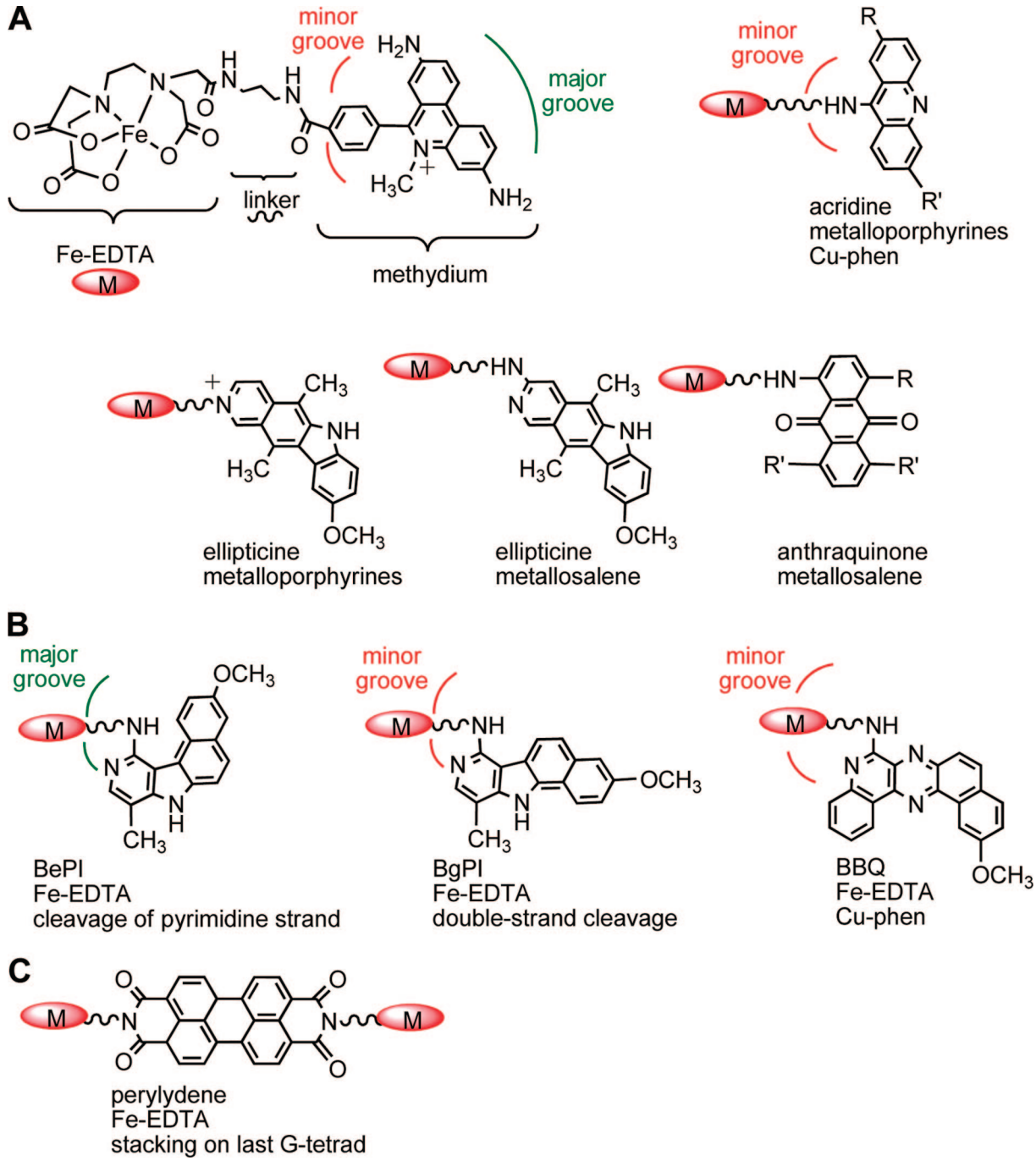

Figure 42. Some typical examples of intercalating agents that have been linked to redox-active metal complexes to target (A) double-stranded DNA, (B) triple helix, and (C) quadruplex DNA. Red balloons stand for the redox-active metal complexes (typical examples that have been used are indicated). Orientation in DNA grooves is discussed in the text.

particular with rhodium complexes able to abstract hydrogen atom at C−H bonds upon light irradiation. Figure 41 shows two typical examples. The first one concerns the dipyrido[2,2′-*d*:2′,3′-*f*]quinoxaline ligand (dpq), which contains one additional aromatic ring compared to phen. Both complexes interact in the minor groove of DNA. Chakravarty et al. also observed an increase of oxidative activity against DNA for ternary copper(II) complexes (CuLL′) where a phenanthroline ligand (L) was replaced by dpq.[338–340] This shows that the increase of affinity for DNA could be a general rule when metal complexes include dpq instead of phen. When dpq was extended with another aromatic cycle to give the larger dipyrido[3,2-*a*:2′,3′-*c*]phenazine ligand (dppz), the octahedral metal complex interacted in the major groove. Rh-complexes including dppz allowed the description of the C3′-oxidation pathway due to the selective binding of this ligand in the DNA major-groove. It can be noted here that the high DNA cleavage activity of a copper-*ortho*-quinacridine complex [Cu(OQ)] developed by Lehn's group, where the metal ion ligand consists of two fused acridine motifs forming an extended phen ligand, belongs also to the same ligand extension strategy.[341] Another example involves extension of 5,6-phenanthrenequinone diimine macrocycle (phi). $Rh^{III}(L_2phi)$ complexes interact with the major groove of DNA, but their selectivity can be modulated by the other ancillary ligands L. The larger chrysene-5,6-quinone diimine ligand (chrysi) interacts with DNA mismatches, abasic sites, or single base bulges because it is too sterically bulky to

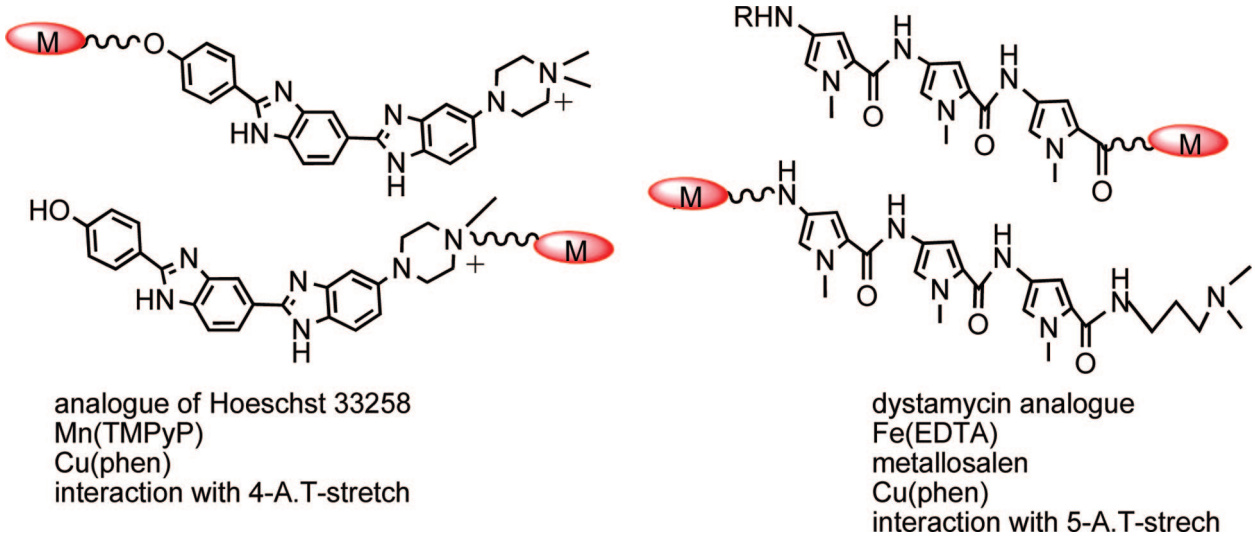

Figure 43. Two typical examples of DNA minor-groove binders that have been linked to redox-active metal complexes. Red balloons stand for the redox-active metal complexes (typical examples that have been used are indicated).

efficiently intercalate into standard B-form DNA.[342] On DNA mismatches, an insertion via the minor groove associated with ejection of the two bases of the mismatch has been characterized by X-ray diffraction.[343]

However, increase of DNA affinity or sequence selectivity is more generally achieved by coupling the metal complex to a DNA binding moiety. Thus, many conjugates of metal complexes with DNA-intercalating agents have been prepared. Some typical examples are shown in Figure 42. Most famous results relate probably to the methidium conjugate of Fe(EDTA) that improves by several orders of magnitude the DNA cleavage efficiency of the negatively charged Fe(EDTA), which has no affinity for DNA by itself. In the case of supercoiled pBR322 DNA, this increase reached between 2 and 3 order of magnitude when ascorbate was used as a reductant.[190] Methidium, acridine, ellipticine, and anthraquinone are some typical intercalators that were used to target successfully a metal complex [Fe(EDTA),[190] metallo-porphyrin,[82,344–346] Cu(phen) derivatives,[347] Cu(salen)[348,349]] toward B-DNA double helix. The length and position of the linker are critical for a good positioning of both parts of the conjugate with respect to DNA and, therefore, for an efficient compound. It can also favor some oxidation pathway as on Fe-EDTA-methydium and conjugates on amino-group of acridine where the covalent attachment of the metal complex to an intercalating moiety can orient the metal reactive part in the minor groove for hydrogen abstraction at C1′, C4′, or C5′ of the deoxyribose unit.[350] Special DNA organizations can be also targeted by incorporation of specific intercalator in the conjugates. Thus, benzopyridoindole BePI[351] and BgPI[351] or benzoquinoquinoxaline (BQQ) efficiently bind DNA-triple helix.[352–354] A comparison of triple helix DNA cleavage by Fe-EDTA-BePI and Fe-EDTA-BgPI has shown that the oxidative events on DNA depend on the choice of the intercalator. Indeed, Fe-EDTA-BePI conjugate cleaves the pyrimidine strand of a DNA duplex target, converted to a triplex by hybridization with a specific pyrimidine-rich ODN, whereas Fe-EDTA-BgPI conjugate performs cleavage on both pyrimidine- and purine-rich strands of the same DNA target. The conjugate between Fe(EDTA) and perylidene was directed toward quadruplex DNA structures by stacking interaction of the perylidene moiety with the last guanine-tetrad.[355]

In the case of B-DNA duplex, the covalent attachment of a metal complex to an intercalating agent generally results in poor sequence selectivity. Higher selectivity has been attained by conjugation to minor-groove DNA binders such as Hoechst 33258 [for Mn-TMPyP[356] or Cu(phen)[357] conjugates] or distamycin analogues [for Fe(EDTA),[358] metallosalen,[359] or Cu(phen) conjugates[322]] that interact selectively with 4 and 5 successive A•T base pairs, respectively, in the DNA minor groove (Figure 43). Interestingly, mechanistic study concerning a conjugate of Cu(3-Clip-Phen) with a distamycin analogue showed that the conjugated molecule selectively directed the metallo-complex toward A•T tract and that the capacity of the Cu(3-Clip-phen) part to oxidize DNA by hydrogen atom abstraction at C1′, C4′, and C5′ in the minor groove was maintained.[127] On the other hand, the results obtained with a conjugate between distamycin and a Cu(salen) reflects the difficulties that can be encountered in the design of conjugates: although the conjugate was able to bind selectively to A•T-rich sequences, as confirmed by footprinting experiments, the DNA cleavage by the conjugate, activated by a reductant in the presence of air, was surprisingly weakly selective.[359] This may be due to a problem of linker optimization.

On the model of DNA recognition by distamycin that interacts (as monomer or dimer) by hydrogen bonding with nucleobases in the minor groove, Dervan's group has optimized minor-groove oligopeptidic binder with varied DNA-sequence selectivity (Figure 44).[287,360] When conjugated to Fe(EDTA), they mediated sequence selective DNA cleavage of a large variety of sequences.[361,362] However, this strategy is limited due to the fact that, when the polypeptide length increases, the interaction with duplex DNA is less optimal. In fact, the polypeptide is a bit over curved when compared to DNA duplex, and above approximately seven base pairs the interaction is less favorable.

In fact, selectivity for long DNA sequence is accessible by conjugation of the metal complex with an oligodeoxynucleotide or an analogue of oligonucleotide (such as PNA, methylphosphonate...). Indeed, the relation between the size of the binding site of an oligonucleotide and the number of distinguishable sequences is related to its length. A 7-mer (that recognizes a DNA sequence of the same length as distamycin) and a 15-mer have a unique site of interaction

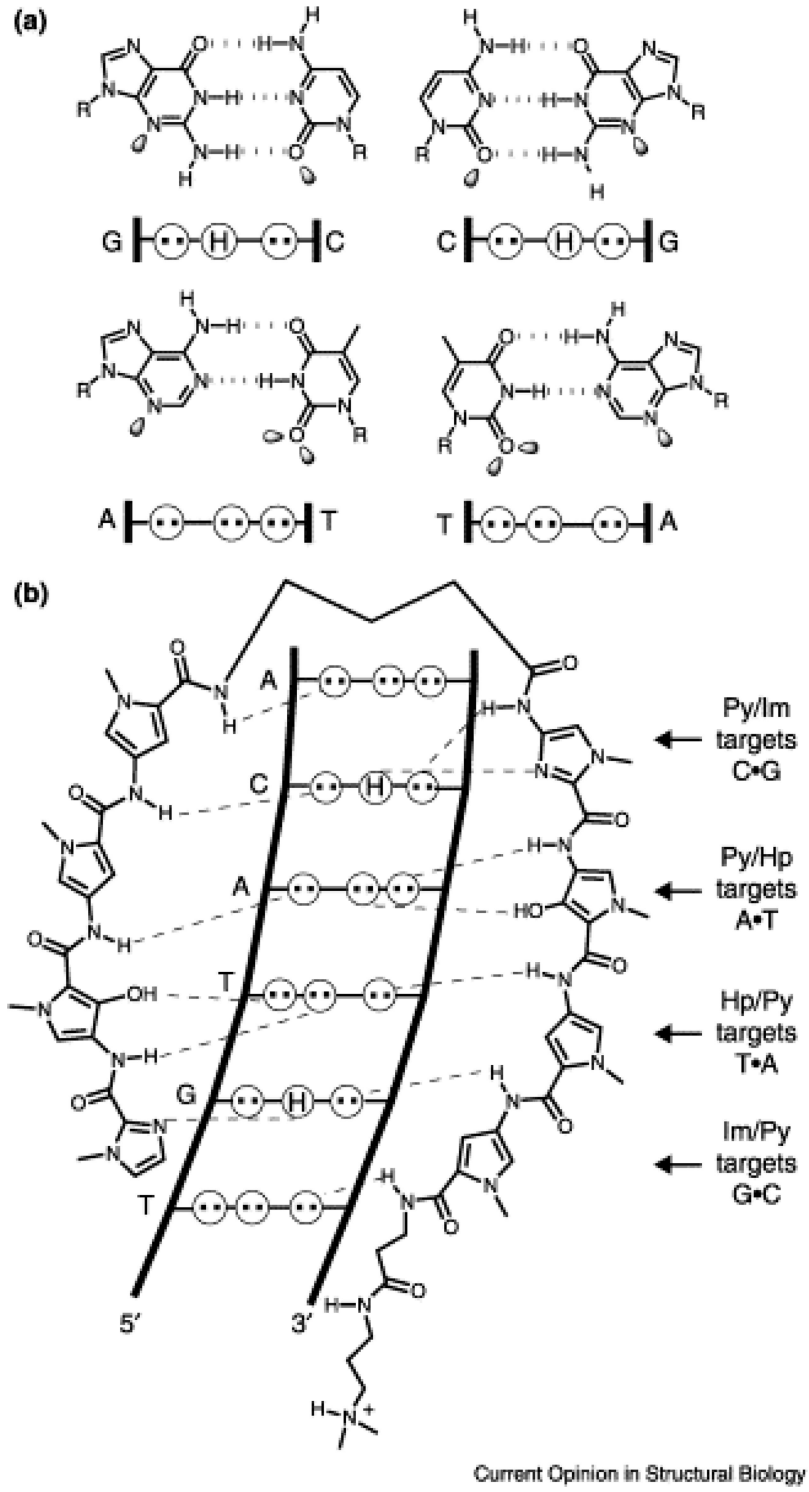

Figure 44. Molecular recognition of the minor groove of DNA. (a) Minor groove hydrogen-bonding patterns of Watson−Crick base pairs. Circles with dots represent lone pairs of N(3) of purines and O(2) of pyrimidines, and circles containing a H represent the 2-amino group of guanine. The R group represents the sugar−phosphate backbone of DNA. Electron lone pairs projecting into the minor groove are represented as shaded orbitals. (b) Binding model for the complex formed between ImHpPyPy-β-ImHpPyPy-β-Dp and a 5′-TGTACA-3′ sequence. Putative hydrogen bonds are shown as dashed lines.[360] Reprinted with permission from ref 360. Copyright 2003 Elsevier.

every 8192 and 536 870 912 nucleotides, respectively, if all four Watson−Crick base pairs are uniformly present! Thus, the formation of Watson−Crick base pairs allows a metal complex covalently bound to an oligonucleotide to select single-stranded DNA with a high specificity. This strategy was used to target a large number of metal complexes such as Fe(EDTA),[363–365] Cu(phen),[366,367] metallo-porphyrin,[368–373] and iron bleomycin.[374] For synthesis facility, coupling was often performed at the end of the oligonucleotide vector, although this position affords different types of orientation for the metal complex toward the DNA target (Figure 45). If one of these interactions dominates, it can change totally the oxidation pathway of a metal complex as observed for instance for some conjugates between ODNs and a Mn(T-MPyP) derivative.[370] In its free form, the activated metal complex attacks selectively hydrogen atom at the C5′ of three successive A·T base pairs, whereas guanine oxidation in the single-stranded part of the DNA target was observed in the

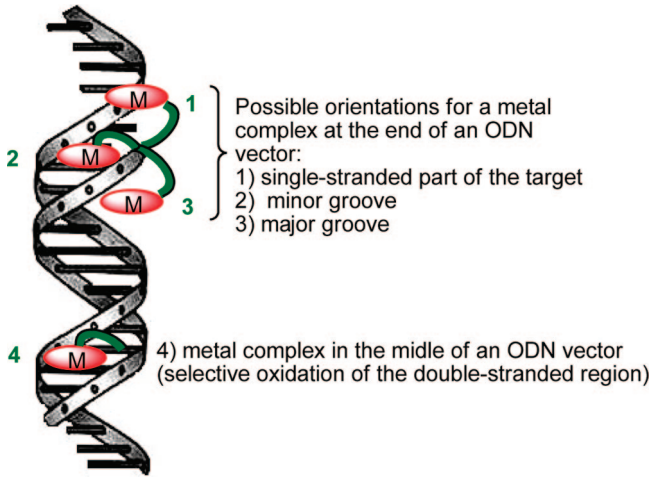

Figure 45. Possible orientations of the redox-active metal complex (red balloon) for conjugates with ODN hybridized with a single-stranded DNA target.

case of the conjugate molecule. Generally, better selectivity for the double-stranded part of the conjugate/target hybrid was obtained for conjugates where the metal complex was included in the middle of the vector sequence. Thus, the DNA oxidation activity of Cu(phen) linked to the N2 of a guanine residue has been efficiently directed in the minor groove of the duplex.[367]

However, when sequence selective oxidation of a DNA duplex target is desired, a triple helix strategy is necessary.[375] It was used successfully with Fe(EDTA),[287,376] Cu(phen),[357,377–380] or metallo-porphyrins[336] as some typical examples. Unfortunately, except if unnatural nucleobases are used,[378,381] this strategy limits the choice of the vector sequence to homopurines or homopyrimidines that are able to interact by Hoogsteen or reverse Hoogsteen interaction in the major groove of homopurine−homopyrimidine sequences of DNA duplex (Figure 46). In addition, the poor stability of DNA triplex lowers the potential of this strategy. The location of the metal complex in the DNA major groove can also have large consequences for the accessibility of the C−H bonds of the duplex target. At this point of the discussion, it can be underlined that a useful alternative is to use a conjugate of the metal complex to an intercalator that is selective for triple helix. Advantages are that these intercalators can stabilize the triplex, and, for some of them, a minor groove orientation can be easily obtained (as for BgPI or BQQ, Figure 42). However, when compared to an oligonucleotide conjugate where the metal complex oxidizes the target duplex only on some base pairs around its link, all of the triplex sequence will be oxidized by the metal complex−intercalator conjugate. Moreover, if an in vivo use is projected, the metal complex−intercalator is restricted to DNA sequence forming "spontaneous triplex", although different other parts of the DNA are probably also accessible with a metal complex−oligonucleotide conjugate.

At this stage, we have to say that an important problem for all of the conjugates with a metal complex able to oxidize DNA, but, obviously, more particularly in the case of conjugates with oligonucleotides, is self-degradation. Self-degradation can release active but unselective metal complex in the experimental medium. Attempts to circumvent this problem may consist of optimization of the linker, use of unnatural oligonucleotides, or metal complexes unable to oxidize single-stranded DNA.

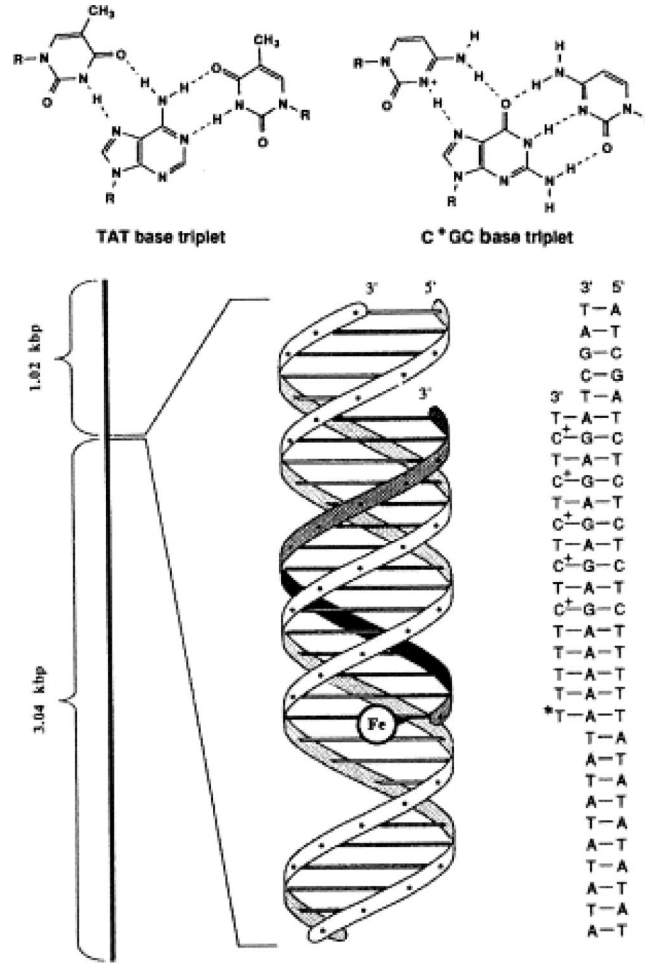

Figure 46. Interaction of a conjugate between a redox-active metal complex and an oligonucleotide with a DNA duplex: triple-helix strategy. (Top) The pyrimidine triple helix motif. Isomorphous base triplets of TAT and CGC. The additional pyrimidine strand is bound by Hoogsteen hydrogen bonds in the major groove to the complementary purine strand of the Watson−Crick duplex.[287] Reprinted with permission from ref 287. Copyright 2001 Elsevier.

Apart from oligonucleotides, proteins are alternative macromolecules able to selectively target large DNA sequences. Different conjugates between proteins showing DNA affinity (Hin recombinase,[382] GCN4 transcriptional activator,[383] Cro and CAP gene activator protein,[384–386] staphylococcal nuclease,[387,388] LexA repressor,[389] Trp repressor,[390] yTBP TATA box binding protein,[391] and NarL response regulatory protein[392]) and Fe(EDTA) or Cu(phen) have been prepared and oxidize selectively DNA around the interaction site of the protein. Metal complex was selectively linked in a covalent way to a well-defined amino acid residue of the protein. Analysis of DNA oxidation allowed the determination of the interaction of this amino acid residue with DNA.

A final strategy for targeting a metal complex to bind DNA consists of the preparation of conjugates with agents able to form a covalent linkage with DNA (Figure 47). Linking of the pyrrolobenzodiazepine alkylating agent to Fe(EDTA) allowed sequence-selective DNA cleavage.[393] DNA adducts were observed for conjugates of Rh-complexes including an alkylating nitrogen mustard[394] or a cisplatin derivative,[395] and they were associated with DNA cleavage (due to photoactivation by rhodium complex) near mismatched nucleotides of the interaction site of the chrysi part of the metal complex.

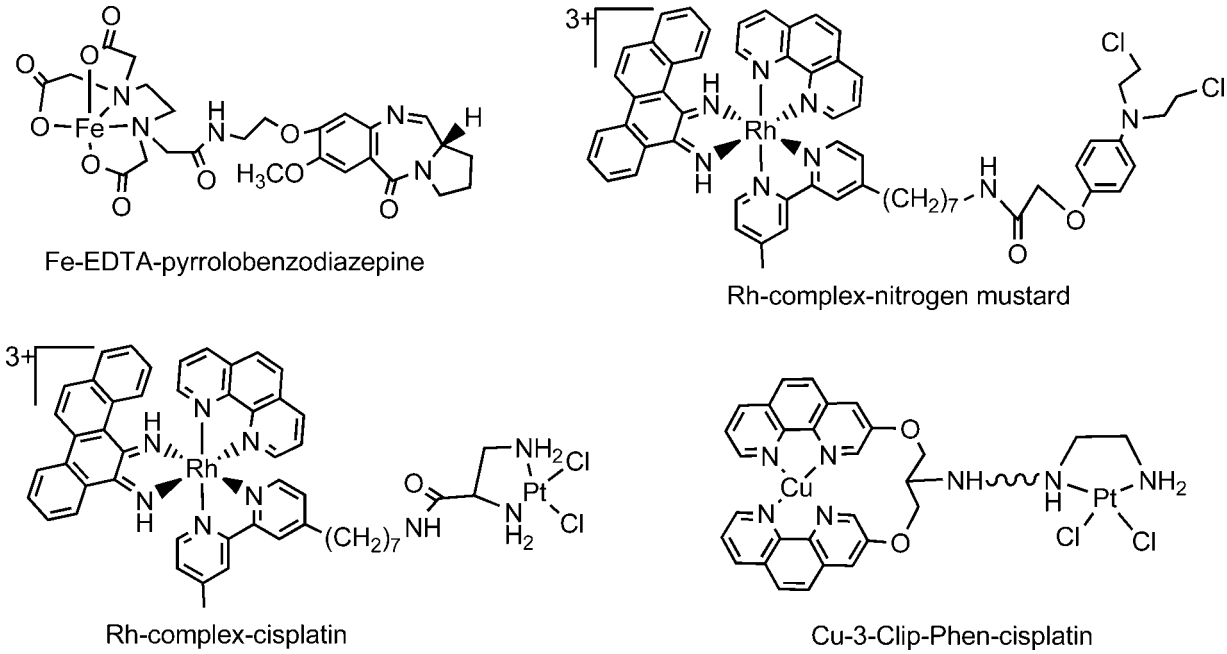

Figure 47. Conjugates of metal complexes with agents able to form covalent links with DNA.

Interesting results were also obtained for conjugates between Cu(3-Clip-Phen) and cisplatin derivative. Conjugation to platinum(II) complexes gave rise to compounds where the platinum part forms covalent adducts essentially at 5′-GG-3′ steps. This anchored the Cu(3-Clip-phen) system performed DNA cleavage restricted to the region of the covalent anchorage. Because the copper system is catalytic, a cluster of DNA oxidation events was produced, and consequently a large increase of the number of "direct" double-strand cleavage events was observed on supercoiled DNA when compared to Cu(3-Clip-phen).[396–398]

In summary, all of these examples show that it is possible to modulate DNA damage mediated by metal complexes with a variety of modifications at different positions. The design of the linker is also of great importance for conjugates with DNA-binders. Modern tools such as molecular modeling may play a part in the optimization of future DNA cleaving agents with tailored specificity.

6. Conclusion

Targeting DNA for C−H bond activation at deoxyribose units with a metal complex is not an easy task. It demands a careful design of the ligand so that the metal complex is a good catalyst and so that a precise fit between the metal center and DNA is achieved. Inspired by bleomycin, a number of metal complexes have been prepared, but none of them have proved fully satisfactory. In general, the poor interaction between the metal complex and DNA did not allow a proper positioning of the metal center with respect to the C−H bond of DNA, and DNA damage was mainly due to radical chemistry (hydroxyl radical production). Despite many efforts, the field of DNA damage by metal complexes led only to the discovery of a few new efficient artificial DNA nucleases within the last 40 years as the two compounds described in this Review. The simplicity of the structure of copper phenanthroline and manganese porphyrin is somehow in contrast to their efficiency as compared to the natural compound bleomycin. However, both of them are endowed with the necessary properties for efficient DNA nucleases. An artificial nuclease must be a strong DNA binder and a strong chelating agent. The metal catalyst must be capable of efficient oxygen activation. Furthermore, it must interact with DNA in such a way that it is within reach of a C−H bond and that it can be activated at the site of its interaction with DNA. A powerful DNA cleaving agent is the result of a sum of structural and chemical parameters, and any structural modification may lower its efficiency. As exemplified in the case of structural modifications of bleomycin or in the case of the various conjugates of metal complexes with sequence selective targeting units, the covalent attachment of a metal complex, itself active as a free reagent, to a DNA binding moiety in general ends up with a change in the positioning of the metal core with respect to DNA double helix and to a modification of the chemistry of DNA damage. At present, the field of artificial nucleases remains a vast challenge for bioinorganic chemists not only at the level of the molecular design of single-strand DNA cleaving agents but at the level of double-strand cleavage of DNA because nature always conceived antibiotic DNA cleavers based on their potency to mediate double-strand breaks.

7. Abbreviations

$(AT)_3$-box	three consecutive A·T base pairs
β-Ala	β-aminoalanine
BePI	benzo[*e*]pyridoindole
BgPI	benzo[*g*]pyridoindole
Bipy	2,2′-bipyridine
BLM	bleomycin
BQQ	benzoquinoquinoxaline
chrysi	chrysene-5,6-quinone diimine
$d^{Br}U$	5-bromodeoxyuridine
DFT	density functional theory
DIP	4,7-diphenyl-1,10-phenanthroline
$d^{I}U$	5-iododeoxyuridine
dpq	dipyrido[2,2′-*d*:2′,3′-*f*]quinoxaline
dppz	dipyrido[3,2-*a*:2′,3′-*c*]phenazine
EDTA	ethylenediaminetetraacetic acid
en	ethylenediamine
ET	electron transfer
β-OH His	β-hydroxyhistidine

KIE	kinetic isotope effect
ODN	oligodeoxyribonucleotide
OQ	*ortho*-quinacridine
$P^{+\bullet}$	porphyrin cation radical
PAGE	polyacrylamide gel electrophoresis
phen	1,10-phenanthroline
phi	9,10-phenanthrenequinone
PNA	peptide nucleic acid
Pyr	pyrimidine
Salen	salicyldialdehyde ethylenediimine
TMPyP	dianion of *meso*-tetrakis(4-methylpyridiniumyl)porphyrin ligand

8. Acknowledgments

We thank Dr. Bernard Meunier for his past guidance and are deeply indebted to the collaborators and co-workers whose names are listed in several references of this Review.

9. References

(1) Poulos, T. L. In *The Porphyrin Handbook*; Kadish, K. M., Smith, K. M., Guillard, R., Eds.; Academic Press: San Diego, CA, 2000; Vol. 4, Chapter 32, pp 189−218.
(2) Meunier, B.; de Visser, S. P.; Shaik, S. *Chem. Rev.* **2004**, *104*, 3947.
(3) Denisov, I. G.; Makris, T. M.; Sligar, S. G.; Schlichting, I. *Chem. Rev.* **2005**, *105*, 2253.
(4) Shaik, S.; Kumar, D.; de Visser, S. P.; Altun, A.; Thiel, W. *Chem. Rev.* **2005**, *105*, 2279.
(5) Costas, M.; Mehn, M. P.; Jensen, M. P.; Que, L., Jr. *Chem. Rev.* **2004**, *104*, 939.
(6) Abu-Omar, M. M.; Loaiza, A.; Hontzeas, N. *Chem. Rev.* **2005**, *105*, 2227.
(7) Krebs, C.; Galonic Fujimori, D.; Walsh, C. T.; Bollinger, J. M., Jr. *Acc. Chem. Res.* **2007**, *40*, 484.
(8) Que, L., Jr.; Tolman, W. B. *Nature* **2008**, *455*, 333.
(9) Solomon, E. I.; Chen, P.; Metz, M.; Lee, S. K.; Palmer, A. E. *Angew. Chem., Int. Ed.* **2001**, *40*, 4570.
(10) Klinman, J. P. *J. Biol. Chem.* **2006**, *281*, 3013.
(11) Mishina, Y.; He, C. *J. Inorg. Biochem.* **2006**, *100*, 670.
(12) Meunier, B.; Robert, A.; Pratviel, G.; Bernadou, J. In *The Porphyrin Handbook*; Kadish, K. M., Smith, K. M., Guillard, R., Eds.; Academic Press: San Diego, CA, 2000; Vol. 4, Chapter 31, pp 119−187.
(13) Groves, J. T. *J. Inorg. Biochem.* **2006**, *100*, 434.
(14) Stubbe, J.; Kozarich, J. W. *Chem. Rev.* **1987**, *87*, 1107.
(15) Pratviel, G.; Bernadou, J.; Meunier, B. *Angew. Chem., Int. Ed. Engl.* **1995**, *34*, 746.
(16) Pogozelski, W. K.; Tullius, T. D. *Chem. Rev.* **1998**, *98*, 1089.
(17) Pitié, M.; Boldron, C.; Pratviel, G. *Adv. Inorg. Chem.* **2006**, *58*, 77.
(18) Newcomb, M.; Toy, P. H. *Acc. Chem. Res.* **2000**, *33*, 449.
(19) Chandrasena, R. E.; Vatsis, K. P.; Coon, M. J.; Hollenberg, P. F.; Newcomb, M. *J. Am. Chem. Soc.* **2004**, *126*, 115.
(20) Jin, S.; Bryson, T. A.; Dawson, J. H. *J. Biol. Inorg. Chem.* **2004**, *9*, 644.
(21) Song, W. J.; Ryu, Y. O.; Song, R.; Nam, W. *J. Biol. Inorg. Chem.* **2005**, *10*, 294.
(22) Li, C.; Wu, W.; Kumar, D.; Shaik, S. *J. Am. Chem. Soc.* **2006**, *128*, 394.
(23) Hirao, H.; Kumar, D.; Que, L., Jr.; Shaik, S. *J. Am. Chem. Soc.* **2006**, *128*, 8590.
(24) Klinker, E. J.; Shaik, S.; Hirao, H.; Que, L., Jr. *Angew. Chem., Int. Ed.* **2009**, *48*, 1291.
(25) Park, M. J.; Lee, J.; Suh, Y.; Kim, J.; Nam, W. *J. Am. Chem. Soc.* **2006**, *128*, 2630.
(26) Seo, M. S.; Kamachi, T.; Kouno, T.; Murata, K.; Park, M. J.; Yoshizawa, K.; Nam, W. *Angew. Chem., Int. Ed.* **2007**, *46*, 2291.
(27) Prigge, S. T.; Eipper, B. A.; Mains, R. E.; Amzel, L. M. *Science* **2004**, *304*, 864.
(28) Crespo, A.; Marti, M. A.; Roitberg, A. E.; Amzel, L. M.; Estrin, D. A. *J. Am. Chem. Soc.* **2006**, *128*, 12817.
(29) Traylor, T. G.; Xu, F. *J. Am. Chem. Soc.* **1990**, *112*, 178.
(30) Fitzpatrick, P. F. *Biochemistry* **2003**, *42*, 14083.
(31) Chen, K.; Que, L., Jr. *J. Am. Chem. Soc.* **2001**, *123*, 6327.
(32) Chen, K.; Costas, M.; Kim, J.; Tipton, A. K.; Que, L., Jr. *J. Am. Chem. Soc.* **2002**, *124*, 3026.
(33) Mas-Balleste, R.; Que, L., Jr. *J. Am. Chem. Soc.* **2007**, *129*, 15964.
(34) Bassan, A.; Blomberg, M. R.; Siegbahn, P. E.; Que, L., Jr. *Chem.-Eur. J.* **2005**, *11*, 692.
(35) Bernadou, J.; Fabiano, A. S.; Robert, A.; Meunier, B. *J. Am. Chem. Soc.* **1994**, *116*, 9375.
(36) Bernadou, J.; Meunier, B. *Chem. Commun.* **1998**, 2167.
(37) Que, L., Jr. *Acc. Chem. Res.* **2007**, *40*, 493.
(38) Nam, W. *Acc. Chem. Res.* **2007**, *40*, 522.
(39) Eser, B. E.; Barr, E. W.; Frantom, P. A.; Saleh, L.; Bollinger, J. M., Jr.; Krebs, C.; Fitzpatrick, P. F. *J. Am. Chem. Soc.* **2007**, *129*, 11334.
(40) Kaizer, J.; Klinker, E. J.; Oh, N. Y.; Rohde, J. U.; Song, W. J.; Stubna, A.; Kim, J.; Munck, E.; Nam, W.; Que, L., Jr. *J. Am. Chem. Soc.* **2004**, *126*, 472.
(41) Oh, N. Y.; Suh, Y.; Park, M. J.; Seo, M. S.; Kim, J.; Nam, W. *Angew. Chem., Int. Ed.* **2005**, *44*, 4235.
(42) Tiago de Oliveira, F.; Chanda, A.; Banerjee, D.; Shan, X.; Mondal, S.; Que, L., Jr.; Bominaar, E. L.; Münck, E.; Collins, T. J. *Science* **2007**, *315*, 835.
(43) Yoon, J.; Wilson, S. A.; Jang, Y. K.; Seo, M. S.; Nehru, K.; Hedman, B.; Hodgson, K. O.; Bill, E.; I., S. E.; Nam, W. *Angew. Chem., Int. Ed.* **2009**, *48*, 1257.
(44) Evans, J. P.; Ahn, K.; Klinman, J. P. *J. Biol. Chem.* **2003**, *278*, 49691.
(45) Chen, P.; Solomon, E. I. *J. Am. Chem. Soc.* **2004**, *126*, 4991.
(46) Yoshizawa, K.; Kihara, N.; Kamachi, T.; Shiota, Y. *Inorg. Chem.* **2006**, *45*, 3034.
(47) Rolff, M.; Tuczek, F. *Angew. Chem., Int. Ed.* **2008**, *47*, 2344.
(48) Cramer, C. J.; Tolman, W. B. *Acc. Chem. Res.* **2007**, *40*, 601.
(49) Balasubramanian, B.; Pogozelski, W. K.; Tullius, T. D. *Proc. Natl. Acad. Sci. U.S.A.* **1998**, *95*, 9738.
(50) von Sonntag, C. *Free-Radical-induced DNA Damage and its Repair, A Chemical Perspective*; Springer-Verlag: Berlin, Heidelberg, New York, 2006.
(51) Dedon, P. C.; Goldberg, I. H. *Chem. Res. Toxicol.* **1992**, *5*, 311.
(52) Beckwith, A. L.; Crich, D.; Duggan, P. J.; Yao, Q. *Chem. Rev.* **1997**, *97*, 3273.
(53) Greenberg, M. M. *Org. Biomol. Chem.* **2007**, *5*, 18.
(54) Chatgilialoglu, C.; O'Neill, P. *Exp. Gerontol.* **2001**, *36*, 1459.
(55) Breen, A. P.; Murphy, J. A. *Free Radical Biol. Med.* **1995**, *18*, 1033.
(56) Close, D. M. *Radiat. Res.* **1997**, *147*, 663.
(57) Sigman, D. S.; Mazumder, A.; Perrin, D. M. *Chem. Rev.* **1993**, *93*, 2295.
(58) Neyhart, G. A.; Cheng, C.-C.; Thorp, H. H. *J. Am. Chem. Soc.* **1995**, *117*, 1463.
(59) Mazzer, P. A.; Maurmann, L.; Bose, R. N. *J. Inorg. Biochem.* **2007**, *101*, 44.
(60) Colson, A.-O.; Sevilla, M. D. *J. Phys. Chem. B* **1995**, *99*, 3867.
(61) Miaskiewicz, K.; Osman, R. *J. Am. Chem. Soc.* **1994**, *116*, 232.
(62) Meijler, M. M.; Zelenko, O.; Sigman, D. S. *J. Am. Chem. Soc.* **1997**, *119*, 1135.
(63) Oyoshi, T.; Sugiyama, H. *J. Am. Chem. Soc.* **2000**, *122*, 6313.
(64) Chatgilialoglu, C.; Ferreri, C.; Bazzanini, R.; Guerra, M.; Choi, S.-Y.; Emanuel, C. J.; Horner, J. H.; Newcomb, M. *J. Am. Chem. Soc.* **2000**, *122*, 9525.
(65) Pitié, M.; Bernadou, J.; Meunier, B. *J. Am. Chem. Soc.* **1995**, *117*, 2935.
(66) Goodman, B. K.; Greenberg, M. M. *J. Org. Chem.* **1996**, *61*, 2.
(67) Emanuel, C. J.; Newcomb, M.; Ferreri, C.; Chatgilialoglu, C. *J. Am. Chem. Soc.* **1999**, *121*, 2927.
(68) Hwang, J.-T.; Greenberg, M. M. *J. Am. Chem. Soc.* **1999**, *121*, 4311.
(69) Tronche, C.; Goodman, B. K.; Greenberg, M. M. *Chem. Biol.* **1998**, *5*, 263.
(70) Tallman, K. A.; Tronche, C.; Yoo, D. J.; Greenberg, M. M. *J. Am. Chem. Soc.* **1998**, *120*, 4903.
(71) Hwang, J. T.; Tallman, K. A.; Greenberg, M. M. *Nucleic Acids Res.* **1999**, *27*, 3805.
(72) Sugiyama, H.; Tsutsumi, Y.; Fujimoto, K.; Saito, I. *J. Am. Chem. Soc.* **1993**, *115*, 4443.
(73) Zheng, Y.; Sheppard, T. L. *Chem. Res. Toxicol.* **2004**, *17*, 197.
(74) Roupioz, Y.; Lhomme, J.; Kotera, M. *J. Am. Chem. Soc.* **2002**, *124*, 9129.
(75) Kappen, L. S.; Goldberg, I. H.; Wu, S. H.; Stubbe, J.; Worth, L. J.; Kozarich, J. W. *J. Am. Chem. Soc.* **1990**, *112*, 2797.
(76) Kappen, L. S.; Chen, C. Q.; Goldberg, I. H. *Biochemistry* **1988**, *27*, 4331.
(77) Bales, B. C.; Pitié, M.; Meunier, B.; Greenberg, M. M. *J. Am. Chem. Soc.* **2002**, *124*, 9062.
(78) Chen, T.; Greenberg, M. M. *J. Am. Chem. Soc.* **1998**, *120*, 3815.
(79) Roginskaya, M.; Bernhard, W. A.; Marion, R. T.; Razskazovskiy, Y. *Radiat. Res.* **2005**, *163*, 85.
(80) Knorre, D. G.; Frolova, E. I. *Russ. Chem. Rev.* **1993**, 62.
(81) Goyne, T. E.; Sigman, D. S. *J. Am. Chem. Soc.* **1987**, *109*, 2846.
(82) Pratviel, G.; Pitié, M.; Bernadou, J.; Meunier, B. *Nucleic Acids Res.* **1991**, *19*, 6283.
(83) Jourdan, M.; Garcia, J.; Defrancq, E.; Kotera, M.; Lhomme, J. *Biochemistry* **1999**, *38*, 3985.
(84) Hong, I. S.; Carter, K. N.; Sato, K.; Greenberg, M. M. *J. Am. Chem. Soc.* **2007**, *129*, 4089.

(85) Hashimoto, M.; Greenberg, M. M.; Kow, Y. W.; Hwang, J. T.; Cunningham, R. P. *J. Am. Chem. Soc.* **2001**, *123*, 3161.
(86) DeMott, M. S.; Beyret, E.; Wong, D.; Bales, B. C.; Hwang, J. T.; Greenberg, M. M.; Demple, B. *J. Biol. Chem.* **2002**, *277*, 7637.
(87) Burrows, C. J.; Muller, J. G. *Chem. Rev.* **1998**, *98*, 1109.
(88) Imoto, S.; Bransfield, L. A.; Croteau, D. L.; Van Houten, B.; Greenberg, M. M. *Biochemistry* **2008**, *47*, 4306.
(89) Hong, I. S.; Carter, K. N.; Greenberg, M. M. *J. Org. Chem.* **2004**, *69*, 6974.
(90) Greenberg, M. M.; Barvian, M. R.; Cook, G. P.; Goodman, B. K.; Matray, T. J.; Tronche, C.; Venkatesan, H. *J. Am. Chem. Soc.* **1997**, *119*, 1828.
(91) Carter, K. N.; Greenberg, M. M. *J. Am. Chem. Soc.* **2003**, *125*, 13376.
(92) Dizdaroglu, M.; Schulte-Frohlinde, D.; Von Sonntag, C. *Z. Naturforsch.* **1977**, *32C*, 1021.
(93) Xu, Y.; Sugiyama, H. *Angew. Chem., Int. Ed.* **2006**, *45*, 1354.
(94) Tashiro, R.; Nakamura, K.; Sugiyama, H. *Tetrahedron Lett.* **2008**, *49*, 428.
(95) Sugiyama, H.; Fujimoto, K.; Saito, I.; Kawashima, E.; Sekine, T.; Ishido, Y. *Tetrahedron Lett.* **1996**, *37*, 1805.
(96) Sugiyama, H.; Tsutsumi, Y.; Saito, I. *J. Am. Chem. Soc.* **1990**, *112*, 6720.
(97) Cook, G. P.; Greenberg, M. M. *J. Am. Chem. Soc.* **1996**, *118*, 10025.
(98) Sugiyama, H.; Fujimoto, K.; Saito, I. *J. Am. Chem. Soc.* **1995**, *117*, 2945.
(99) Kim, J.; Weledji, Y. N.; Greenberg, M. M. *J. Org. Chem.* **2004**, *69*, 6100.
(100) Greenberg, M. M.; Weledji, Y. N.; Kroeger, K. M.; Kim, J. *Biochemistry* **2004**, *43*, 15217.
(101) Greenberg, M. M.; Kreller, C. R.; Young, S. E.; Kim, J. *Chem. Res. Toxicol.* **2006**, *19*, 463.
(102) Kawai, K.; Saito, I.; Sugiyama, H. *J. Am. Chem. Soc.* **1999**, *121*, 1391.
(103) Li, M. J.; Liu, L.; Wei, K.; Fu, Y.; Guo, Q. X. *J. Phys. Chem. B* **2006**, *110*, 13582.
(104) Sitlani, A.; Long, E. C.; Pyle, A. M.; Barton, J. K. *J. Am. Chem. Soc.* **1992**, *114*, 2303.
(105) Shields, T. P.; Barton, J. K. *Biochemistry* **1995**, *34*, 15037.
(106) Zeglis, B. M.; Pierre, V. C.; Barton, J. K. *Chem. Commun.* **2007**, 4565.
(107) Lahoud, G. A.; Hitt, A. L.; Bryant-Friedrich, A. C. *Chem. Res. Toxicol.* **2006**, *19*, 1630.
(108) Collins, C.; Awada, M. M.; Zhou, X.; Dedon, P. C. *Chem. Res. Toxicol.* **2003**, *16*, 1560.
(109) Awada, M.; Dedon, P. C. *Chem. Res. Toxicol.* **2001**, *14*, 1247.
(110) Murata-Kamiya, N.; Kamiya, H.; Iwamoto, N.; Kasai, H. *Carcinogenesis* **1995**, *16*, 2251.
(111) Bryant-Friedrich, A. C. *Org. Lett.* **2004**, *6*, 2329.
(112) Sitlani, A.; Barton, J. K. *Biochemistry* **1994**, *33*, 12100.
(113) Claussen, C. A.; Long, E. C. *Chem. Rev.* **1999**, *99*, 2797.
(114) Burger, R. M. *Chem. Rev.* **1998**, *98*, 1153.
(115) Ajmera, S.; Wu, J. C.; Worth, L. J.; Rabow, L. E.; Stubbe, J.; Kozarich, J. W. *Biochemistry* **1986**, *25*, 6586.
(116) McGall, G. H.; Rabow, L. E.; Ashley, G. W.; Wu, S. H.; Kozarich, J. W.; Stubbe, J. *J. Am. Chem. Soc.* **1992**, *114*, 4958.
(117) Burger, R. M.; Projan, S. J.; Horwitz, S. B.; Peisach, J. *J. Biol. Chem.* **1986**, *261*, 15955.
(118) McGall, G. H.; Rabow, L. E.; Stubbe, J.; Kozarich, J. W. *J. Am. Chem. Soc.* **1987**, *109*, 2836.
(119) Rashid, R.; Langfinger, D.; Wagner, R.; Schuchmann, H. P.; von Sonntag, C. *Int. J. Radiat. Biol.* **1999**, *75*, 101.
(120) Giese, B.; Beyrich-Graf, X.; Erdmann, P.; Giraud, L.; Imwinkelried, P.; Mueller, S. N.; Schwitter, U. *J. Am. Chem. Soc.* **1995**, *117*, 6146.
(121) Giese, B.; Beyrich-Graf, X.; Erdmann, P.; Petretta, M.; Schwitter, U. *Chem. Biol.* **1995**, *2*, 367.
(122) Dussy, A.; Meggers, E.; Giese, B. *J. Am. Chem. Soc.* **1998**, *120*, 7399.
(123) Giese, B.; Dussy, A.; Meggers, E.; Petretta, M.; Schwitter, U. *J. Am. Chem. Soc.* **1997**, *119*, 11130.
(124) Junker, H. D.; Hoehn, S. T.; Bunt, R. C.; Marathius, V.; Chen, J.; Turner, C. J.; Stubbe, J. *Nucleic Acids Res.* **2002**, *30*, 5497.
(125) Kuwabara, M.; Yoon, C.; Goyne, T.; Thederahn, T.; Sigman, D. S. *Biochemistry* **1986**, *25*, 7401.
(126) Giloni, L.; Takeshita, M.; Johnson, F.; Iden, C.; Grollman, A. P. *J. Biol. Chem.* **1981**, *256*, 8608.
(127) Pitié, M.; Burrows, C. J.; Meunier, B. *Nucleic Acids Res.* **2000**, *28*, 4856.
(128) Zhou, X.; Taghizadeh, K.; Dedon, P. C. *J. Biol. Chem.* **2005**, *280*, 25377.
(129) Szekely, J.; Rizzo, C. J.; Marnett, L. J. *J. Am. Chem. Soc.* **2008**, *130*, 2195.
(130) Dedon, P. C.; Jiang, Z. W.; Goldberg, I. H. *Biochemistry* **1992**, *31*, 1917.
(131) Rabow, L. E.; Stubbe, J.; Kozarich, J.; McGall, G. H. *J. Am. Chem. Soc.* **1990**, *112*, 3203.
(132) Chen, J.; Stubbe, J. *Biochemistry* **2004**, *43*, 5278.
(133) Kim, J.; Gil, J. M.; Greenberg, M. M. *Angew. Chem., Int. Ed.* **2003**, *42*, 5882.
(134) Sugiyama, H.; Xu, C.; Murugesan, N.; Hecht, S. M. *J. Am. Chem. Soc.* **1985**, *107*, 4104.
(135) Sugiyama, H.; Xu, C.; Murugesan, N.; Hecht, S. M.; van der Marel, G. A.; van Boom, J. H. *Biochemistry* **1988**, *27*, 58.
(136) Rabow, L. E.; Stubbe, J.; Kozarich, J. W.; McGall, G. H. *J. Am. Chem. Soc.* **1990**, *112*, 3196.
(137) Chen, J.; Dupradeau, F. Y.; Case, D. A.; Turner, C. J.; Stubbe, J. *Biochemistry* **2007**, *46*, 3096.
(138) Regulus, P.; Duroux, B.; Bayle, P. A.; Favier, A.; Cadet, J.; Ravanat, J. L. *Proc. Natl. Acad. Sci. U.S.A.* **2007**, *104*, 14032.
(139) Dizdaroglu, M.; Von Sonntag, C.; Schulte-Frohlinde, D. *J. Am. Chem. Soc.* **1975**, *97*, 2277.
(140) Beesk, F.; Dizdaroglu, M.; Schulte-Frohlinde, D.; von Sonntag, C. *Int. J. Radiat. Biol. Relat. Stud. Phys. Chem. Med.* **1979**, *36*, 565.
(141) Meggers, E.; Dussy, A.; Schafer, T.; Giese, B. *Chem.-Eur. J.* **2000**, *6*, 485.
(142) Meggers, E.; Kusch, D.; Spichty, M.; Wille, U.; Giese, B. *Angew. Chem., Int. Ed.* **1998**, *37*, 460.
(143) Pitié, M.; Pratviel, G.; Bernadou, J.; Meunier, B. *Proc. Natl. Acad. Sci. U.S.A.* **1992**, *89*, 3967.
(144) Mourgues, S.; Kupan, A.; Pratviel, G.; Meunier, B. *ChemBioChem* **2005**, *6*, 2326.
(145) Pratviel, G.; Duarte, V.; Bernadou, J.; Meunier, B. *J. Am. Chem. Soc.* **1993**, *115*, 7939.
(146) Wietzerbin, K.; Muller, J. G.; Jameton, R. A.; Pratviel, G.; Bernadou, J.; Meunier, B.; Burrows, C. J. *Inorg. Chem.* **1999**, *38*, 4123.
(147) Goldberg, I. H. *Acc. Chem. Res.* **1991**, *24*, 191.
(148) Dix, T. A.; Hess, K. M.; Medina, M. A.; Sullivan, R. W.; Tilly, S. L.; Webb, T. L. *Biochemistry* **1996**, *35*, 4578.
(149) Pitié, M., Pratviel, G., Bernadou, J., Meunier, B. In *The Activation of Dioxygen and Homogeneous Catalytic Oxidation*. Barton, D. H. R., Martell, A. E., Sawyer, D. T., Eds. Plenum: New York, 1993; pp 333−346.
(150) Boussicault, F.; Kaloudis, P.; Caminal, C.; Mulazzani, Q. G.; Chatgilialoglu, C. *J. Am. Chem. Soc.* **2008**, *130*, 8377.
(151) Chin, D. H.; Carr, S. A.; Goldberg, I. H. *J. Biol. Chem.* **1984**, *259*, 9975.
(152) Angeloff, A.; Dubey, I.; Pratviel, G.; Bernadou, J.; Meunier, B. *Chem. Res. Toxicol.* **2001**, *14*, 1413.
(153) Kodama, T.; Greenberg, M. M. *J. Org. Chem.* **2005**, *70*, 9916.
(154) Pratviel, G.; Pitié, M.; Perigaud, C.; Gausselin, G.; Bernadou, J.; Meunier, B. *J. Chem. Soc., Chem. Commun.* **1993**, 149.
(155) Kappen, L. S.; Goldberg, I. H. *Biochemistry* **1983**, *22*, 4872.
(156) Kawabata, H.; Takeshita, H.; Fujiwara, T.; Sugiyama, H.; Matsuura, T.; Saito, I. *Tetrahedron Lett.* **1989**, *30*, 4263.
(157) Chin, D. H.; Kappen, L. S.; Goldberg, I. H. *Proc. Natl. Acad. Sci. U.S.A.* **1987**, *84*, 7070.
(158) Murphy, J. A.; Griffiths, J. *Nat. Prod. Rep.* **1993**, *10*, 551.
(159) Chen, B.; Bohnert, T.; Zhou, X.; Dedon, P. C. *Chem. Res. Toxicol.* **2004**, *17*, 1406.
(160) Chen, B.; Vu, C. C.; Byrns, M. C.; Dedon, P. C.; Peterson, L. A. *Chem. Res. Toxicol.* **2006**, *19*, 982.
(161) Jiang, T.; Zhou, X.; Taghizadeh, K.; Dong, M.; Dedon, P. C. *Proc. Natl. Acad. Sci. U.S.A.* **2007**, *104*, 60.
(162) Jaruga, P.; Dizdaroglu, M. *DNA Repair* **2008**, *7*, 1413.
(163) Dirksen, M. L.; Blakely, W. F.; Holwitt, E.; Dizdaroglu, M. *Int. J. Radiat. Biol.* **1988**, *54*, 195.
(164) Miaskiewicz, K.; Miller, J. H.; Fuciarelli, A. F. *Nucleic Acids Res.* **1995**, *23*, 515.
(165) Romieu, A.; Gasparutto, D.; Molko, D.; Cadet, J. *J. Org. Chem.* **1998**, *63*, 5245.
(166) Chatgilialoglu, C.; Guerra, M.; Mulazzani, Q. G. *J. Am. Chem. Soc.* **2003**, *125*, 3839.
(167) Manetto, A.; Georganakis, D.; Leondiadis, L.; Gimisis, T.; Mayer, P.; Carell, T.; Chatgilialoglu, C. *J. Org. Chem.* **2007**, *72*, 3659.
(168) Pratviel, G.; Meunier, B. *Chem.-Eur. J.* **2006**, *12*, 6018.
(169) Neeley, W. L.; Essigmann, J. M. *Chem. Res. Toxicol.* **2006**, *19*, 491.
(170) Cadet, J.; Douki, T.; Gasparutto, D.; Ravanat, J. L. *Mutat. Res.* **2003**, *531*, 5.
(171) Evans, M. D.; Dizdaroglu, M.; Cooke, M. S. *Mutat. Res.* **2004**, *567*, 1.
(172) Wagner, J. R.; van Lier, J. E.; Berger, M.; Cadet, J. *J. Am. Chem. Soc.* **1994**, *116*, 2235.
(173) Tofigh, S.; Frenkel, K. *Free Radical Biol. Med.* **1989**, *7*, 131.
(174) Frenkel, K.; Tofigh, S. *Biol. Trace Elem. Res.* **1989**, *21*, 351.
(175) Mellac, S.; Fazakerley, G. V.; Sowers, L. C. *Biochemistry* **1993**, *32*, 7779.

(176) Tsunoda, M.; Karino, N.; Ueno, Y.; Matsuda, A.; Takenaka, A. *Acta Crystallogr., Sect. D: Biol. Crystallogr.* **2001**, *57*, 345.
(177) Vu, H. M.; Pepe, A.; Mayol, L.; Kearns, D. R. *Nucleic Acids Res.* **1999**, *27*, 4143.
(178) Pasternack, L. B.; Bramham, J.; Mayol, L.; Galeone, A.; Jia, X.; Kearns, D. R. *Nucleic Acids Res.* **1996**, *24*, 2740.
(179) Rogstad, D. K.; Heo, J.; Vaidehi, N.; Goddard, W. A., III; Burdzy, A.; Sowers, L. C. *Biochemistry* **2004**, *43*, 5688.
(180) Hong, I. S.; Ding, H.; Greenberg, M. M. *J. Am. Chem. Soc.* **2006**, *128*, 485.
(181) Box, H. C.; Budzinski, E. E.; Dawidzik, J. D.; Wallace, J. C.; Evans, M. S.; Gobey, J. S. *Radiat. Res.* **1996**, *145*, 641.
(182) Bellon, S.; Ravanat, J. L.; Gasparutto, D.; Cadet, J. *Chem. Res. Toxicol.* **2002**, *15*, 598.
(183) Labet, V.; Morell, C.; Grand, A.; Cadet, J.; Cimino, P.; Barone, V. *Org. Biomol. Chem.* **2008**, *6*, 3300.
(184) Hong, H.; Cao, H.; Wang, Y. *Chem. Res. Toxicol.* **2006**, *19*, 614.
(185) Zhang, Q.; Wang, Y. *Nucleic Acids Res.* **2005**, *33*, 1593.
(186) Nackerdien, Z.; Rao, G.; Cacciuttolo, M. A.; Gajewski, E.; Dizdaroglu, M. *Biochemistry* **1991**, *30*, 4873.
(187) Hong, I. S.; Greenberg, M. M. *J. Am. Chem. Soc.* **2005**, *127*, 3692.
(188) Ding, H.; Greenberg, M. M. *Chem. Res. Toxicol.* **2007**, *20*, 1623.
(189) Pogozelski, W. J.; McNeese, T. J.; Tullius, T. D. *J. Am. Chem. Soc.* **1995**, *117*, 6428.
(190) Hertzberg, R. P.; Dervan, P. B. *Biochemistry* **1984**, *23*, 3934.
(191) Moser, H. E.; Dervan, P. B. *Science* **1987**, *238*, 645.
(192) Dervan, P. B. *Science* **1986**, *232*, 464.
(193) Aso, M.; Kondo, M.; Suemune, H.; Hecht, S. M. *J. Am. Chem. Soc.* **1999**, *121*, 9023.
(194) Tullius, T. D.; Greenbaum, J. A. *Curr. Opin. Chem. Biol.* **2005**, *9*, 127.
(195) Jain, S. S.; Tullius, T. D. *Nat. Protocol* **2008**, *3*, 1092.
(196) Umezaxa, H.; Maeda, K.; Takeuchi, T.; Okami, Y. *J. Antibiot.* **1966**, *19*, 200.
(197) Chen, J.; Stubbe, J. *Nat. Rev. Cancer* **2005**, *5*, 102.
(198) Hecht, S. M. *Bioconjugate Chem.* **1994**, *5*, 513.
(199) Abraham, A. T.; Lin, J. J.; Newton, D. L.; Rybak, S.; Hecht, S. M. *Chem. Biol.* **2003**, *10*, 45.
(200) Ekimoto, H.; Takahashi, K.; Matsuda, A.; Takita, T.; Umezawa, H. *J. Antibiot.* **1985**, *38*, 1077.
(201) Petering, D.; Byrnes, R. W.; Antholine, W. E. *Chem. Biol. Interact.* **1990**, *73*, 133.
(202) Petering, D. H.; Mao, Q.; Li, W.; DeRose, E.; Antholine, W. E. *Metal Ions Biol. Syst.* **1996**, *33*, 619.
(203) Boger, D. L.; Cai, H. *Angew. Chem., Int. Ed.* **1999**, *38*, 449.
(204) Hecht, S. M. *J. Nat. Prod.* **2000**, *63*, 158.
(205) Burger, R. M. *Struct. Bonding (Berlin)* **2000**, *97*, 287.
(206) Chen, J.; Stubbe, J. *Curr. Opin. Chem. Biol.* **2004**, *8*, 175.
(207) Byrnes, R. W.; Templin, J.; Sem, D.; Lyman, S.; Petering, D. H. *Cancer Res.* **1990**, *50*, 5275.
(208) Radtke, K.; Lornitzo, F. A.; Byrnes, R. W.; Antholine, W. E.; Petering, D. H. *Biochem. J.* **1994**, *302*, 655.
(209) Ehrenfeld, G. M.; Shipley, J. B.; Heimbrook, D. C.; Sugiyama, H.; Long, E. C.; van Boom, J. H.; van der Marel, G. A.; Oppenheimer, N. J.; Hecht, S. M. *Biochemistry* **1987**, *26*, 931.
(210) Chang, C.-H.; Meares, C. F. *Biochemistry* **1984**, *23*, 2268.
(211) Wu, W.; Vanderwall, D. E.; Lui, S. M.; Tang, X. J.; Turner, C. J.; Kozarich, J. W.; Stubbe, J. *J. Am. Chem. Soc.* **1996**, *118*, 1268.
(212) Rajani, C.; Kincaid, J. R.; Petering, D. H. *J. Am. Chem. Soc.* **2004**, *126*, 3829.
(213) Goodwin, K. D.; Lewis, M. A.; Long, E. C.; Georgiadis, M. M. *Proc. Natl. Acad. Sci. U.S.A.* **2008**, *105*, 5052.
(214) Sugiyama, M.; Kumagai, T.; Hayashida, M.; Maruyama, M.; Matoba, Y. *J. Biol. Chem.* **2002**, *277*, 2311.
(215) Danshiitsoodol, N.; de Pinho, C. A.; Matoba, Y.; Kumagai, T.; Sugiyama, M. *J. Mol. Biol.* **2006**, *360*, 398.
(216) Leitheiser, C. J.; Smith, K. L.; Rishel, M. J.; Hashimoto, S.; Konishi, K.; Thomas, C. J.; Li, C.; McCormick, M. M.; Hecht, S. M. *J. Am. Chem. Soc.* **2003**, *125*, 8218.
(217) Ma, Q.; Xu, Z.; Schroeder, B. R.; Sun, W.; Wei, F.; Hashimoto, S.; Konishi, K.; Leitheiser, C. J.; Hecht, S. M. *J. Am. Chem. Soc.* **2007**, *129*, 12439.
(218) Chapuis, J. C.; Schmaltz, R. M.; Tsosie, K. S.; Belohlavek, M.; Hecht, S. M. *J. Am. Chem. Soc.* **2009**, *131*, 2438.
(219) Iitaka, Y.; Nakamura, H.; Nakatani, T.; Muraoka, Y.; Fujii, A.; Takita, T.; Umezawa, H. *J. Antibiot.* **1978**, *31*, 1070.
(220) Xu, R. X.; Nettesheim, D.; Otvos, J. D.; Petering, D. H. *Biochemistry* **1994**, *33*, 907.
(221) Wu, W.; Vanderwall, D. E.; Turner, C. J.; Kozarich, J. W.; Stubbe, J. *J. Am. Chem. Soc.* **1996**, *118*, 1281.
(222) Vanderwall, D. E.; Lui, S. M.; Wu, W.; Turner, C. J.; Kozarich, J. W.; Stubbe, J. *Chem. Biol.* **1997**, *4*, 373.
(223) Caceres-Cortes, J.; Sugiyama, H.; Ikudome, K.; Saito, I.; Wang, H.-J. *Eur. J. Biochem.* **1997**, *244*, 818.
(224) Caceres-Cortes, J.; Sugiyama, H.; Ikudome, K.; Saito, I.; Wang, A. H. *Biochemistry* **1997**, *36*, 9995.
(225) Hoehn, S. T.; Junker, H. D.; Bunt, R. C.; Turner, C. J.; Stubbe, J. *Biochemistry* **2001**, *40*, 5894.
(226) Fedeles, F.; Zimmer, M. *Inorg. Chem.* **2001**, *40*, 1557.
(227) Zhao, C.; Xia, C.; Mao, Q.; Forsterling, H.; DeRose, E.; Antholine, W. E.; Subczynski, W. K.; Petering, D. H. *J. Inorg. Biochem.* **2002**, *91*, 259.
(228) Xia, C.; Forsterling, F. H.; Petering, D. H. *Biochemistry* **2003**, *42*, 6559.
(229) Fulmer, P.; Zhao, C. Q.; Li, W. B.; DeRose, E.; Antholine, W. E.; Petering, D. H. *Biochemistry* **1997**, *36*, 4367.
(230) Maruyama, M.; Kumagai, T.; Matoba, Y.; Hayashida, M.; Fujii, T.; Hata, Y.; Sugiyama, M. *J. Biol. Chem.* **2001**, *276*, 9992.
(231) Lehmann, T. E. *J. Biol. Inorg. Chem.* **2004**, *9*, 323.
(232) Lehmann, T. E. *J. Biol. Inorg. Chem.* **2002**, *7*, 305.
(233) Lehmann, T. E.; Ming, L. J.; Rosen, M. E.; Que, L., Jr. *Biochemistry* **1997**, *36*, 2807.
(234) Akkerman, M. A. J.; Neijman, E. W. J. F.; Wijmenga, S. S.; Hilbers, C. W.; Bermel, W. *J. Am. Chem. Soc.* **1990**, *112*, 7462.
(235) Keck, M. V.; Manderville, R. A.; Hecht, S. M. *J. Am. Chem. Soc.* **2001**, *123*, 8690.
(236) Sucheck, S. J.; Ellena, J. F.; Hecht, S. M. *J. Am. Chem. Soc.* **1998**, *120*, 7450.
(237) Akkerman, M. A. J.; Haasnoot, C. A. G.; Hilbers, C. W. *Eur. J. Biochem.* **1988**, *173*, 211.
(238) Manderville, R. A.; Ellena, J. F.; Hecht, S. M. *J. Am. Chem. Soc.* **1994**, *116*, 10851.
(239) Manderville, R. A.; Ellena, J. F.; Hecht, S. M. *J. Am. Chem. Soc.* **1995**, *117*, 7891.
(240) Lehmann, T. E.; Serrano, M. L.; Que, L., Jr. *Biochemistry* **2000**, *39*, 3886.
(241) Loeb, K. E.; Zaleski, J. M.; Hess, C. D.; Hecht, S. M.; Solomon, E. I. *J. Am. Chem. Soc.* **1998**, *120*, 1249.
(242) Wasinger, E. C.; Zaleski, L.; Hedman, B.; Hodgson, K. O.; Solomon, E. I. *J. Biol. Inorg. Chem.* **2002**, *7*, 157.
(243) Akiyama, Y.; Ma, Q.; Edgar, E.; Laikhter, A.; Hecht, S. M. *J. Am. Chem. Soc.* **2008**, *130*, 9650.
(244) Ma, Q.; Akiyama, Y.; Xu, Z.; Konishi, K.; Hecht, S. M. *J. Am. Chem. Soc.* **2009**, *131*, 2013.
(245) Mao, Q. K.; Fulmer, P.; Li, W. B.; DeRose, E. F.; Petering, D. H. *J. Biol. Chem.* **1996**, *271*, 6185.
(246) Li, W.; Zhao, C.; Xia, C.; Antholine, W. E.; Petering, D. H. *Biochemistry* **2001**, *40*, 7559.
(247) Stubbe, J. K. J. W.; Wu, W.; Vanderwall, D. E. *Acc. Chem. Res.* **1996**, *29*, 322.
(248) Kumar, D.; Hirao, H.; Shaik, S.; Kozlowski, P. M. *J. Am. Chem. Soc.* **2006**, *128*, 16148.
(249) Abraham, A. T.; Zhou, X.; Hecht, S. M. *J. Am. Chem. Soc.* **2001**, *123*, 5167.
(250) Chen, J.; Ghorai, M. K.; Kenney, G.; Stubbe, J. *Nucleic Acids Res.* **2008**, *36*, 3781.
(251) Chikira, M.; Iiyama, T.; Sakamoto, K.; Antholine, W. E.; Petering, D. H. *Inorg. Chem.* **2000**, *39*, 1779.
(252) Kemsley, J. N.; Zaleski, K. L.; Chow, M. S.; Decker, A.; Shishova, E. Y.; Wasinger, E. C.; Hedman, B.; Hodgson, K. O.; Solomon, E. I. *J. Am. Chem. Soc.* **2003**, *125*, 10810.
(253) Burger, R. M.; Peisach, J.; Horwitz, S. B. *J. Biol. Chem.* **1981**, *256*, 11636.
(254) Sam, J. W.; Tang, X. J.; Peisach, J. *J. Am. Chem. Soc.* **1994**, *116*, 5250.
(255) Burger, R. M.; Tian, G. C.; Drlica, K. *J. Am. Chem. Soc.* **1995**, *117*, 1167.
(256) Burger, R. M.; Kent, T. A.; Horwitz, S. B.; Munck, E.; Peisach, J. *J. Biol. Chem.* **1983**, *258*, 1559.
(257) Veselov, A.; Burger, R. M.; Scholes, C. P. *J. Am. Chem. Soc.* **1998**, *120*, 1030.
(258) Westre, T. E.; Loeb, K. E.; Zaleski, J. M.; Hedman, B.; Hodgson, K. O.; Solomon, E. I. *J. Am. Chem. Soc.* **1995**, *117*, 1309.
(259) Peisach, J. *Int. Congress Ser.* **2002**, *1233*, 511.
(260) Burger, R. M.; Usov, O. M.; Grigoryants, V. M.; Scholes, C. P. *J. Phys. Chem. B* **2006**, *110*, 20702.
(261) Neese, F.; Zaleski, J. M.; Zaleski, K. L.; Solomon, E. I. *J. Am. Chem. Soc.* **2000**, *122*, 11703.
(262) Solomon, E. I.; Decker, A.; Lehnert, N. *Proc. Natl. Acad. Sci. U.S.A.* **2003**, *100*, 3589.
(263) Decker, A.; Chow, M. S.; Kemsley, J. N.; Lehnert, N.; Solomon, E. I. *J. Am. Chem. Soc.* **2006**, *128*, 4719.
(264) Chow, M. S.; Liu, L. V.; Solomon, E. I. *Proc. Natl. Acad. Sci. U.S.A.* **2008**, *105*, 13241.

(265) Solomon, E. I.; Wong, S. D.; Liu, L. V.; Decker, A.; Chow, M. S. *Curr. Opin. Chem. Biol.* **2009**, *13*, 99.
(266) Aikens, J.; Sligar, S. G. *J. Am. Chem. Soc.* **1994**, *116*, 1143.
(267) Ogliaro, F.; de Visser, S. P.; Groves, J. T.; Shaik, S. *Angew. Chem., Int. Ed.* **2001**, *40*, 2874.
(268) Schunemann, V.; Lendzian, F.; Jung, C.; Contzen, J.; Barra, A. L.; Sligar, S. G.; Trautwein, A. X. *J. Biol. Chem.* **2004**, *279*, 10919.
(269) Ehrenfeld, G. M.; Murugesan, N.; Hecht, S. M. *Inorg. Chem.* **1984**, *23*, 1496.
(270) Natrajan, A.; Hecht, S. M.; Vandermarel, G. A.; Vanboom, J. H. *J. Am. Chem. Soc.* **1990**, *112*, 4532.
(271) Heimbrook, D. C.; Carr, S. A.; Mentzer, M. A.; Long, E. C.; Hecht, S. M. *Inorg. Chem.* **1987**, *26*, 3835.
(272) Murugesan, N.; Hecht, S. M. *J. Am. Chem. Soc.* **1985**, *107*, 493.
(273) Worth, L., Jr.; Frank, B. L.; Christner, D. F.; Absalon, M. J.; Stubbe, J.; Kozarich, J. W. *Biochemistry* **1993**, *32*, 2601.
(274) Khenkin, A. M.; Shilov, A. E. *New J. Chem.* **1989**, *13*, 659.
(275) Sawyer, D. T.; Kang, C.; Llobet, A.; Redman, C. *J. Am. Chem. Soc.* **1993**, *115*, 5817.
(276) Gelb, M. H.; Heimbrook, D. C.; Malkonen, P.; Sligar, S. G. *Biochemistry* **1982**, *21*, 370.
(277) Groves, J. T.; McClusky, G. A. *Biochem. Biophys. Res. Commun.* **1978**, *81*, 154.
(278) Padbury, G.; Sligar, S. G.; Labeque, R.; Marnett, L. J. *Biochemistry* **1988**, *27*, 7846.
(279) Kozarich, J. W.; Worth, L.; Frank, B. L.; Christner, D. F.; Vanderwall, D. E.; Stubbe, J. *Science* **1989**, *245*, 1396.
(280) Chen, B.; Zhou, X.; Taghizadeh, K.; Chen, J.; Stubbe, J.; Dedon, P. C. *Chem. Res. Toxicol.* **2007**, *20*, 1701.
(281) Groves, J. T.; Lee, J. B.; Marla, S. S. *J. Am. Chem. Soc.* **1997**, *119*, 6269.
(282) Jin, N.; Groves, J. T. *J. Am. Chem. Soc.* **1999**, *121*, 2923.
(283) Prince, S.; Korber, F.; Cooke, P. R.; Smith, J. R. L.; Mazid, M. A. *Acta Crystallogr., Sect. C* **1993**, *49*, 1158.
(284) Geacintov, N. E.; Ibanez, V.; Rougee, M.; Bensasson, R. V. *Biochemistry* **1987**, *26*, 3087.
(285) Sehlstedt, U.; Kim, S. K.; Carter, P.; Goodisman, J.; Vollano, J. F.; Norden, B.; Dabrowiak, J. C. *Biochemistry* **1994**, *33*, 417.
(286) Arnaud, P.; Zakrzewska, K.; Meunier, B. *J. Comput. Chem.* **2003**, *24*, 797.
(287) Dervan, P. B. *Bioorg. Med. Chem.* **2001**, *9*, 2215.
(288) Dabrowiak, J. C.; Ward, B.; Goodisman, J. *Biochemistry* **1989**, *28*, 3314.
(289) Vialas, C.; Pratviel, G.; Meunier, B. *Biochemistry* **2000**, *39*, 9514.
(290) Makarska, M.; Pratviel, G. *J. Biol. Inorg. Chem.* **2008**, *13*, 973.
(291) Kupan, A.; Sauliere, A.; Broussy, S.; Seguy, C.; Pratviel, G.; Meunier, B. *ChemBioChem* **2006**, *7*, 125.
(292) Sigman, D. S.; Graham, D. R.; D'Aurora, V.; Stern, A. M. *J. Biol. Chem.* **1979**, *254*, 12269.
(293) Sigman, D. S. *Acc. Chem. Res.* **1986**, *19*, 180.
(294) Sigman, D. S. *NATO Adv. Study Inst. Ser., Ser. C* **1996**, *479*, 119.
(295) Chen, C. B.; Milne, L.; Landgraf, R.; Perrin, D. M.; Sigman, D. S. *ChemBioChem* **2001**, *2*, 735.
(296) James, B. R.; Williams, R. J. P. *J. Chem. Soc.* **1961**, 2007.
(297) In *Stability Constants of Metal-Ion Complexes*. Sillen, L. G., Martell, A. E., Society, C., Eds. The Chemical Society London Publication: London, 1971.
(298) Dobson, J. F.; Green, B. E.; Healy, P. C.; Kennard, C. H. L.; Pakawatchai, C.; White, A. H. *Aust. J. Chem.* **1984**, *37*, 649.
(299) Nakai, H.; Deguchi, Y. *Bull. Chem. Soc. Jpn.* **1975**, *48*, 2557.
(300) Robertazzi, A.; Magistrato, A.; de Hoog, P.; Carloni, P.; Reedijk, J. *Inorg. Chem.* **2007**, *46*, 5873.
(301) Marshall, L. E.; Graham, D. R.; Reich, K. A.; Sigman, D. S. *Biochemistry* **1981**, *20*, 244.
(302) Johnson, G. R. A.; Nazhat, N. B. *J. Am. Chem. Soc.* **1987**, *109*, 1990.
(303) Thederahn, T. B.; Kuwabara, M. D.; Larsen, T. A.; Sigman, D. S. *J. Am. Chem. Soc.* **1989**, *111*, 4941.
(304) Veal, J. M.; Rill, R. L. *Biochemistry* **1991**, *30*, 1132.
(305) Veal, J. M.; Merchant, K.; Rill, R. L. *Nucleic Acids Res.* **1991**, *19*, 3383.
(306) Veal, J. M.; Rill, R. L. *Biochemistry* **1988**, *27*, 1822.
(307) Veal, J. M.; Rill, R. L. *Biochemistry* **1989**, *28*, 3243.
(308) Schaeffer, F.; Rimsky, S.; Spassky, A. *J. Mol. Biol.* **1996**, *260*, 523.
(309) Stockert, J. C. *J. Theor. Biol.* **1989**, *137*, 107.
(310) Yoon, C.; Kuwabara, M. D.; Law, R.; Wall, R.; Sigman, D. S. *J. Biol. Chem.* **1988**, *263*, 8458.
(311) Pope, L. E.; Sigman, D. S. *Proc. Natl. Acad. Sci. U.S.A.* **1984**, *81*, 3.
(312) Sigman, D. S.; Spassky, A.; Rimsky, S.; Buc, H. *Biopolymers* **1985**, *24*, 183.
(313) Murakawa, G. J.; Chen, C. H.; Kuwabara, M. D.; Nierlich, D. P.; Sigman, D. S. *Nucleic Acids Res.* **1989**, *17*, 5361.
(314) Pope, L. M.; Reich, K. A.; Graham, D. R.; Sigman, D. S. *J. Biol. Chem.* **1982**, *257*, 12121.
(315) Sy, D.; Savoye, C.; Begusova, M.; Michalik, V.; Charlier, M.; Spotheim-Maurizot, M. *Int. J. Radiat. Biol.* **1997**, *72*, 147.
(316) Zelenko, O.; Gallagher, J.; Xu, Y.; Sigman, D. S. *Inorg. Chem.* **1998**, *37*, 2198.
(317) Frelon, S.; Douki, T.; Favier, A.; Cadet, J. *Chem. Res. Toxicol.* **2003**, *16*, 191.
(318) Pitié, M.; Sudres, B.; Meunier, B. *Chem. Commun.* **1998**, 2597.
(319) Pitié, M.; Boldron, C.; Gornitzka, H.; Hemmert, C.; Donnadieu, B.; Meunier, B. *Eur. J. Inorg. Chem.* **2003**, 528.
(320) de Hoog, P.; Louwerse, M. J.; Gamez, P.; Pitié, M.; Baerends, E. J.; Meunier, B.; Reedijk, J. *Eur. J. Inorg. Chem.* **2008**, 612.
(321) Pitié, M.; Burrows, C. J.; Meunier, B. *Nucleic Acids Res.* **2000**, *28*, 4856.
(322) Pitié, M.; Van Horn, J. D.; Brion, D.; Burrows, C. J.; Meunier, B. *Bioconjugate Chem.* **2000**, *11*, 892.
(323) Bales, B. C.; Kodama, T.; Weledji, Y. N.; Pitié, M.; Meunier, B.; Greenberg, M. M. *Nucleic Acids Res.* **2005**, *33*, 5371.
(324) Hannon, M. J. *Chem. Soc. Rev.* **2007**, *36*, 280.
(325) Strekowski, L.; Wilson, B. *Mutat. Res.* **2007**, *623*, 3.
(326) Thomas, J. R.; Hergenrother, P. J. *Chem. Rev.* **2008**, *108*, 1171.
(327) Dixon, I. M.; Lopez, F.; Tejera, A. M.; Esteve, J. P.; Blasco, M. A.; Pratviel, G.; Meunier, B. *J. Am. Chem. Soc.* **2007**, *129*, 1502.
(328) Muller, B. C.; Raphael, A. L.; Barton, J. K. *Proc. Natl. Acad. Sci. U.S.A.* **1987**, *84*, 1764.
(329) Barton, J. K.; Raphael, A. L. *Proc. Natl. Acad. Sci. U.S.A.* **1985**, *82*, 6460.
(330) Thyagarajan, S.; Murthy, N. N.; Narducci Sarjeant, A. A.; Karlin, K. D.; Rokita, S. E. *J. Am. Chem. Soc.* **2006**, *128*, 7003.
(331) Li, L.; Karlin, K. D.; Rokita, S. E. *J. Am. Chem. Soc.* **2005**, *127*, 520.
(332) Blondeau, P.; Segura, M.; Perez-Fernandez, R.; de Mendoza, J. *Chem. Soc. Rev.* **2007**, *36*, 198.
(333) Pitié, M.; Meunier, B. *Bioconjugate Chem.* **1998**, *9*, 604.
(334) Pitié, M.; Croisy, A.; Carrez, D.; Boldron, C.; Meunier, B. *ChemBioChem* **2005**, *6*, 686.
(335) Jakobs, A.; Bernadou, J.; Meunier, B. *J. Org. Chem.* **1997**, *62*, 3505.
(336) Pitié, M.; Meunier, B. *J. Biol. Inorg. Chem.* **1996**, *1*, 239.
(337) Erkkila, K. E.; Odom, D. T.; Barton, J. K. *Chem. Rev.* **1999**, *99*, 2777.
(338) Patra, A. K.; Nethaji, M.; Chakravarty, A. R. *J. Inorg. Biochem.* **2007**, *101*, 233.
(339) Patra, A. K.; Dhar, S.; Nethaji, M.; Chakravarty, A. R. *Dalton Trans.* **2005**, 896.
(340) Dhar, S.; Nethaji, M.; Chakravarty, A. R. *Inorg. Chem.* **2005**, *44*, 8876.
(341) Baudoin, O.; Teulade-Fichou, M.-P.; Vigneron, J.-P.; Lehn, J.-M. *Chem. Commun.* **1998**, 2349.
(342) Zeglis, B. M.; Boland, J. A.; Barton, J. K. *J. Am. Chem. Soc.* **2008**, *130*, 7530.
(343) Pierre, V. C.; Kaiser, J. T.; Barton, J. K. *Proc. Natl. Acad. Sci. U.S.A.* **2007**, *104*, 429.
(344) Hashimoto, Y.; Iijima, H.; Nozaki, Y.; Shudo, K. *Biochemistry* **1986**, *25*, 5103.
(345) Lown, J. W.; Sondhi, S. M.; Ong, C. W.; Skorobogaty, A.; Kishikawa, H.; Dabrowiak, J. C. *Biochemistry* **1986**, *25*, 5111.
(346) Ding, L.; Etemad-Moghadam, G.; Meunier, B. *Biochemistry* **1990**, *29*, 7868.
(347) Boldron, C.; Ross, S. A.; Pitie, M.; Meunier, B. *Bioconjugate Chem.* **2002**, *13*, 1013.
(348) Routier, S.; Cotelle, N.; Catteau, J. P.; Bernier, J. L.; Waring, M. J.; Riou, J. F.; Bailly, C. *Bioorg. Med. Chem.* **1996**, *4*, 1185.
(349) Routier, S.; Bernier, J. L.; Catteau, J. P.; Colson, P.; Houssier, C.; Rivalle, C.; Bisagni, E.; Bailly, C. *Bioconjugate Chem.* **1997**, *8*, 789.
(350) Baguley, B. C. *Anti-Cancer Drug Des.* **1991**, *6*, 1.
(351) Marchand, C.; Nguyen, C. H.; Ward, B.; Sun, J. S.; Bisagni, E.; Garestier, T.; Helene, C. *Chem.-Eur. J.* **2000**, *6*, 1559.
(352) Zaid, A.; Sun, J. S.; Nguyen, C. H.; Bisagni, E.; Garestier, T.; Grierson, D. S.; Zain, R. *ChemBioChem* **2004**, *5*, 1550.
(353) Zain, R.; Polverari, D.; Nguyen, C. H.; Blouquit, Y.; Bisagni, E.; Garestier, T.; Grierson, D. S.; Sun, J. S. *ChemBioChem* **2003**, *4*, 856.
(354) Zain, R.; Marchand, C.; Sun, J.; Nguyen, C. H.; Bisagni, E.; Garestier, T.; Helene, C. *Chem. Biol.* **1999**, *6*, 771.
(355) Tuntiwechapikul, W.; Salazar, M. *Biochemistry* **2001**, *40*, 13652.
(356) Frau, S.; Bernadou, J.; Meunier, B. *Bioconjugate Chem.* **1997**, *8*, 222.
(357) Chen, C. H.; Mazumder, A.; Constant, J. F.; Sigman, D. S. *Bioconjugate Chem.* **1993**, *4*, 69.
(358) Taylor, J. S.; Schultz, P. G.; Dervan, P. B. *Tetrahedron* **1984**, *40*, 457.
(359) Routier, S.; Bernier, J.-L.; Catteau, J.-P.; Bailly, C. *Bioorg. Med. Chem. Lett.* **1997**, *7*, 1729.

(360) Dervan, P. B.; Edelson, B. S. *Curr. Opin. Struct. Biol.* **2003**, *13*, 284.
(361) Swalley, S. E.; Baird, E. E.; Dervan, P. B. *J. Am. Chem. Soc.* **1996**, *118*, 8198.
(362) White, S.; Baird, E. E.; Dervan, P. B. *Biochemistry* **1996**, *35*, 12532.
(363) Boidot-Forget, M.; Thuong, N. T.; Chassignol, M.; Helene, C. C. R. *Acad. Sci. Paris, Ser. II* **1986**, *302*, 75.
(364) Chu, B. C.; Orgel, L. E. *Proc. Natl. Acad. Sci. U.S.A.* **1985**, *82*, 963.
(365) Lin, S. B.; Blake, K. R.; Miller, P. S.; Ts'o, P. O. *Biochemistry* **1989**, *28*, 1054.
(366) Sun, J. S.; Francois, J. C.; Lavery, R.; Saison-Behmoaras, T.; Montenay-Garestier, T.; Thuong, N. T.; Helene, C. *Biochemistry* **1988**, *27*, 6039.
(367) Bergstrom, D. E.; Gerry, N. P. *J. Am. Chem. Soc.* **1994**, *116*, 12067.
(368) Frolova, E. I.; Ivanova, E. M.; Zarytova, V. F.; Abramova, T. V.; Vlassov, V. V. *FEBS Lett.* **1990**, *269*, 101.
(369) Frolova, E. I.; Fedorova, O. S.; Knorre, D. G. *Biochimie* **1993**, *75*, 5.
(370) Mestre, B.; Nascimben, S.; Pratviel, G.; Meunier, B. *C. R. Acad. Sci., Ser. IIc* **1998**, *1*, 725.
(371) Bigey, P.; Sonnichsen, S. H.; Meunier, B.; Nielsen, P. E. *Bioconjugate Chem.* **1997**, *8*, 267.
(372) Mestre, B.; Pitié, M.; Loup, C.; Claparols, C.; Pratviel, G.; Meunier, B. *Nucleic Acids Res.* **1997**, *25*, 1022.
(373) Pitié, M.; Casas, C.; Lacey, C. J.; Pratviel, G.; Bernadou, J.; Meunier, B. *Angew. Chem., Int. Ed. Engl.* **1993**, *32*, 557.
(374) Vorobjev, P. E.; Smith, J. B.; Pyshnaya, I. A.; Levina, A. S.; Zarytova, V. F.; Wickstrom, E. *Bioconjugate Chem.* **2003**, *14*, 1307.
(375) Escudé, C.; Sun, J.-S. *Top. Curr. Chem.* **2005**, *253*, 109.
(376) Singleton, S. F.; Dervan, P. B. *J. Am. Chem. Soc.* **1992**, *114*, 6957.
(377) Francois, J. C.; Saison-Behmoaras, T.; Barbier, C.; Chassignol, M.; Thuong, N. T.; Helene, C. *Proc. Natl. Acad. Sci. U.S.A.* **1989**, *86*, 9702.
(378) Shimizu, M.; Inoue, H.; Ohtsuka, E. *Biochemistry* **1994**, *33*, 606.
(379) Francois, J. C.; Helene, C. *Biochemistry* **1995**, *34*, 65.
(380) Cannata, F.; Brunet, E.; Perrouault, L.; Roig, V.; Ait-Si-Ali, S.; Asseline, U.; Concordet, J. P.; Giovannangeli, C. *Proc. Natl. Acad. Sci. U.S.A.* **2008**, *105*, 9576.
(381) Griffin, L. C.; Kiessling, L. L.; Beal, P. A.; Gillespie, P.; Dervan, P. B. *J. Am. Chem. Soc.* **1992**, *114*, 7976.
(382) Mack, D. P.; Sluka, J. P.; Shin, J. A.; Griffin, J. H.; Simon, M. I.; Dervan, P. B. *Biochemistry* **1990**, *29*, 6561.
(383) Oakley, M. G.; Dervan, P. B. *Science* **1990**, *248*, 847.
(384) Ebright, Y. W.; Chen, Y.; Pendergrast, P. S.; Ebright, R. H. *Biochemistry* **1992**, *31*, 10664.
(385) Pendergrast, P. S.; Ebright, Y. W.; Ebright, R. H. *Science* **1994**, *265*, 959.
(386) Bruice, T. W.; Wise, J. G.; Rosser, D. S. E.; Sigman, D. S. *J. Am. Chem. Soc.* **1991**, *113*, 5446.
(387) Ermacora, M. R.; Delfino, J. M.; Cuenoud, B.; Schepartz, A.; Fox, R. O. *Proc. Natl. Acad. Sci. U.S.A.* **1992**, *89*, 6383.
(388) Ermacora, M. R.; Ledman, D. W.; Hellinga, H. W.; Hsu, G. W.; Fox, R. O. *Biochemistry* **1994**, *33*, 13625.
(389) Dumoulin, P.; Ebright, R. H.; Knegtel, R.; Kaptein, R.; Granger-Schnarr, M.; Schnarr, M. *Biochemistry* **1996**, *35*, 4279.
(390) Pfau, J.; Arvidson, D. N.; Youderian, P.; Pearson, L. L.; Sigman, D. S. *Biochemistry* **1994**, *33*, 11391.
(391) Cox, J. M.; Hayward, M. M.; Sanchez, J. F.; Gegnas, L. D.; van der Zee, S.; Dennis, J. H.; Sigler, P. B.; Schepartz, A. *Proc. Natl. Acad. Sci. U.S.A.* **1997**, *94*, 13475.
(392) Xiao, G.; Cole, D. L.; Gunsalus, R. P.; Sigman, D. S.; Chen, C. H. *Protein Sci.* **2002**, *11*, 2427.
(393) Thurston, D. E.; Morris, S. J.; Hartley, J. A. *Chem. Commun.* **1996**, 563.
(394) Schatzschneider, U.; Barton, J. K. *J. Am. Chem. Soc.* **2004**, *126*, 8630.
(395) Petitjean, A.; Barton, J. K. *J. Am. Chem. Soc.* **2004**, *126*, 14728.
(396) de Hoog, P.; Boldron, C.; Gamez, P.; Sliedregt-Bol, K.; Roland, I.; Pitié, M.; Kiss, R.; Meunier, B.; Reedijk, J. *J. Med. Chem.* **2007**, *50*, 3148.
(397) de Hoog, P.; Pitié, M.; Amadei, G.; Gamez, P.; Meunier, B.; Kiss, R.; Reedijk, J. *J. Biol. Inorg. Chem.* **2008**, *13*, 575.
(398) Ozalp-Yaman, S.; de Hoog, P.; Amadei, G.; Pitié, M.; Gamez, P.; Dewelle, J.; Mijatovic, T.; Meunier, B.; Kiss, R.; Reedijk, J. *Chem.-Eur. J.* **2008**, *14*, 3418.

CR900247M